University of Stavanger

Faculty of Science and Technology

MASTER'S THESIS

Study program/ Specialisation: Master of Science: Environmental Engineering	Spring semester, 2018 Open access
Writer: Katja S. Håheim	Katja S. Håheim ..... (Writer's signature)
Faculty supervisors: Magne O. Sydnes	
Thesis title: Synthesis of Isocryptolepine and Analogues for Antimalarial Evaluation	
Credits (ECTS): 30 points	
Key words: Malaria, Isocryptolepine, Isocryptolepine analogues, Natural products	Pages: 97 (Including Appendix) Enclosure: Spectroscopic data Sandnes, 15th July 2018

UNIVERSITY OF STAVANGER

MASTER'S THESIS

Synthesis of Isocryptolepine and Analogues for Antimalarial Evaluation

Author:
Katja S. Håheim

Supervisor:
Magne O. Sydnes

July 12, 2018

University of Stavanger

Abstract

Malaria is considered a serious global health concern, causing 445 000 deaths annually. With the increasing apperance of drug resistant cases of *Plasmodium* strains, discovery of new treatments are of paramount importance. The natural product isocryptolepine (**4**) is known to display potent antimalarial activity, with preliminary studies indicating that its analogues may display even greater activities.

Isocryptolepine (**4**) was successfully synthesized in four steps starting from 3-bromoquinoline in a total yield of 31%. $Pd(OAc)_2$ was examined as a possible catalyst for the microwave-assisted ring closure to obtain 5*H*-indolo[3,2-*c*]quinoline, where $PdCl_2$(dppf) performed better at low scales. Attempts to utilize both $Pd(OAc)_2$ and $PdCl_2$(dppf) to achieve a gram-scale synthesis of the natural product **4** were unsuccessful.

Two novel C6-alkylated isocryptolepine analogues were synthesized in six steps starting from 3-bromoquinoline in total yields of 25-45% and 3-4% for analogues **41a** and **41b**, respectively. The key synthetic strategies in the pathway towards analogues **41** include *N*-oxidation, iodine-catalyzed alkenylation, Suzuki-Miyaura cross-coupling reaction, Pd/C catalyzed reduction, tandem C-H activation and C-N bond formation and *N*-methylation.

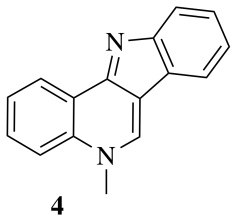

4

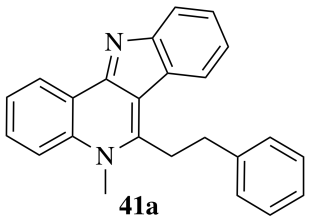

41a

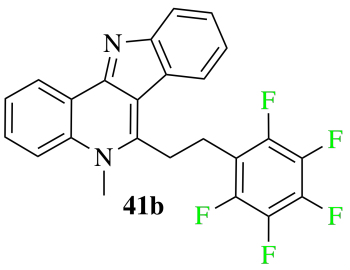

41b

Acknowledgements

All work conducted on this thesis was done at the University of Stavanger, Department of Chemistry, Bioscience and Environmental Technology, Norway, as part of my Master's Degree in Environmental Engineering. First and foremost, I would like to express my sincere gratitude to Associate Professor Dr. Magne O. Sydnes for his excellent guidance throughout this project. Despite residing in Japan for mostly all of my thesis, you always had time for Skype meetings and never failed to lend your expertise and support.

Secondly, I would like to thank the members of our research group: Associate Professor Dr. Emil Lindbäck, PhD student Vebjørn Eikemo and PhD student Marianne Bore Haarr. Your constant guidance and support made my time working at the laboratory truly enjoyable. Thanks for your help in the lab and for assisting me with my NMR interpretations. I would also like to thank fellow master's students Caroline Vaaland and Mojgan Khodakaram for contributing to a fun and positive working environment in the lab.

Furthermore, thanks to Associate Professor Dr. Kåre B. Jørgensen for his help with the NMR instrument, which was not always cooperative. Also, a thanks to Kåre's research group consisting of PhD student Sindhu Kancherla, PhD student Hiwot Minwuyelet and Bachelor's student Steffen Høie for readily lending us solvents and chemicals when necessary and in general for contributing to a great working environment.

A special thanks to Associate Professor Dr. Ronny Helland and the University of Tromsø for his enormous effort in analyzing our mystery compound by X-ray crystallography. Without his help, a tentative identification could not be possible.

Finally, thanks to my friends and family for their relentless support during my time as a master's student. Special thanks to Ådne Tobiesen, Elina Alfsvåg and Kenneth M. Boholm for always believing in me and encouraging me to do better. Lastly, a special thanks to my brother, Eirik Håheim, for providing last minute proof-reading.

Selected abbreviations

Ar	Aryl
atm	Atmosphere
DFT	Density functional theory
DCM	Dichloromethane
DMSO	Dimethyl sulfoxide
DVFC	Dry vacuum flash chromatography
EDG	Electron-donating group
EWG	Electron-withdrawing group
FTIR	Fourier transform infrared spectroscopy
Hz	Hertz
HMBC	Heteronuclear multiple bond correlation spectroscopy
HSQC	Heteronuclear single-quantum correlation spectroscopy
HRMS	High resolution mass spectrometry
h	Hour(s)
LRMS	Low resolution mass spectrometry
MW	Microwave
NHC	*N*-heterocyclic carbene ligand
S_NA	Nucleophilic aromatic substitution
PFA	Paraformaldehyde
PE	Petroleum ether
PPA	Polyphosphoric acid
R_f	Retardation factor
TFA	Trifluoroacetic acid
WHO	World Health Organization

Contents

1 Introduction

1.1 Malaria

Infection caused by the parasitic disease malaria represents a major global health concern.[1,2] Malaria is a tropical disease caused by one of the five protozoan *Plasmodium* strains;[3] *P. vivax*, *P. falciparum*, *P. ovale*, *P. knowlesi* and *P. malariae*, where the *P. falciparum* strain is the most deadly.[4] The spread to humans is by disease-borne, female anopheline mosquitoes[2,5] and occurs most frequently in countries near the equator.[6] In 2017, the World Health Organization (WHO) reported that 91 countries had ongoing malaria transmissions,[7] causing approximately 47% of the world's countries to suffer from the threat of malaria. Consequently, millions of lives are affected by the disease annually,[1,3] with 216 million reported cases and a mortality of 445 000 in 2017 alone.[7]

Malaria was traditionally treated by herbal remedies,[8] until the discovery of the natural alkaloid quinine (Figure 1) in the 17th century.[9] From its discovery until 1920, quinine was the main treatment for malaria until more effective semi-synthetic compounds became available.[9] A semi-synthetic analogue of quinine, chloroquine (Figure 1) became one of the new lead compounds in order to combat malaria.[9] Chloroquine has historically been the cheapest and most effective antimalarial drug.[8] However, following heavy use, chloroquine resistant strains of *P. falciparum* began to appear in the 1950s and by 1980 the resistance was spread to nearly all areas endemic to the strain.[9] Today, the treatment consists of a variety of antimalarial drugs, such as quinine, chloroquine, mefloquine and artemisinin (Figure 1), often in combination. However, with the increasing number of resistant strains, new and better drugs are in great need to outcompete the appearing resistances.

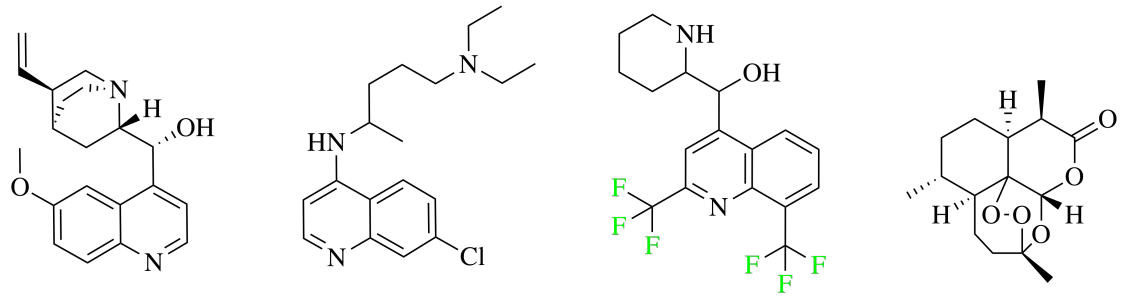

Quinine Chloroquine Mefloquine Artemisinin

Figure 1: The antimalarial agents quinine, chloroquine, mefloquine and artemisinin.

1.2 Natural products as antimalarial agents

When searching for new antimalarial drugs, natural products are of particularly high interest as they have been the most successful leads in the discovery of medicinal compounds in the past.[10,11] Natural products have historically played a key role in drug discovery and have been documented to exhibit antiproliferative, antiviral, antibacterial, antiparasitic and antifungal properties, among other therapeutic effects.[12] Two natural products that have greatly benefited human health since their discovery are penicillin G and salicylic acid, the precursor of acetylsalicylic acid (Aspirin) (Figure 2).[13] The discovery of penicillin has been called one of the most important developments in medicinal history, and in 1945 Alexander Fleming was awarded the Nobel Prize in Medicine for its discovery.[14]

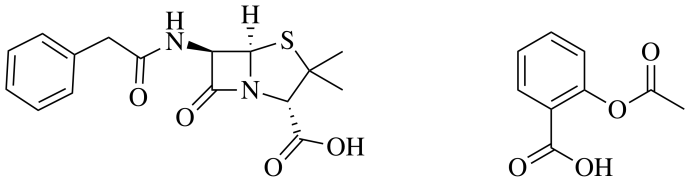

Penicillin G Aspirin

Figure 2: Penicillin G and Aspirin.

In 2015, the Nobel Prize in Medicine was awarded to Tu Youyou for her contributions in the discovery of Artemisinin (Figure 1).[6,15] The drug is said to have helped save millions from death by malaria. Moreover, Youyou's discovery is being labelled as a paradigm shift in antimalarial drug development.

A number of natural alkaloids have been found to possess antimalarial activity, including the aforementioned quinine.[9] Isolated from the West African climbing shrub *Cryptolepis sanguinolenta*, cryptolepine, neocryptolepine and isocryptolepine (Figure 3) were found to contain significant antimalarial activity.[1–3,8] These alkaloids can be classified as indoloquinolines; which are composed of a fused quinoline and indole moiety.[16] Indoloquinolines show a variety of bioactivities, including antibacterial, antifungal, antiprotozoan, antitumoral and antimalarial.[16] While cryptolepine and neocryptolepine have been extensively studied, isocryptolepine has been mostly overlooked.[1] Furthermore, while cryptolepine has displayed the most potent antimalarial properties of the three, it has also been found to inhibit topoisomerase II, resulting in cytotoxicity, interfering with its therapeutic effects.[8] Antimalarial studies have shown that isocryptolepine has lower cytotoxicity than cryptolepine,[8] and its analogues may thus be developed into new antimalarial agents.[6]

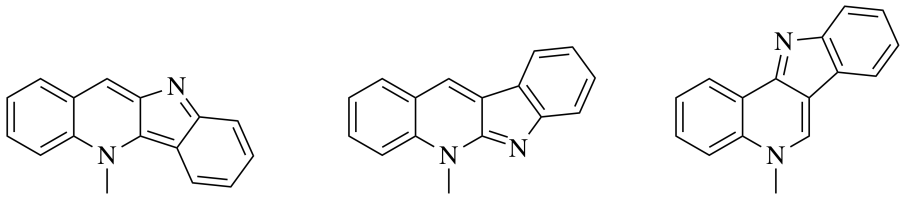

Figure 3: Bioactive compounds isolated from *Cryptolepis sanguinolenta.*

1.3 Syntheses of isocryptolepine (4) in the literature

A variety of total syntheses of isocryptolepine (**4**) are described in the literature, where most of the methods report using compounds containing quinolines or indoles as their starting materials.[10] Some synthetic strategies include palladium-catalyzed couplings, Fischer indole cyclizations, aza-Wittig reactions, photochemical cyclizations, Pictet-Spengler cyclizations[17] and Graebe-Ullmann reactions.[10,18] The number of syntheses of isocryptolepine are too numerous for all paths to be explored in detail in this thesis, however, four selected methods will be examined briefly.

Whittell *et al.*[19] outlined a three-step synthesis using a modified Graebe-Ullmann reaction to arrive at isocryptolepine (**4**) (Scheme 1). The synthesis commences with a thermally induced

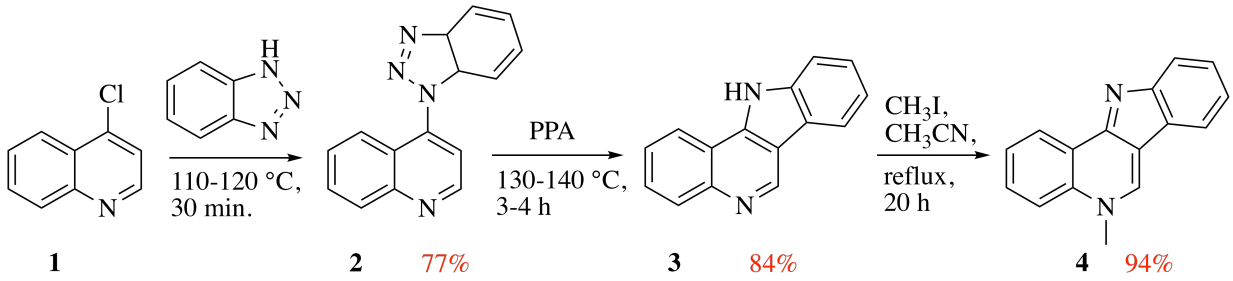

Scheme 1: Whittell *et al.*'s synthesis of isocryptolepine (**4**).[19]

coupling between 4-chloroquinoline (**1**) and benzotriazole, followed by an acid-catalyzed cyclization of compound **2** using polyphosphoric acid (PPA), *via* a modified Graebe-Ullmann-type mechanism. Subsequent *N*-methylation of compound **3** afforded the hydroiodo salt of isocryptolepine (**4**), which was converted to its basic form in an overall yield of 61%, upon treatment with base.

Agarwal *et al.*[17] developed a synthetic route towards isocryptolepine (**4**) which utilizes a Fisher indole synthesis followed by a modified Pictet-Spengler cyclization (Scheme 2). *o*-

Aminoacetophenone (**5**) and phenylhydrazine (**6**) is treated with acetic acid, ethanol and PPA to yield indole **7**. The Pictet-Spengler cyclization was initiated by treating compound **7** with paraformaldehyde (PFA) in the presence of trifluoroacetic acid (TFA) creating intermediate **8**, which upon spontaneous aerial oxidation produced compound **9** in 86% yield. Finally, *N*-methylation of compound **9** furnished isocryptolepine (**4**) in an overall yield of 67%.

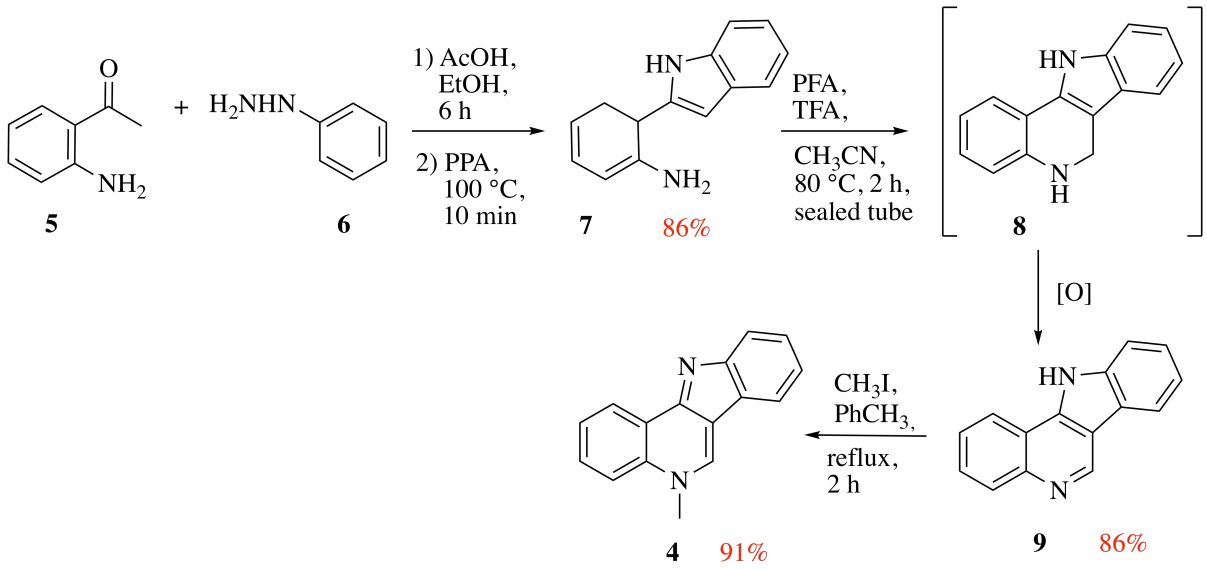

Scheme 2: Synthesis of isocryptolepine (**4**) using a modified Pictet-Spengler approach, as described by Agarwal *et al.*.[17]

Helgeland and Sydnes[3] presented a short and concise synthesis of isocryptolepine (**4**), wherein the key step is a Suzuki-Miyaura cross-coupling reaction (Scheme 3). 3-Bromoquinoline (**10**) is coupled to 2-aminophenylboronic acid hydrochloride (**11**) under optimized Suzuki-Miyaura cross-coupling conditions, catalyzed by $PdCl_2$(dppf) using K_2CO_3 as base. Coupling product **12** is then subjected to a tandem C-H activation and intramolecular C-N bond formation into the ring system **13**. The strategy towards ring closure was a microwave (MW) induced palladium-catalyzed reaction in the presence of H_2O_2 and 1,3-bis(2,4,6-trimethylphenyl)-imidazolium (I-Mes). The resulting product **13** was finally *N*-methylated to yield isocryptolepine (**4**) in an overall yield of 38%.

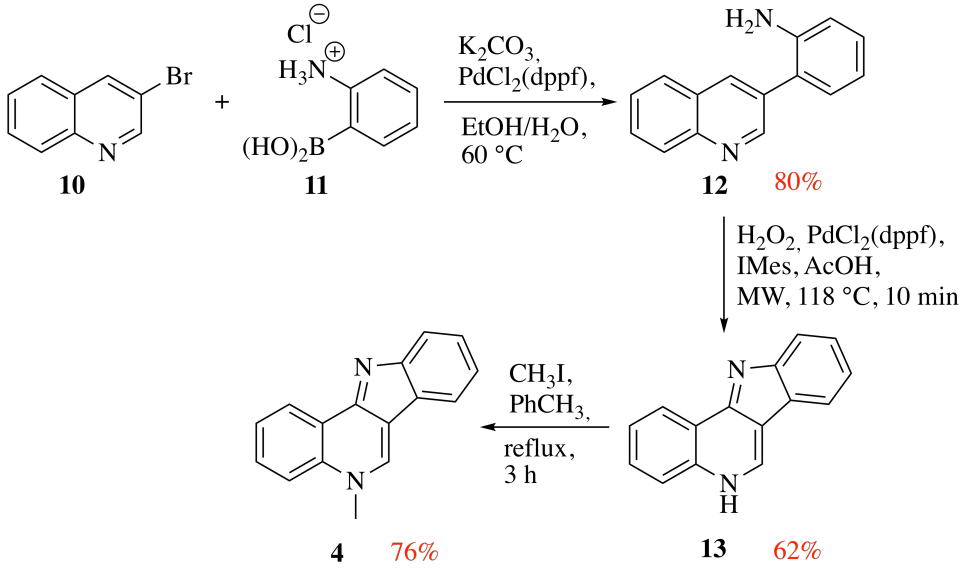

Scheme 3: Total synthesis of isocryptolepine (**4**) as conducted by Helgeland and Sydnes.[3]

By making slight modifications to their synthesis, Helgeland and Sydnes developed a two-step one-pot approach to synthesize isocryptolepine (**4**). Their method combines the cross coupling between compounds **10** and **11** with the MW-induced cyclization of coupling product **12** to form indoloquinoline **13** in a 32% yield. Upon *N*-methylation of indoloquinoline **13**, the natural product **4** is formed in a total yield of 24%.

One-pot chemistry is a growing field within the synthesis of *N*-heterocycles and a recent study by Aksenov's group[20] presented a one-pot synthesis of isocryptolepine (**4**) starting from *o*-aminoacetophenone (**5**) and phenylhydrazine (**6**) (Scheme 4). The reaction is initiated by addition of catalytical amounts of acetic acid, resulting in the formation of intermediate **14**. The formation of indole **15** is achieved by an acid-catalyzed Fischer indolization of intermediate **14**, which upon addition of 1,3,5-triazine and further treatment by PPA furnishes isocryptolepine (**4**) in an 82% yield.

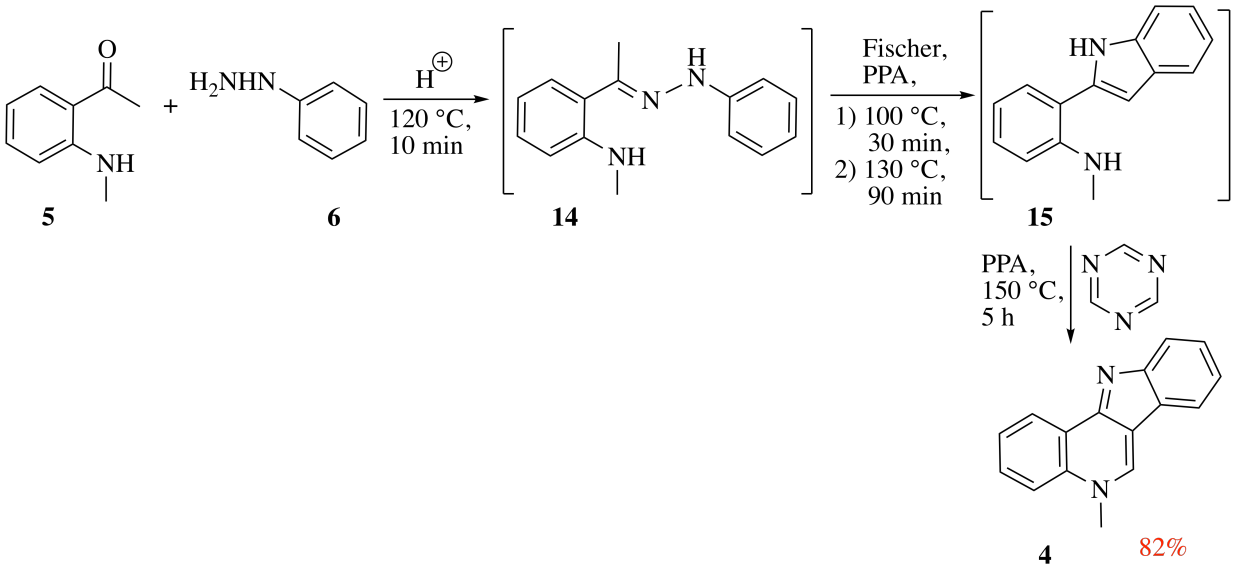

Scheme 4: One-pot synthesis of isocryptolepine (**4**) carried out by Aksenov *et al.*.[20]

1.3.1 Isocryptolepine derivatives

Analogues of bioactive compounds are often more potent than their parent molecules and additionally less cytotoxic.[10,19] However, the amount of literature available concerning the antimalarial activity of isocryptolepine derivatives is marginal compared to that of cryptolepine and neocryptolepine. Consequently, the full potential of isocryptolepine analogues as antimalarial compounds is not known.[19] Recent studies indicate two major developments: (1) di-halogenated derivatives displayed increased potency, particularly derivatives with a halogen at the C2,[1,19] C3[1] and C8[19] positions; (2) methyl-branched chains at the C6 position showed increased activity.[8] Similarly, a study by Teguh *et al.*[21] demonstrated that alkylation at the C2 position of 4-aminoquinolines increased the bioactivity against *P. falciparum* (see Figure 4 for the ring numbering in quinolines and indoloquinolines). As isocryptolepine (**4**) and its analogues can be viewed as 4-aminoquinoline derivatives, it provides yet another lead in the search for new compounds.

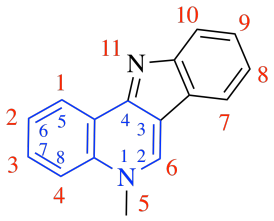

Figure 4: Ring numbering of *N*-heterocycles such as quinoline (blue) and indoloquinoline (red) demonstrated using the structure of isocryptolepine (**4**).

The methyl-branched chain analogue (**16**) (Figure 5) synthesized by Wang *et al.*[8] was found to exhibit an IC_{50} of 17.5 nM against the chloroquine resistant, or K1, strain of *P. falciparum*.[8] The lower the concentration of antiplasmodial activity, the more active the compound, meaning the methyl-branched chain analogue is a factor of approximately 45 times more active than the parent compound, namely isocryptolepine (**4**) (IC_{50} = 780 nM). Moreover, compound **16** displayed a toxicity of around 1/4 that of isocryptolepine (**4**) (Table 1).

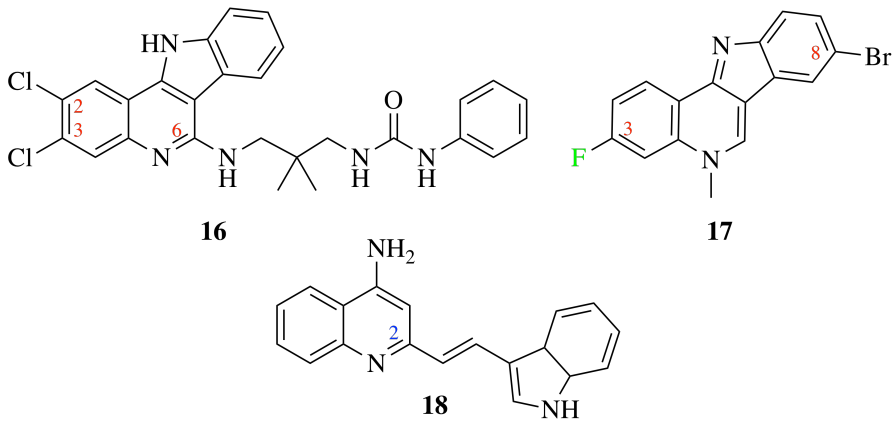

Figure 5: Structures of some bioactive compounds in recent literature.

The 3-fluoro-8-bromo analogue **17** (Figure 5) synthesized by Aroonkit *et al.*[1] revealed similar results; increased antiplasmodial activity and significantly decreased cytotoxicity (Table 1).[1] Teguh *et al.*'s[21] alkylated 4-aminoquinoline **18** (Figure 5) displayed an antiplasmodial activity which is twice that of isocryptolepine[21] (Table 1), making it the least active of the analogues depicted in Figure 5. However, it is unknown how it would affect the bioactivity having an alkyl moiety at the C6 position of isocryptolepine (**4**).

Table 1: Bioactivities of recently published structures (Figure 5) compared with isocryptolepine (**4**).

Compound	Cytotoxicity; IC_{50} [nM]	Antiplasmodial activity; IC_{50} [nM]
Isocryptolepine (**4**)	1190^{a} [8]	780^{b} [8]
16	4105.3^{a} [8]	17.5^{b} [8]
17	26279^{c} [1]	61.8^{b} [1]
18	-	390^{a} [21]

[a] *In vitro* activity against L6 cells; [b] *In vitro* activity against *Plasmodium falciparum* (K1 strain); [c] *In vitro* activity against MRC-5 cells

1.4 Suzuki-Miyaura cross-coupling reaction

A frequently used technique in the synthesis of natural products is the Suzuki-Miyaura C-C cross coupling.[22] The reaction can be defined as a palladium-catalyzed addition of an aryl, alkenyl or alkyl halide, triflate or sulfonate to organo boronic acids or organo boronates.[22–24] The Suzuki-Miyaura cross-coupling reaction has several advantages, such as the abundance of commercially available starting materials, tolerance to a broad range of functionalities, its mild reaction conditions and high product yields and also its low toxicity compared to other coupling reactions.[25] Additionally, the stability and water solubility of the boronic acids makes water an excellent solvent for the reaction, allowing for green chemistry. However, the stability of the boronic acids require the presence of a base in order to activate it as a coupling partner. Some bases commonly used in the Suzuki-Miyaura cross coupling are K_2CO_3, NaOH or *t*-BuOK,[24] depending on the type of boronic acid utilized.

The palladium catalyst is employed in different forms in the Suzuki-Miyaura cross-coupling reaction, most commonly as a complex aided by ligands. Nevertheless, palladium by itself has also proven to be an effective catalyst; palladium on charcoal (Pd/C) is known to catalyze several coupling reactions. The interaction between the palladium species and the ligands is not fully understood, as it has been shown that an assumed pure sample of palladium may contain up to 40% Pd nanoparticles.[26] Whether the catalysis proceeds in a homogenous or heterogenous manner is then uncertain,[26] but the presence of ligands is considered instrumental to a majority of palladium-catalyzed C-C couplings.[27] The phosphines have thus far been the most important ligands in organometallic and inorganic chemistry, playing a particularly important role in catalysis.[27] The success can be attributed to their ability to donate σ-electrons from the lone pair on the phosphorus.[27] Moreover, by controlling the electron density and bulkiness of the R groups, the stereochemistry of the product can be controlled.[27] Three phosphine-based ligands that have proven successful in the Suzuki-Miyaura cross coupling are 1,1'-bis(diphenylphosphino)ferrocene (dppf), triphenylphospine (PPh_3) and 2-dicyclohexyl- phosphino-2',4',6'-triisopropylbiphenyl (XPhos) (Figure 6).[22–24] In addition to phosphorous-based ligands, *N*-heterocyclic carbene ligands (NHC) are utilized for C-C couplings as they are also strong σ-donors[28] and significantly less toxic than the phosphines.[27] An NHC frequently used in the Suzuki-Miyaura cross coupling is IMes (Figure 6), which has been shown to behave quite similarly to the phosphorous ligands.[28]

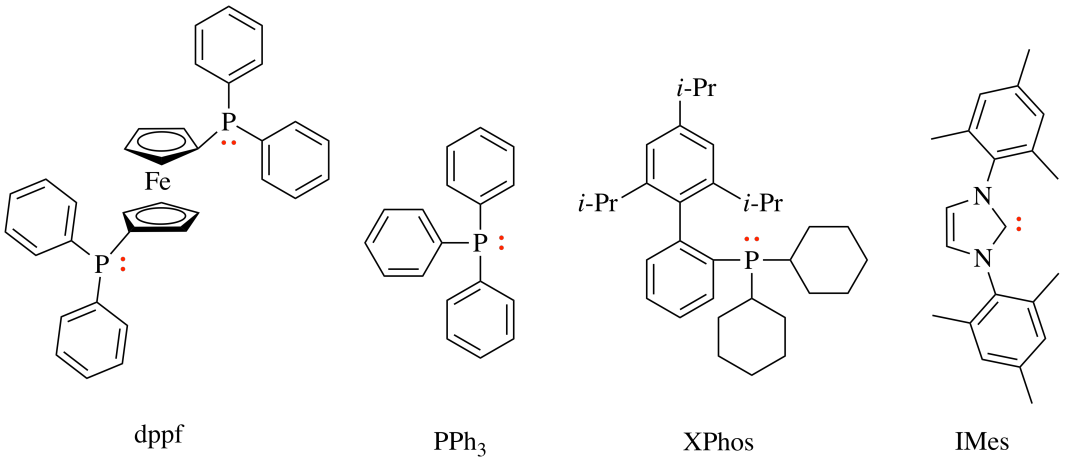

Figure 6: Some common ligands in Suzuki-Miyaura cross-coupling reactions.[22–24,28]

The role of palladium in the catalytic cycle of the Suzuki-Miyaura cross coupling has been extensively studied, as has its intermediates.[29] The cycle is known to contain three main steps: (i) oxidative addition, (ii) transmetallation and (iii) reductive elimination (Figure 5).[27] In oxidative addition, the organohalide coordinates to the palladium species forming the organopalladium complex, [L_2Pd-R^1X], which after attack from the base expels the halide, yielding [L_2Pd-R^1OH].[27] For transmetallation to occur, the boronic acid must be activated by the presence of a base to create a more reactive boronate complex,[29] further reacting with the palladium complex, creating [L_2Pd-R^1R^2]. Finally, reductive elimination affords the coupling product R^1-R^2 and subsequent regeneration of the palladium catalyst.[27]

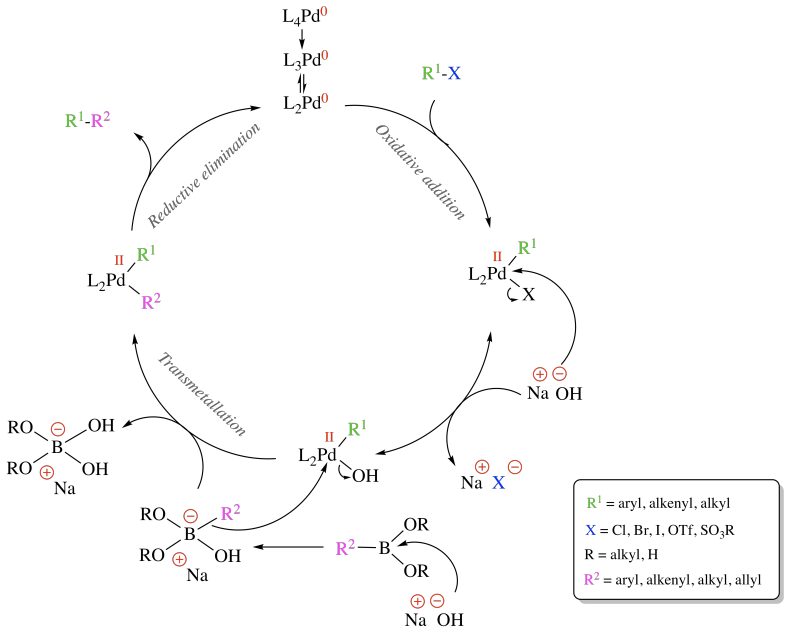

Scheme 5: Catalytic cycle of the Suzuki-Miyaura cross coupling.[24,29]

1.5 Objectives

1.5.1 Larger scale synthesis of isocryptolepine (4)

Helgeland and Sydnes[3] previously demonstrated the effectiveness of a short synthetic route towards isocryptolepine (**4**) at modest scales (50-100 mg) (Scheme 3). It is of interest to examine the performance of their synthesis on a larger scale (1-5 g). The aim is to carry out and describe the scale-up of the synthesis.

1.5.2 Synthesis of novel isocryptolepine analogues

As indicated by previous studies into the bioactivity of isocryptolepine analogues, the analogues may possess greater antiplasmodial activity than the natural alkaloid itself.[19] Furthermore, they often display less cytotoxicity providing for excellent lead compounds.[19] The effect of ring-substituted halogen analogues has been the major investigative focus in the past, yielding promising results.[8,19] Given the success of alkylation at the C2 position of 4-aminoquinolines as described by Teguh *et al.*,[21] and the addition of methyl-branched chains at the C6 position of isocryptolepine (**4**) outlined by Wang *et al.*,[8] it is desired to create novel C6-alkylated analogues. The aim is to investigate synthetic strategies towards the synthesis of the desired analogues and carry them out with the intent to hopefully create novel compounds displaying increased bioactivity. Based on work by Zhang *et al.*,[30] synthesis of analgoues containing ethylbenzene and 1-ethyl-2,3,4,5,6-pentafluorobenzene (Figure 7) at C6 is to be conducted. The analogues will be tested for a range of bioactivities, including antiproliferative and antimalarial, though cataloging and describing those activities is not the focus of this work. Instead, the focus will lie in the synthetic route towards said analogues and determination of our synthesis as a competitive path towards the creation of novel compounds.

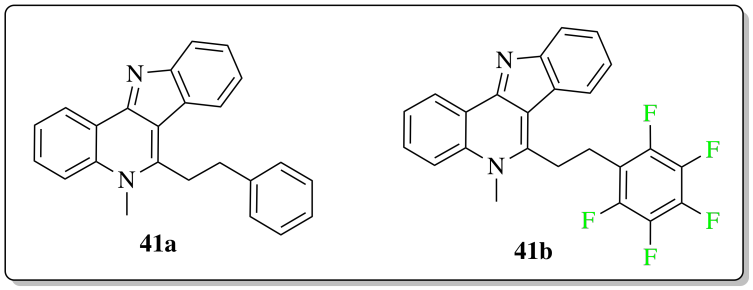

Figure 7: Suggested analogues for this project.

2 Results and discussion

2.1 Scale-up of Helgeland and Sydnes' method

The formation of 2-(quinolin-3-yl)aniline (**12**) follows a standard Suzuki-Miyaura cross-coupling mechanism (Figure 5), where 2-aminophenylboronic acid hydrochloride (**11**) is easily transformed into the more active borate using K_2CO_3 as the base. While using K_2CO_3, water has to be present in the reaction medium due to its poor solubility in any of the organic solvents commonly used in Suzuki-Miyaura cross couplings. Being a robust synthetic method, the scale-up of the coupling reaction in Helgeland and Sydnes' [3] method was thus expected to give excellent results. Indeed, coupling product **12** was synthesized in an 84% yield after two consequtive purifications by silica gel chromatography when starting from 5 grams of 3-bromoquinoline (**10**) (Scheme 6).

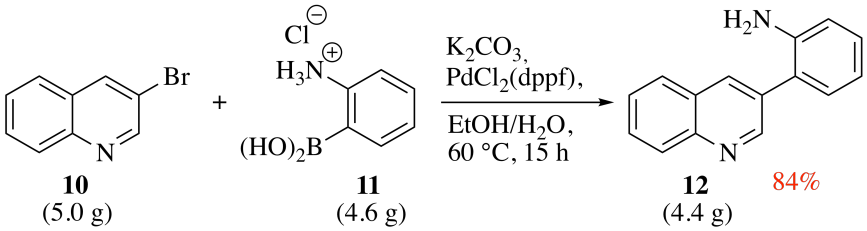

10 (5.0 g) + **11** (4.6 g) → **12** (4.4 g)

Scheme 6: Scale-up of Suzuki-Miyaura cross-coupling to form coupling product **12** in excellent yields.

Having prepared in excess of 4 grams of phenylquinoline **12**, the next step in the scale-up process was the MW-assisted ring closure of coupling product **12** to obtain 5*H*-indolo[3,2-*c*]quinoline (**13**) (Scheme 7). Surprisingly, the reaction was a failure, due to the MW terminating the experiment after detecting rapid pressure build-up within the reaction vessel.

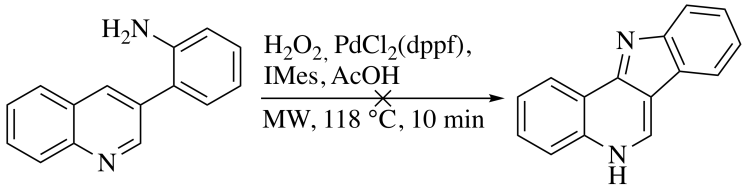

12 → **13**

Scheme 7: Failed scale-up of the MW-induced tandem C-H activation and C-N bond formation to yield the tetracyclic ring-system **13**.

After some literature work, it became apparant that the use of hydrogen peroxide is considered unconventional in MW-assisted experiments, though it may still be used under controlled conditions.[31] Hydrogen peroxide will naturally decompose under high temperatures, producing

oxygen gas and water,[32] followed by subsequent pressure build-up inside the closed vessel. The presence of Fe(II) in the palladium catalyst within the mixture accelerates the decomposition by becoming oxidized to Fe(III). Due to the added effect of an acidic environment, Fe(III) will then be reduced back to Fe(II), decomposing hydrogen peroxide into oxygen gas and water. The stoichiometric reactions describing the process can be expressed as follows:

$$Fe^{2+} + H_2O_2 + 2H^+ + e^- \rightarrow Fe^{3+} + 2H_2O$$
$$Fe^{3+} + 2H_2O_2 + e^- \rightarrow Fe^{2+} + O_2 + 2H_2O$$

In all likeliness, the small scale reaction to form indoloquinoline **13** starting from 70 milligrams of coupling product **12** as conducted by Helgeland and Sydnes[3] was successful because the scale was small enough for the reaction vessel to equalize the added pressure formed by the build-up of gas.

2.1.1 Modified Helgeland and Sydnes approach

Work by Bjørsvik and Elumalai[2] report the use of $Pd(OAc)_2$ as the catalyst of choice to achieve tandem C-H activation and C-N bond formation in order to obtain carbazoles. Wanting to compare the efficiency of the acetate and dppf-based catalysts and the possibility of using $Pd(OAc)_2$ for a large-scale reaction, ring closure of coupling product **12** using $Pd(OAc)_2$ was undertaken, providing indoloquinoline **13** in a 53% yield after two consecutive purifications by flash chromatography.

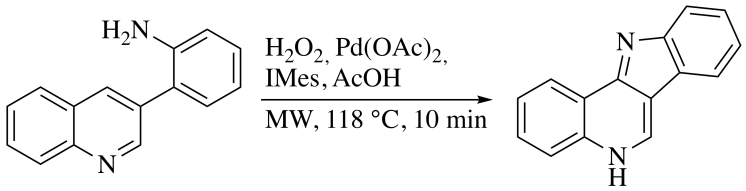

12 **13** 53%

Scheme 8: $Pd(OAc)_2$ catalyzed tandem C-H activation and C-N bond formation to obtain indoloquinoline **13**.

Using thin-layer chromatography (TLC) and low resolution mass spectrometry (LRMS) as aids in order to follow the ring closure reaction, the crude was revealed to still contain unreacted starting material. However, Bjørsvik and Elumalai[2] reported lower yields of the desired product and increased formation of undesired side products with increasing reaction times with $Pd(OAc)_2$ as the catalyst. Thus, prolonging the reaction time was not attempted.

Satisfied with a 53% yield of indoloquinoline **13** obtained with $Pd(OAc)_2$, a scale-up using 3 grams of 2-(quinolin-3-yl)aniline (**12**) was initiated. Again, the results were disappointing, providing the desired product in a modest 4% yield after purification. During the MW experiment, the reaction vessel was filled to approximately 50% capacity, which turned out to be a too high loading to accommodate the decomposition of hydrogen peroxide. The reaction was thus terminated after a run-time of roughly 2 minutes. Upon inspection of the crude mixture on TLC and LRMS, it was discovered that indoloquinoline **13** was already formed. The presence of side products in the reaction mixture caused the purification of the product to be unusually challenging, particularly removal of one byproduct overlapping with the desired product. A total of 7 purifications by conventional chromatography, DVFC and an automated flash chromatography system was necessary to obtain the pure fractions. Hoping that a smaller scale would solve these problems, a 500 milligram reaction was attempted to furnish indoloquinoline **13**. After three consecutive purifications no more than 12% was isolated. However, in addition to the product, the starting material was recovered in a 25% yield and the troublesome side product was isolated in a 3% yield (for identification of side product, see Section 2.1.2).

As this new attempt was yet again regarded as a failure to produce large quantities of compound **13**, a last effort was made by removing the hydrogen peroxide from the reaction mixture in its entirety and replace it with another reagent. It was decided to use pure oxygen gas, which was introduced into the mixture in a steady flow through a syringe. TLC of the crude after 10 minutes showed only trace amounts of product. More oxygen gas was introduced into the mixture before placing it for 10 more minutes in the MW. Sadly, TLC indicated no significant change in the amounts of the desired product **13**, hence the experiment was terminated. A full summary of the efforts towards a large-scale synthesis of indoloquinoline **13** is presented in Table 2.

Table 2: Efforts towards a large-scale synthesis of indoloquinoline **13** by a MW-assisted ring closure of phenylquinoline **12** with variable parameters.

Scale (mg **12**)	Catalyst	Oxygen source	Reaction time (min)	Isolated yield (%)
2470	$PdCl_2$(dppf)	H_2O_2	10	-[a]
70	$Pd(OAc)_2$	H_2O_2	10	53
3000	$Pd(OAc)_2$	H_2O_2	2	4
500	$Pd(OAc)_2$	H_2O_2	10	12[b]
100	$Pd(OAc)_2$	O_2	20	-[a]

[a]No product was isolated; [b]Unreacted starting material **12** was recovered in a 25% yield and additionally 3% side product was isolated.

Despite the failure to synthesize indoloquinoline **13** at large scales, the total synthesis of isocryptolepine (**4**) was nonetheless completed by subjecting compound **13** to *N*-methylation. Commonly used methylating agents include iodomethane and dimethyl sulfate,[3,17,19,33] where iodomethane was the more obvious choice due to its lower toxicity. The *N*-methylation observed in this reaction proceeds *via* an S_N2-type mechanism, where an alkyl halide reacts with a secondary amine to yield an alkylated quaternary ammonium salt as an intermediate. This type of methylation reaction is referred to as the Menshutkin reaction, in which the choice of solvent plays an important role.[34] It is thought that the use of aprotic solvents, such as acetonitrile, will enhance the rate of which the S_N2 reaction occurs, while protic solvents, such as water, will deter it. Of course, other factors naturally play a role, such as the nucleophilicity of the reactant towards the methylating agent.

By subjecting indoloquinoline **13** to a large excess of iodomethane in refluxing acetonitrile for 19 hours, the hydroiodide salt (**19**) of isocryptolepine (**4**) was obtained. The hydroiodo salt **19** was subjected to purification by dry vacuum flash chromatography (DVFC), which upon treatment with an aqueous solution of ammonia liberated isocryptolepine (**4**) as the free base in excellent yields (Scheme 9).

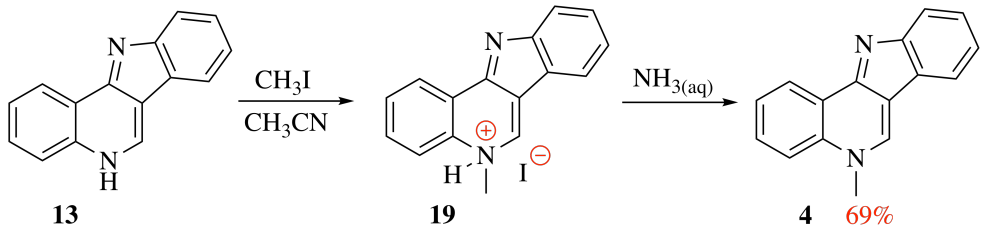

Scheme 9: Synthesis of isocryptolepine (**4**) from indoloquinoline **13** *via* the formation of a quaternary ammonium salt.

The choice was made to deviate from Helgeland and Sydnes' approach and use acetonitrile as the solvent in place of toluene. Whittell and coworkers[19] report the use of 100 equivalents when refluxing in acetonitrile, versus 200 equivalents in toluene, as reported by Helgeland and Sydnes.[3] Additionally, acetonitrile seemed to be better able to dissolve indoloquinoline **13** than toluene, however Helgeland and Sydnes report a yield of 76% in toluene, while the yield in acetonitrile was 69%. Nevertheless, no direct comparison can be made between the two, as the amount of iodomethane used together with toluene could possibly have affected the solubility of the indoloquinoline in the reaction mixture.

2.1.2 Side product(s) in the MW-assisted synthesis of indoloquinoline 13

In Bjørsvik and Elumalai's work,[2] they identified two side products associated with the ring closure of 2-aminobiphenyl (**20**) to yield carbazole (**21**); 2-nitrobiphenyl (**22**) and 2-acetamidobiphenyl (**23**) (Scheme 10). Owing to the low yields and multiple spots apparent on TLC of the crudes, it seemed natural to look for similar byproducts in our own MW-assisted reactions.

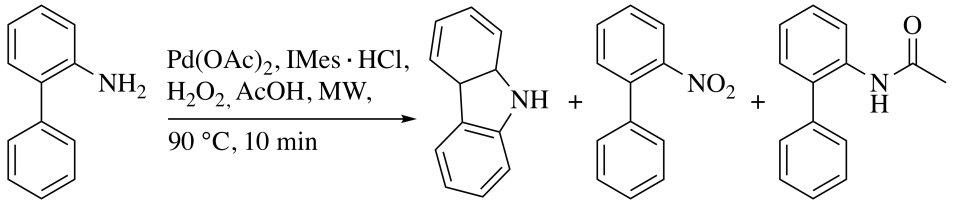

20 **21** (67%) **22** (2%) **23** (28%)

Scheme 10: Side products observed by Bjørsvik and Elumalai[2] during the ring closure of 2-aminobiphenyl (**20**) to furnish carbazole (**21**).

The formation of side products **22** and **23**, as well as the desired carbazole (**21**), in Bjørsvik and Elumalai's work[2] is supported by a proposed reaction mechanism (Scheme 11). Their proposed mechanism is based on prior work carried out by Buchwald and collaborators,[35,36] in which 2-acetamidobiphenyl (**23**) was subjected to C-H activation and subsequent C-N bond formation aided by a Pd(II) complex. The mechanism described by Bjørsvik and Elumalai[2] follows the same steps as outlined by Buchwald and collaborators,[35,36] where the catalytic cycle is initiated by the coordination of the palladium species to the amino moiety of biphenyl **20**. Subsequent *ortho*-palladation results in loss of aromaticity, followed by the release of acetic acid to form a six-membered palladacyclic intermediate to restore the aromatic system. Loss of a second unit of acetic acid and reductive elimination of palladium furnishes the carbazole scaffold (**21**) and simultaneously regenerates the palladium catalyst through oxidation.

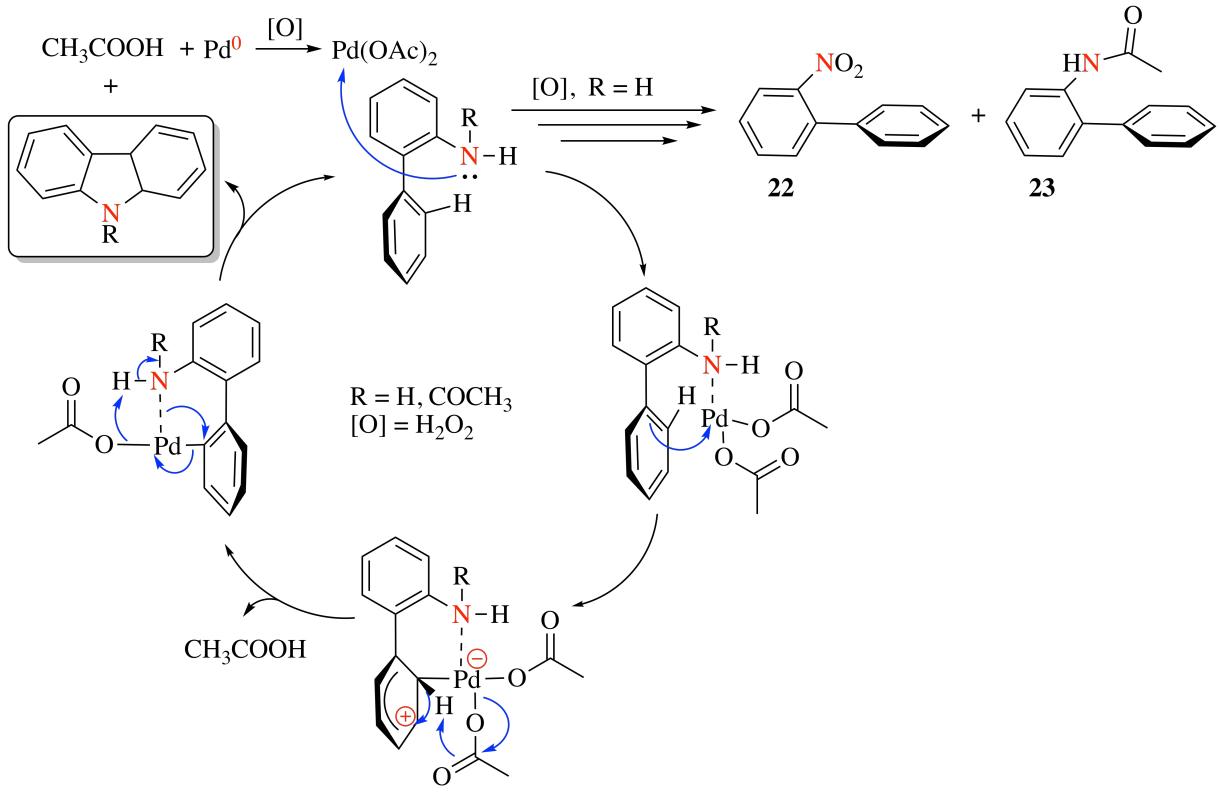

Scheme 11: Proposed mechanism by Bjørsvik and Elumalai[2] for the tandem C-H activation and C-N bond formation furnishing the carbazole scaffold (**21**) when 2-aminobiphenyl (**20**) is used as the substrate.

Bjørsvik and Elumalai's proposed mechanism[2] does not account for the formation of the two side products. However, the formation of 2-nitrobiphenyl (**22**) is thought to be a product of a parasite reaction occurring as a consequence of the highly oxidative conditions in the reaction vessel.[2] The presence of 2-acetamidobiphenyl (**23**) may not be explained by an oxidative process, hence other pathways must be considered. Acetamides are usually synthesized from acetic anhydride or acetyl chloride under various conditions.[37,38] Acetic acid is known to thermally decompose reversibly into acetic anhydride, ketene and water in the temperature range of 268-330 °C.[39] It is not unlikely that some degree of decomposition is observed at lower temperature intervals, providing a possible reaction pathway to the formation of the acetamide observed by Bjørsvik and Elumalai. The formation of 2-acetamidobiphenyl (**23**) may then begin with thermal decomposition of acetic acid into acetic anhydride. Nucleophilic attack from the lone pair electrons of the amine ensues, which upon intramolecular rearrangement furnishes a six-membered intermediate. Hydrogen transfer from the amine to the acid results in the loss of acetic acid, yielding the desired acetamide (Scheme 12).

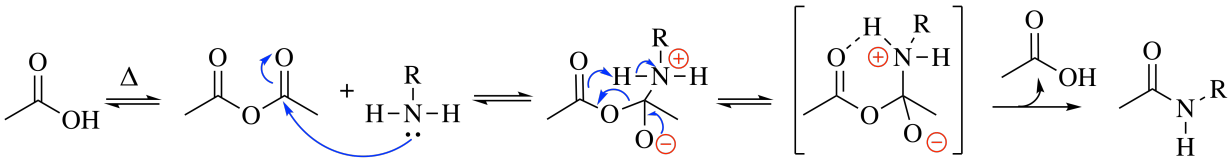

Scheme 12: Reaction between acetic anhydride and amines to produce the corresponding amides.

Furthermore, acetic acid by itself is reported to function as an acetylating agent in MW syntheses.[40,41] The exact mechanism by which the acetylation occurs is unknown, but it has been argued by some that it proceeds by nucleophilic attack of the amine onto the carbonyl of the acid.[41] In this case, the effect exhibited by the MW must somehow increase the electrophilicity of the acid to initiate nucleophilic attack, as acetic acid is significantly less electrophilic than its anhydride. Another possibility is that it alters the kinetics of the reaction, accelerating the rate determining step and leading to formation of the acetamide.[41]

Work by Charville's group[42] presented a density functional theory (DFT) supported mechanistic approach to explain the direct formation of amides from their corresponding amines through carboxylic acid dimers. Intermolecular hydrogen bonding fascilitates carboxylic acid dimerisation, creating a more reactive carboxylic acid species enabling nucleophilic attack from the amine. The attack occurs on the carbonyl moiety of one of the acids in the dimer, while the other carboxylic acid acts as a proton acceptor. The loss of a carboxylic acid and a concerted proton transfer from the amine to the acid creates an intermediate which readily releases water to generate the amide (Scheme 13).

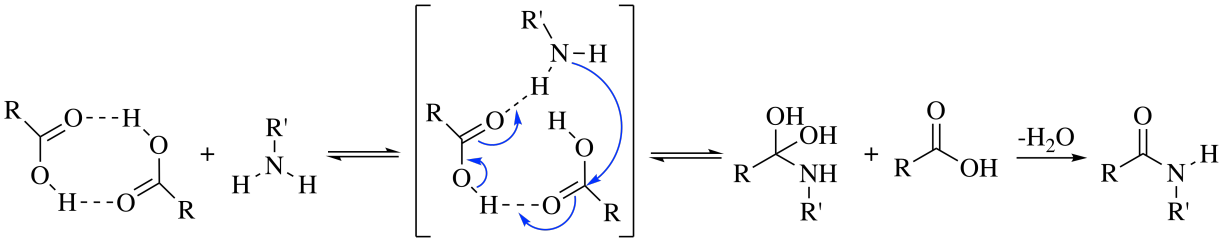

Scheme 13: DFT supported mechanism for the formation of amides through dimerisations of carboxylic acids as suggested by Charville *et al.*.[42]

Charville *et al.*'s findings[42] are supported by recent work by Sharley and Williams,[43] where amides are readily synthesized using acetic acid as a catalyst and ethyl acetate as the acetyl source. In combination, this makes for a realistic explanation for the *N*-acetylation observed by Bjørsvik and Elumalai.[2]

Incidentally, identification of the side product isolated in a 3% yield during the attempted scale-up of indoloquinoline **13** corresponds perfectly with the results reported by Bjørsvik and Elumalai.[2] *N*-Acetylation of coupling product **12** had transpired yielding *N*-(2-(quinolin-3-yl)phenyl)acetamide (**24**) (Scheme 14), corroborating their findings.

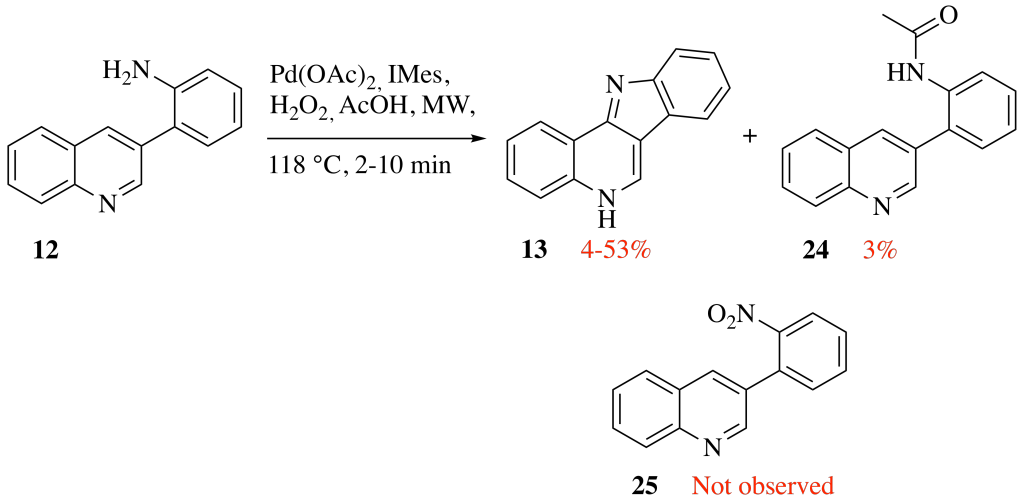

12 **13** 4-53% **24** 3%

25 Not observed

Scheme 14: *N*-Acetylation during MW-assisted ring closure of compound **12** to yield acetanilide **24** as a side product.

The first evidence that formation of acetanilide **24** had occurred was during LRMS analysis of the crude. A mass of 263.3 was observed (Figure 8), which corresponds well with the protonated mass of acetanilide **24** ([M + H^+] = 263.1).

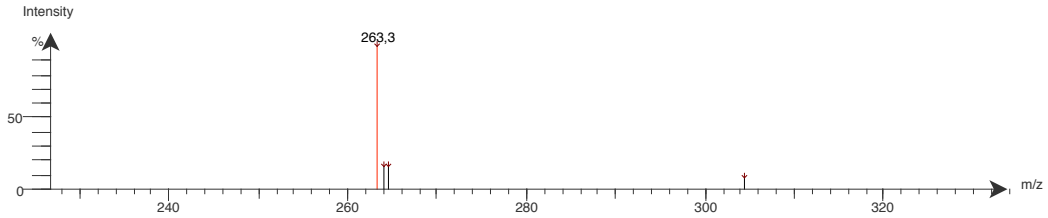

Figure 8: LRMS spectrum of acetanilide **24**.

By LRMS analysis, we also expected to identify a mass belongning to 3-(2-nitrophenyl)quinoline (**25**), but no such mass was observed. The solvent mixture used during the LRMS experiments is slightly acidic and easily protonates most of the studied *N*-heterocycles. It is possible that quinoline **25** was resistant to protonation and with the use of a different solvent the mass would appear. Moreover, Bjørsvik and Elumalai[2] report only small amounts of conversion into nitrobiphenyl **22**, indicating a less favorable transformation. As no other spots from TLC

of the crude was isolated than the main product **13** and acetanilide **24**, this was not explored further.

^{1}H-NMR of compound **24** shows a singlet at δ 2.00 ppm integrated to three protons, confirming the presence of a methyl group in the molecule (Figure 9). Examining the chemical shifts of methyl groups with similar chemical environments seem to support the claim that the methyl group is neighbouring an aromatic amide. The chemical shift is nearly identical to that of acetanilides **23** ($\Delta\delta = 0.01$)[44] and **26** ($\Delta\delta = 0.04$ ppm).[45] While the N-H signal of acetanilide **24** is visible on ^{1}H-NMR as a broad singlet, it is not for acetanilides **23** and **26**. There, it is reported as doublets, showing *ortho*-couplings ($J_{\mathbf{23}}$ = 8.1 Hz;[44] $J_{\mathbf{25}}$ = 8.4 Hz)[45] to the neighboring proton.

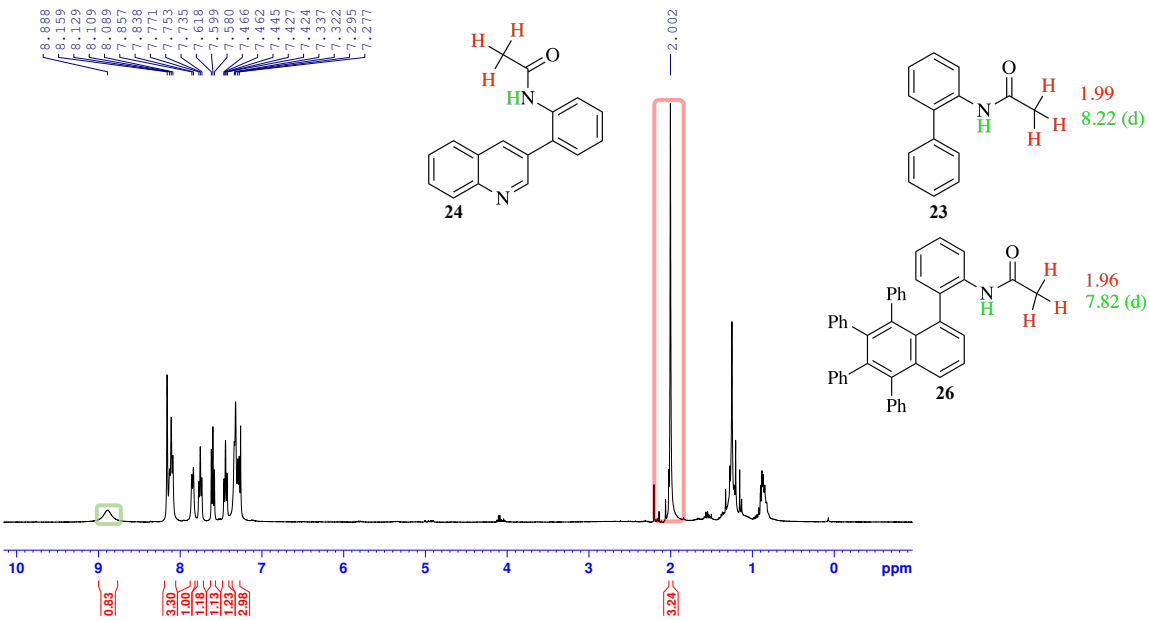

Figure 9: ^{1}H-NMR spectrum of acetanilide **24**.

By obtaining an infrared (IR) spectrum of compound **24**, the main functional groups in the molecule could be identified. The analysis was in agreement with the conclusions drawn from ^{1}H-NMR and LRMS and revealed a typical N-H stretch (ν 3233 cm^{-1}) and carbonyl stretch (ν 1662 cm^{-1}) at the expected wavenumbers (Figure 10).[44–46]

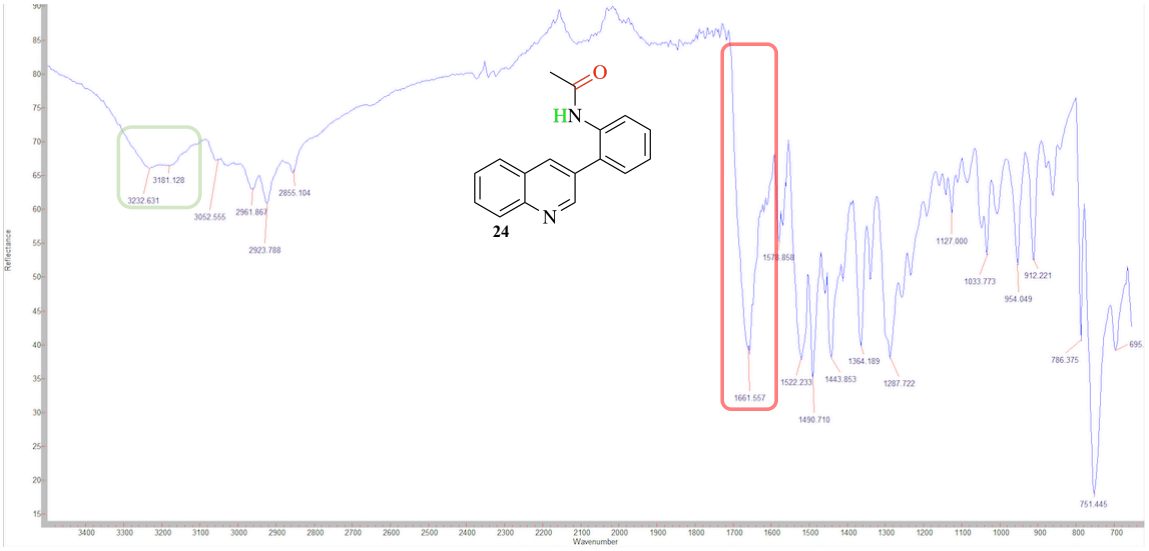

Figure 10: IR spectrum of acetanilide **24**.

Bjørsvik and Elumalai's work[2] rationalize the formation of the undersired acetanilide **24**, however, it fails to account for the low to modest yields of carbazole **13** in our case. The 25% recovery of starting material **12** using $Pd(OAc)_2$ indicates an unfavorable reaction, possibly due to a non-optimal catalyst. $PdCl_2$(dppf) is clearly superior as a catalyst at small scales, per the yields reported by Helgeland and Sydnes (published yield: 62%,[3] unpublished yield: 73%[60]). Determination of the optimal catalyst has long been revered as the goal of catalysis and predicting the success of a catalyst can be tricky.[47] Assuming the catalysis with $PdCl_2$(dppf) follows the same mechanism as outlined by Bjørsvik and Elumalai,[2] comparing the coordination of the two palladium species with the amino group of 2(quinolin-3-yl)aniline (**12**) (as outlined in Schemes 15a and b) might be helpful in understanding the diffence in yields. Unlike 2-aminobiphenyl (**20**), coupling product **12** might experience significant strain while coupled to palladium acetate due to the bulkiness of the acetate groups. Following the same logic, it seems likely that the palladium complex only experiences a weak coordination to the amine. As a result, the starting material is favored over the palladacyclic intermediate, leading to reduced formation of indoloquinoline **13**.

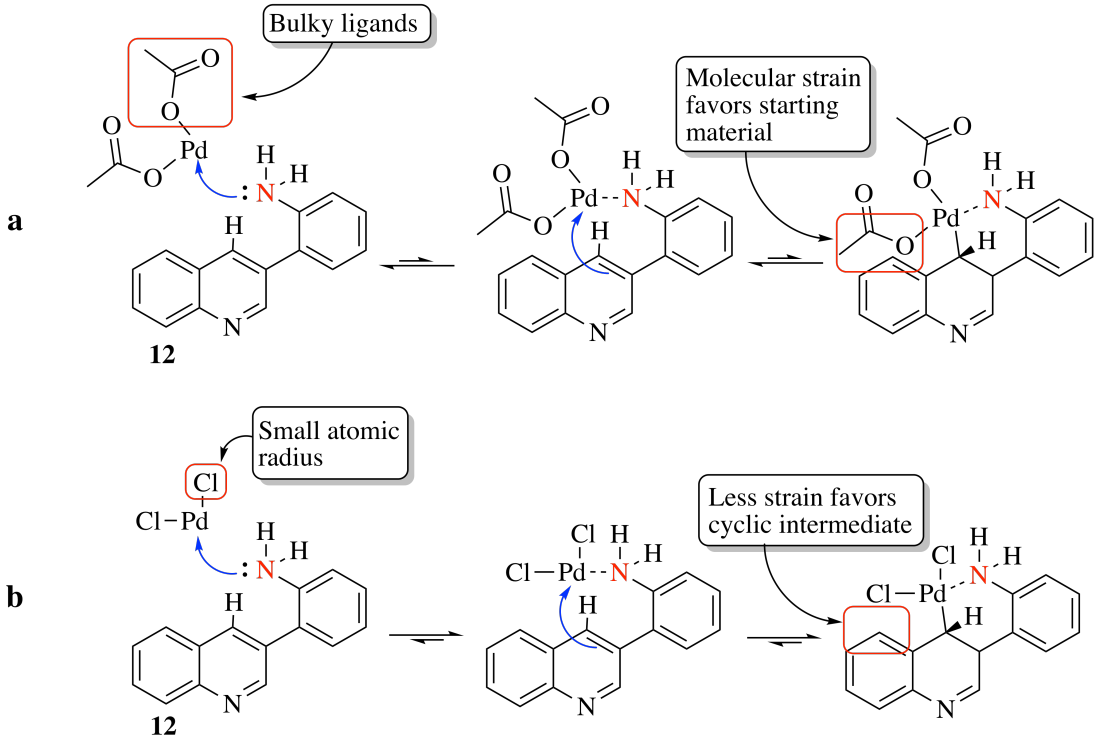

Scheme 15: Comparison of palladium acetate (**a**) and palladium chloride (**b**) as catalysts in the synthesis of indoloquinoline **13**.

With its fairly minimal atomic radius, chlorine proves to be a much better ligand for this particular system, allowing for the palladium complex to easily coordinate to the amine and initiate catalysis. Of course, there could be other factors involved in determining the success of the catalysts. The effects of solvents and temperature are known to be instrumental to successful catalysis.[47] Moreover, the exact nature of the IMes and dppf ligands in the reaction mechanism is also uncertain. However, Bjørsvik and Elumalai[2] reported favorable yields with IMes as a ligand.

2.2 Synthesis of isocryptolepine analogues

2.2.1 *N*-Oxidation of 3-bromoquinoline (10)

In order to activate C2 of 3-bromoquinoline (**10**) for subsequent alkenylation, *N*-oxidation to yield the corresponding *N*-oxide took place. The *N*-oxidation of heterocycles such as pyridines and quinolines can be fascilitated by the use of a peroxide, typically hydrogen peroxide or a peroxy acid, such as *m*-chloroperoxybenzoic acid (*m*CPBA). The employment of hydrogen peroxide is often associated with the use of an activating solvent, in order to increase the peroxide's electrophilicity towards the *N*-heterocycle. Acetic acid serves this purpose, as it readily protonates the peroxide and thereby activates it as an electrophile. Subsequent nucleophilic

attack from the *N*-heterocycle yields the desired *N*-oxide. In this thesis, hydrogen peroxide in acetic acid was chosen as the synthetic strategy. Unsurprisinlgy, 3-bromoquinoline-*N*-oxide (**19**) was furnished from 3-bromoquinoline (**10**) (Scheme 16) in good yields after purification, compared to previously reported literature.[48]

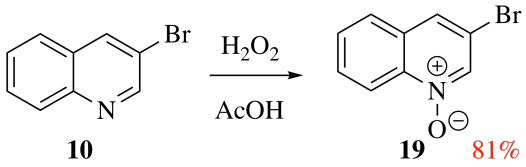

Scheme 16: Synthesis of 3-bromoquinoline-*N*-oxide (**19**).

2.2.2 Iodine-catalyzed alkenylation of *N*-oxide 19

Direct C-H activation can be regarded as the most straightforward method of achieving C-C bond formation in organic synthesis.[49–51] The most common strategy is transition metal-catalyzed activations under various conditions, however, recent work by Zhang *et al.*[30] has demonstrated iodine's potential as a catalyst. Their work describes the reaction of some styrenes with azaheterocycle *N*-oxides using iodine as the catalyst to yield the corresponding alkenylated azaheterocycles. Using the conditions described by Zhang *et al.*,[30] (*E*)-3-bromo-2-styrylquinoline (**27a**) and (*E*)-3-bromo-2-(2-(perfluorophenyl)vinyl)quinoline (**27b**) were synthesized from styrene and 2,3,4,5,6-pentafluorostyrene respectively, in modest to excellent yields following purification (**27a**: 61-89%, **27b**: 49-54%) (Scheme 17). Being described by Zhang's group[30] already, the spectroscopic and spectrometric data of compound **27a** will not be discussed in detail as it is in accordance with their findings.

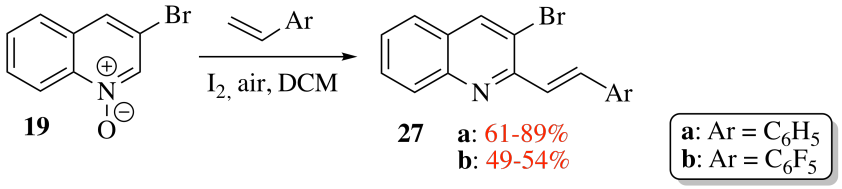

Scheme 17: Iodine-catalyzed alkenylation of *N*-oxide **19** with styrenes.

The successful formation of the pentafluorostyryl product **27b** was confirmed by ^{1}H-NMR, showing two doublets at δ 8.13 ppm (J = 16.0 Hz) and δ 7.97 ppm (J = 16.0 Hz), whose coupling constants indicate the presence of a *trans* alkene (Figure 11). The olefinic protons of **27b** experiences deshielding to a greater extent than those in **27a** ($\Delta\delta$ = 0.08, 0.26 ppm) and are shifted downfield as a consequence of the inductive effect from the fluorines.

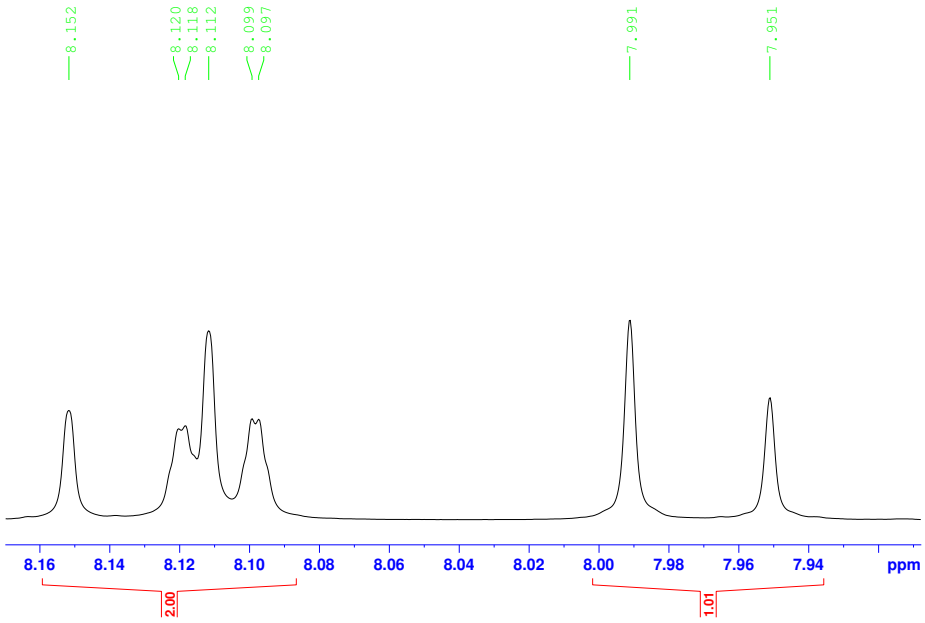

Figure 11: ^{1}H-NMR spectrum of the *trans* alkene present in compound **27b**.

It was difficult to find NMR data on similar compounds in the literature that could be used to corroborate the presence of a *trans* alkene in compound **27b**. Instead, an indirect comparison can be made by reviewing systems containing aromatic vinyls with and without the presence of fluorines. This might demonstrate the effect fluorines exhibit on the chemical shifts of olefinic protons. Using styrene and 2,3,4,5,6-pentafluorostyrene as examples, the effect of the different environments is apparent (Figure 12). Two of the protons of the pentafluorostyrene have been shifted downfield ($\Delta\delta$ = 0.34 ppm; $\Delta\delta$ = 0.21 ppm) while the proton adjacent to the benzene moiety has experienced a shift upfield ($\Delta\delta$ = 0.25 ppm) due to anisotropy from both the aromat and the alkene. Consequently, it does not seem unlikely that a shift downfield in the olefinic protons is to be expected for compounds containing pentafluorostyryls.

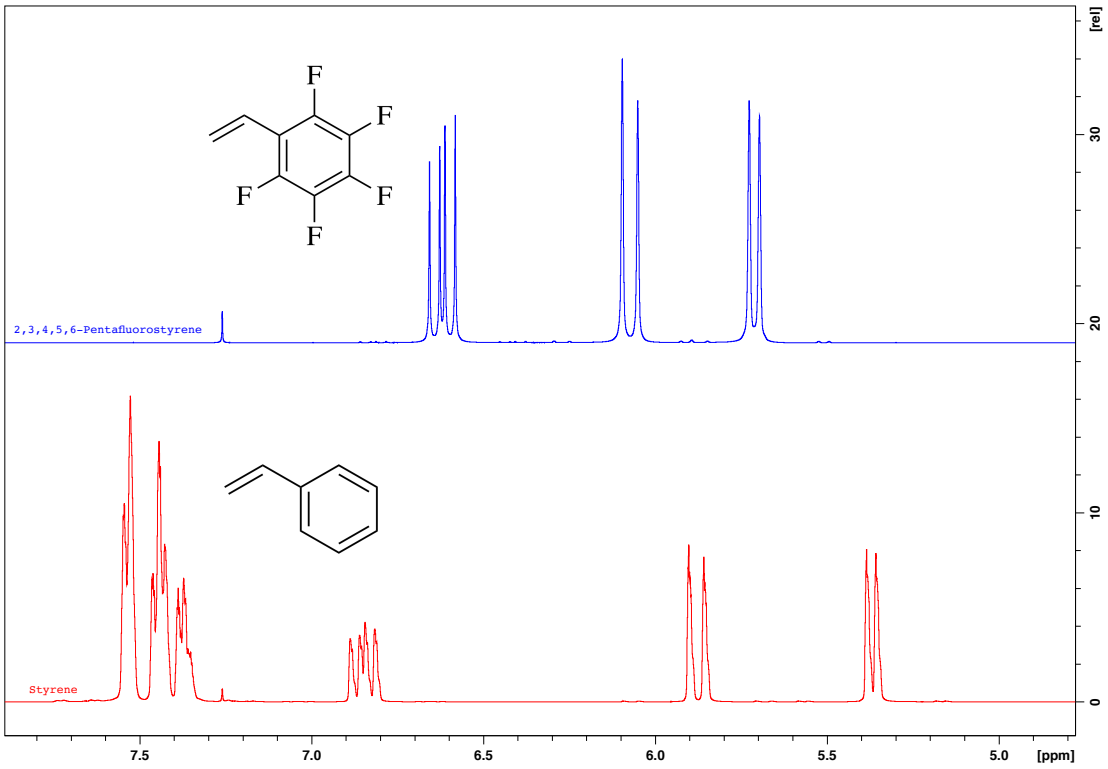

Figure 12: ^{1}H-NMR spectra comparing the shifts of styrene (red) with 2,3,4,5,6-pentafluorostyrene (blue).

Examining the difference in yields of compounds **27a** and **27b**, it appears that the fluorines impact the yield negatively. Incidentally, it was noted by Zhang *et al.* [30] that styrenes containing electron-donating groups (EDG) gave higher yields than those with electron-withdrawing groups (EWG), a trend which might be explained by their proposed reaction mechanism (Scheme 18). The key feature of the mechanism as outlined by Zhang's group [30] and supported by previous literature, [52–54] is the addition of iodine to the oxygen atom in the quinoline-*N*-oxide, creating a quaternary ammonium salt intermediate. Upon intramolecular rearrangement, styrene is added at C2 of quinoline through nucleophilic addition, leading to the formation of a positively charged phenethyl intermediate. Finally, rearrangement of the intermediate yields the alkenylated quinoline, HI and HIO, which upon a redox reaction releases water and regenerates the iodine catalyst.

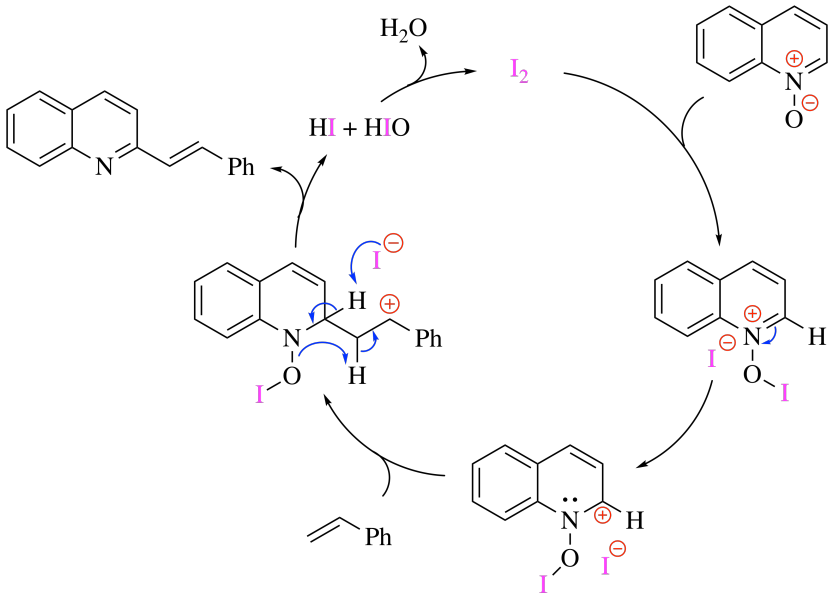

Scheme 18: Proposed mechanism for the direct C-H alkenylation of azaheterocycle *N*-oxides by Zhang *et al.*.[30]

Having examined the proposed mechanism by Zhang's group,[30] the lower yields with EWG can be explained by their destabilizing effect of the benzylic carbocation in the catalytic cycle. On the other hand, EDG have a stabilizing effect and favors product formation.

While the crude mixture of **27a** was fairly clean and contained only a few additional spots on TLC, it was a different matter with the fluoro analogue. The crude of compound **27b** contained 7 spots visible on TLC, where two spots were high in intensity. Analysis of the crude mixture on LRMS revealed that both of the high-intensity spots had a mass roughly matching that of the desired product (i.e. **27b**), hence both spots were isolated and analyzed by NMR. ^{1}H-NMR successfully identified the spot with the highest R_f value to be compound **27b**, while the other spot turned out to be much harder to identify with a high level of confidence through NMR alone. LRMS revealed that the side product contained a bromine molecule by displaying two peaks of identical intensity two mass units appart (Figure 13).

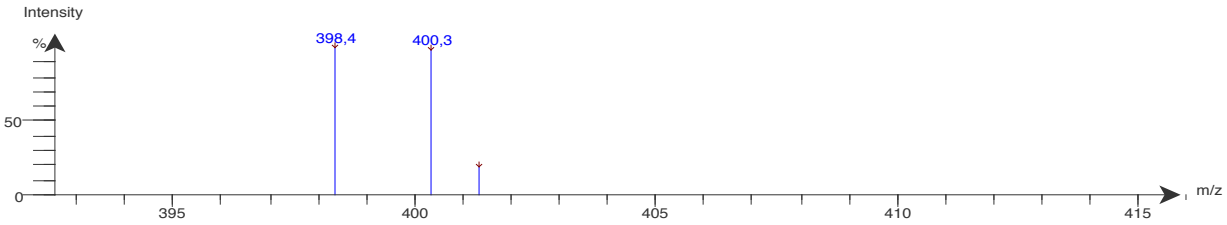

Figure 13: LRMS spectrum of side product isolated from the crude mixture of the reaction to yield compound **27b**.

These results were obtained using a solvent mixture containing acetonitrile, ammonium acetate, water and formic acid. However, using pure acetonitrile as the solvent resulted in a mass of 418, demonstrating that ESI is not adequate for determining the mass of this particular compound. Unable to get an accurate mass and a proton NMR which was hard to interpret, the compound was recrystallized using ethanol and sent to the University of Tromsø (UiT) for X-ray analysis. The crystal turned out to be difficult to analyze by X-ray, possibly due to its quality being subpar, hence no definite structure has been identified currently. Based on the preliminary X-ray results, the side product is tentatively suggested to be an iodoethyl quinoline, namely 3-bromo-2-(2-iodo-2-(perfluorophenyl)ethyl)quinoline (**28**) (Figure 14). Further crystallization experiments are ongoing and a new sample will be sent to UiT for further analysis when complete.

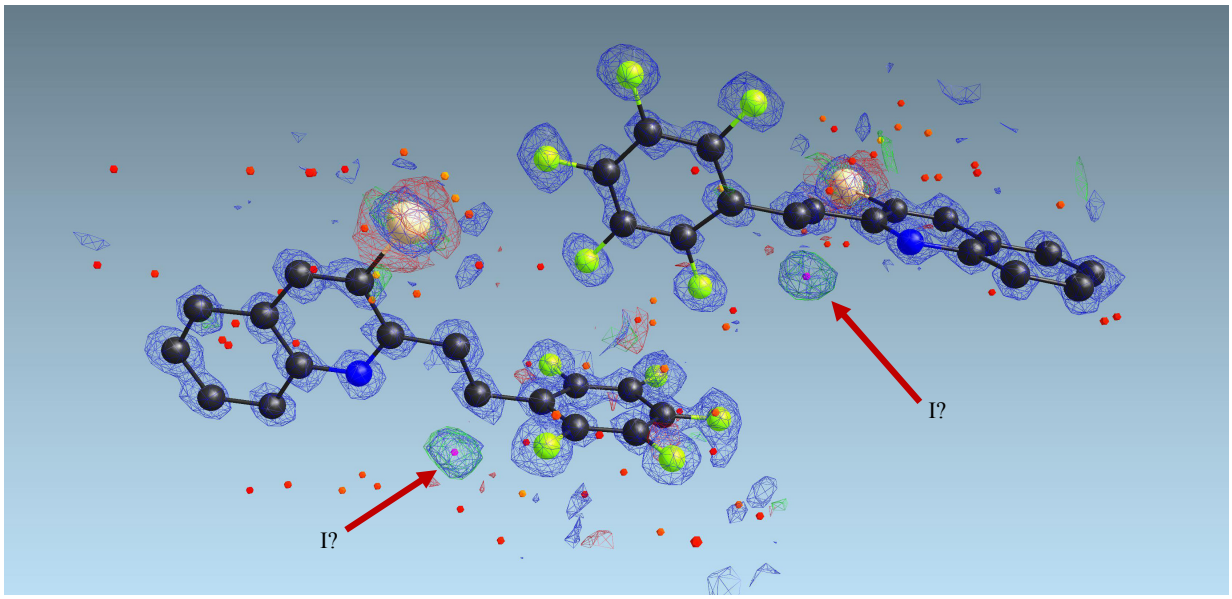

Figure 14: Preliminary X-ray results of compound **28**.

What can be said with some confidence based on the preliminary X-ray analysis is that the molecule contains a 3-bromoquinoline which is linked through two carbons to a pentafluorophenyl. The presence of five fluorines in the molecule is supported by ^{19}F-NMR (Figure 15).

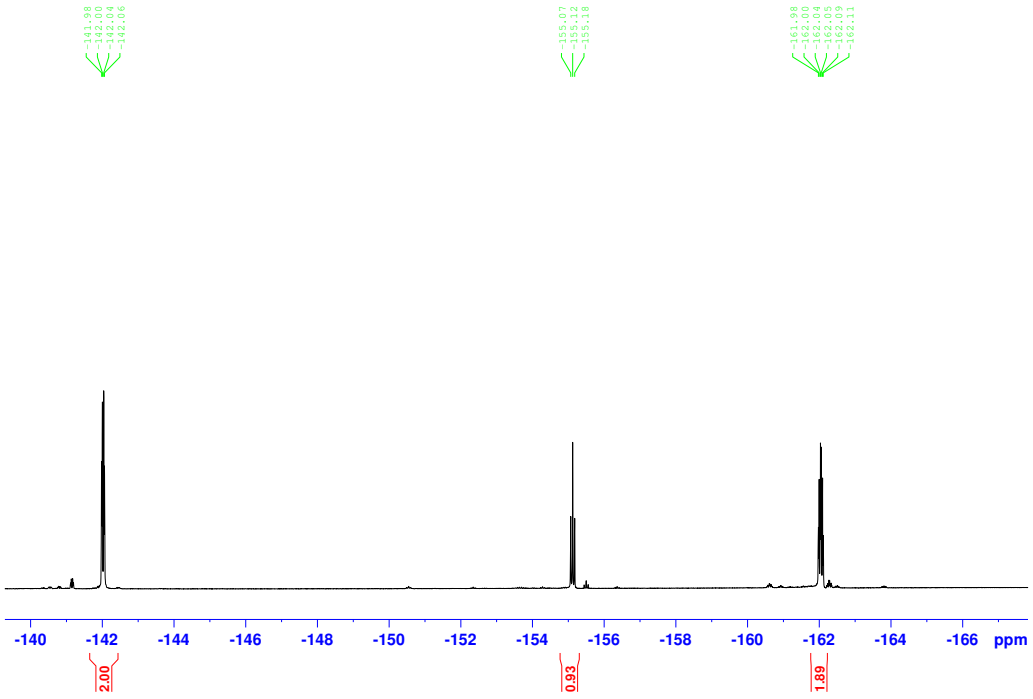

Figure 15: ^{19}F-NMR spectrum of compound **28**.

There appears to be a high electron density surrounding the carbon closest to the pentafluorophenyl, possibly representing an iodine atom. The linkage between the quinoline and benzene moieties would then be an alkane and not an alkene, as the splitting indicates. Using heteronuclear single quantum coherence spectroscopy (HSQC) and heteronuclear multiple-bond correlation spectroscopy (HMBC), the location of the three alkane protons were identified and are indicated on Figure 16.

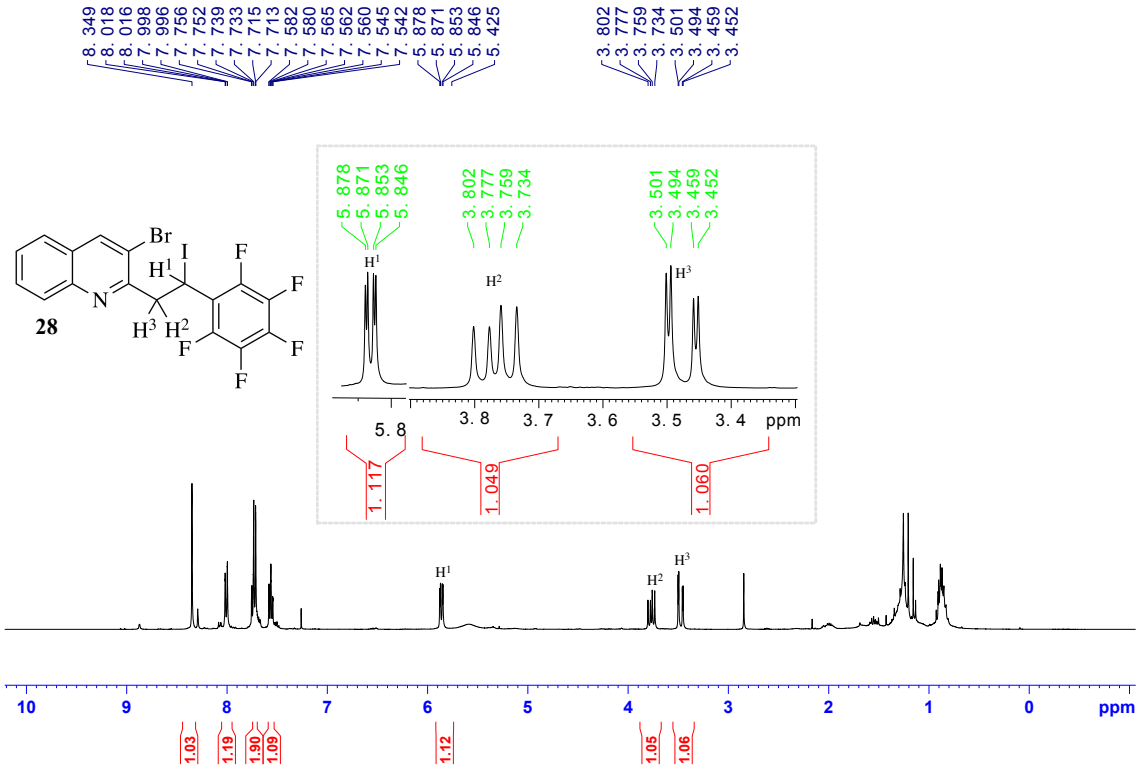

Figure 16: ^{1}H-NMR spectrum of compound **28**.

The protons behave as those of an alkene, displaying both geminal and vicinal couplings (δ 5.86 ppm, J = 9.7 Hz, 16.8 Hz; δ 3.77 ppm, J = 2.7 Hz, 9.9 Hz; δ 3.48 ppm, J = 2.7 Hz, 17.2 Hz), but the chemical shifts, in particular those of protons H^2 and H^3, are more akin to those of an alkane. Normally, alkanes will have free rotation about their bonds, resulting in different splittings than those observed, something which may not occur in this case due to electronic and steric effects. The massive size of the iodine and the presence of bulky halogenated aromats on either side of the alkane, could be sufficient to keep the bond locked in place and could possibly account for both the observed splitting pattern and the chemical shifts.

An argument can be made for the formation of iodoethyl **28** being the result of an iodation of the alkene in the main product (**27b**). Despite being less reactive than chlorine and bromine, the hydroiodation of alkenes is known in the literature.[55,56] After compound **27b** is furnished through the catalytic cycle, HI reacts with HIO to regenerate the iodine catalyst (Scheme 18). However, if the HI instead adds to the alkene in a typical hydrohalogen reaction, iodoethyl **28** is formed.

2.2.3 Suzuki-Miyaura cross-coupling of styrylquinolines 27

Under standard Suzuki-Miyaura cross-coupling conditions as described by Helgeland and Sydnes,[3] styrylquinolines **27** were coupled with boronic acid **11** to furnish the corresponding coupling products in good to excellent yields (**30a**: 67-78%, **30b**: 51%) (Scheme 19).

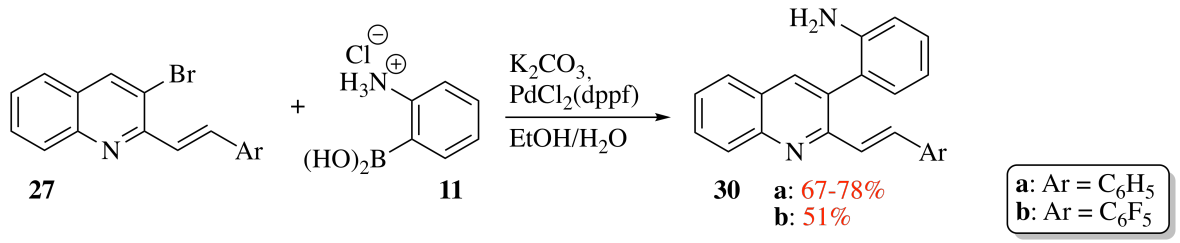

Scheme 19: Suzuki-Miyaura cross coupling of styrylquinolines **27** to yield coupling products **30**.

The successful formation of the coupling products could be identified through ^{1}H-NMR, showing the addition of four new aromatic protons (Figure 17). Coupling product **30b** also shows a broad singlet at δ 3.62 ppm, verifying the presence of a primary amine.

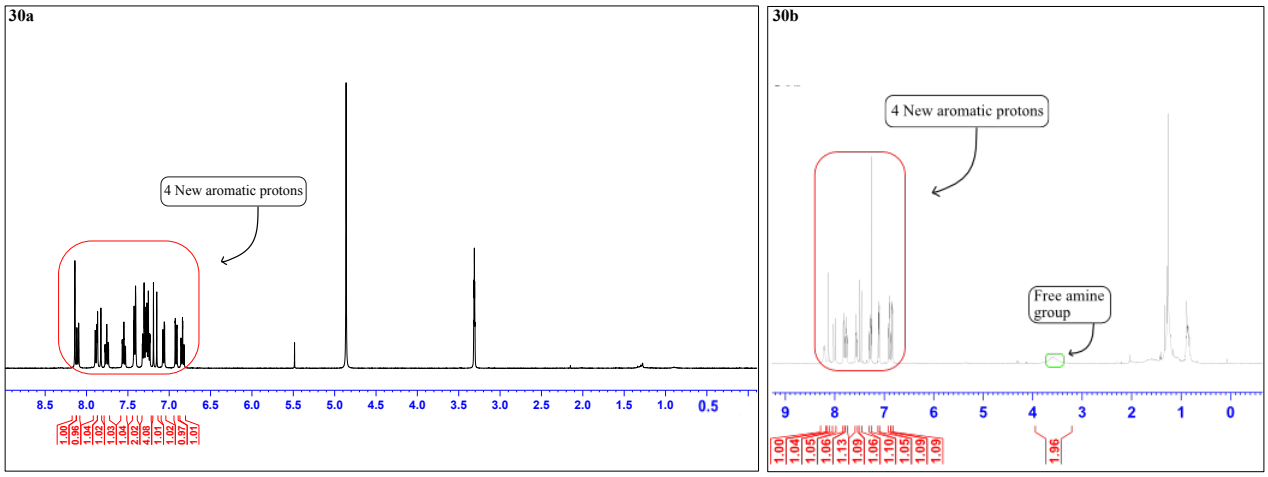

Figure 17: ^{1}H-NMR spectra of coupling products **30a** and **30b**.

The amino functionality of compound **30a** is however not visible on ^{1}H-NMR, presumably due to hydrogen-deuterium exchange with the deuterated methanol. Positive identification of compound **30a** as the desired coupling product thus had to be assisted by IR. The IR spectrum clearly showed two amine stretches (ν 3462 cm^{-1}, ν 3380cm $^{-1}$) at the expected wavenumbers (Figure 18), confirming that coupling product **30a** contains a primary amine. A closer inspection of the amine region shows a third peak at ν 3207 cm^{-1}, possibly representing an amine shoulder, a phenomenon commonly observed in the IR spectra of primary amines. This

is believed to occur as an overtone of the N-H bending band usually found at wavelenghts of roughly ν 1600 cm^{-1}.[57]

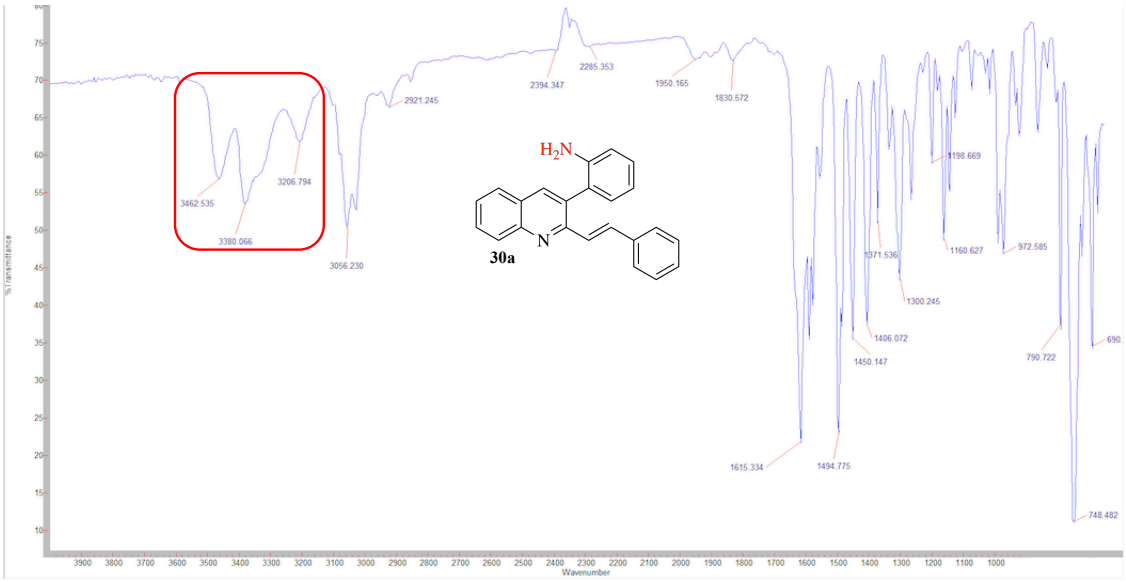

Figure 18: IR spectrum of coupling product **30a** showing the presence of a primary amine.

The difference in yields observed for the two coupling produts prompted us to try and synthesize coupling product **30b** using a different solvent mixture, as it was noted that the starting material (**27b**) was only slightly soluble in EtOH/H_2O. Pentafluorostyrl **27b** appears to be a highly non-polar compound and was only solvated by non-polar solvents, such as petroleum ether, but hardly soluble at all in any kind of polar solvent. It was thus decided to replace water for the less polar solvent tetrahydrofuran (THF) and hope that the difference in yields was due to a solubility problem. Unfortunately, analysis of the crude mixture on LRMS showed only trace amounts of coupling product **30b** and upon purification no product was isolated owing to the small amounts.

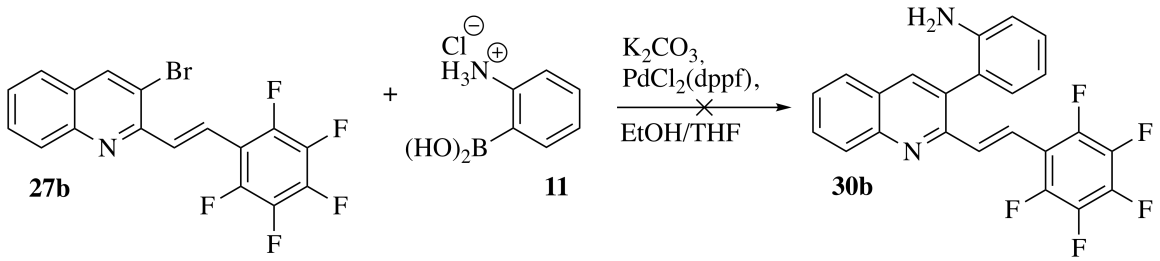

Scheme 20: Failed synthesis of coupling product **30b** using EtOH/THF as the solvent mixture.

TLC did however show one spot of high intensity, which was isolated by flash chromatography. The spot had a mass of 426.2 on LRMS, and still contained a bromine.

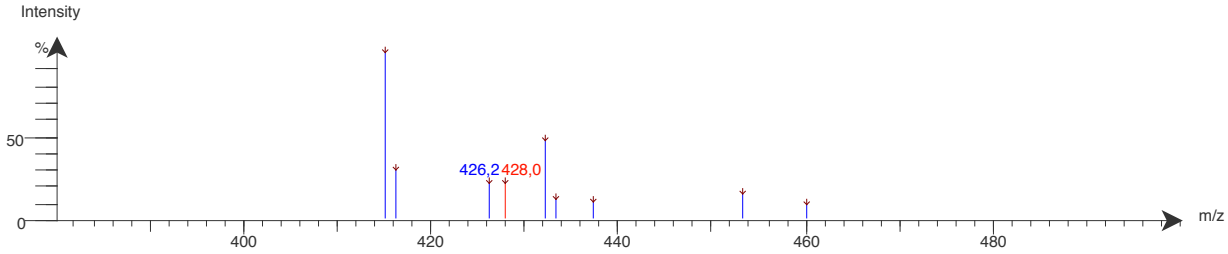

Figure 19: LRMS spectrum of the isolated compound during modified Suzuki-Miyaura cross-coupling conditions to synthesize coupling product **30b**.

Examination of ^{19}F-NMR, revealed that the compound had lost the fluorine *para* to the alkene (Figure 20).

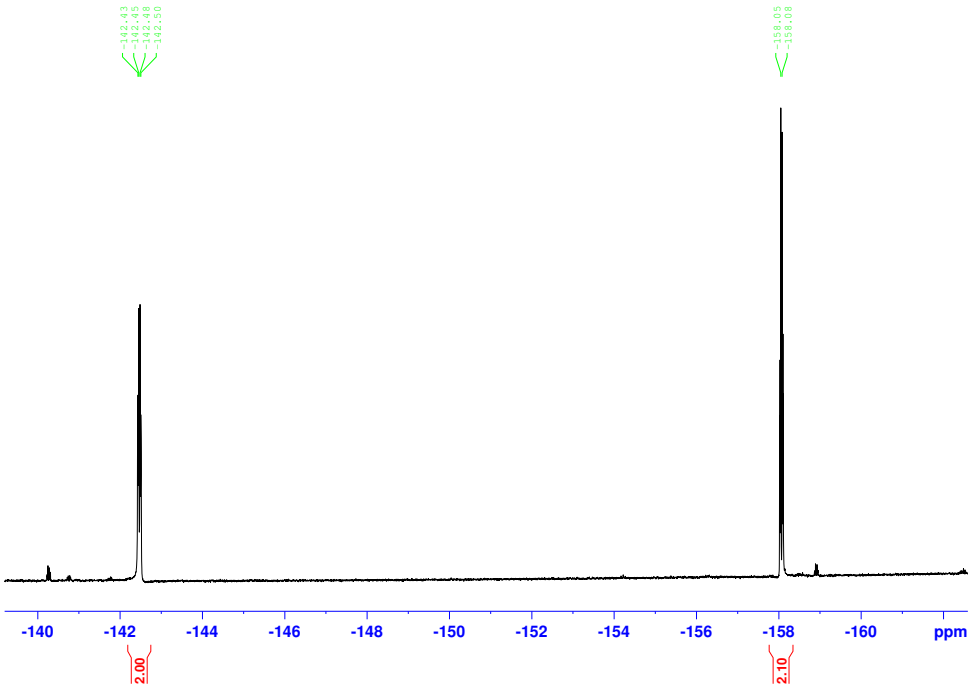

Figure 20: ^{19}F-NMR spectrum of compound **31**.

After discovery of an ethoxy group on ^{1}H-NMR (Figure 21), it became evident that the fluorine *para* to the alkene likely had been removed through nucleophilic aromatic substitution (S_NA) with the ethanol used as the solvent. S_NA reactions of pentafluorophenyls have been observed

previously for different systems, and it has been noted that the fluorine in the *para* position was especially prone to undergo substitution.[58,59]

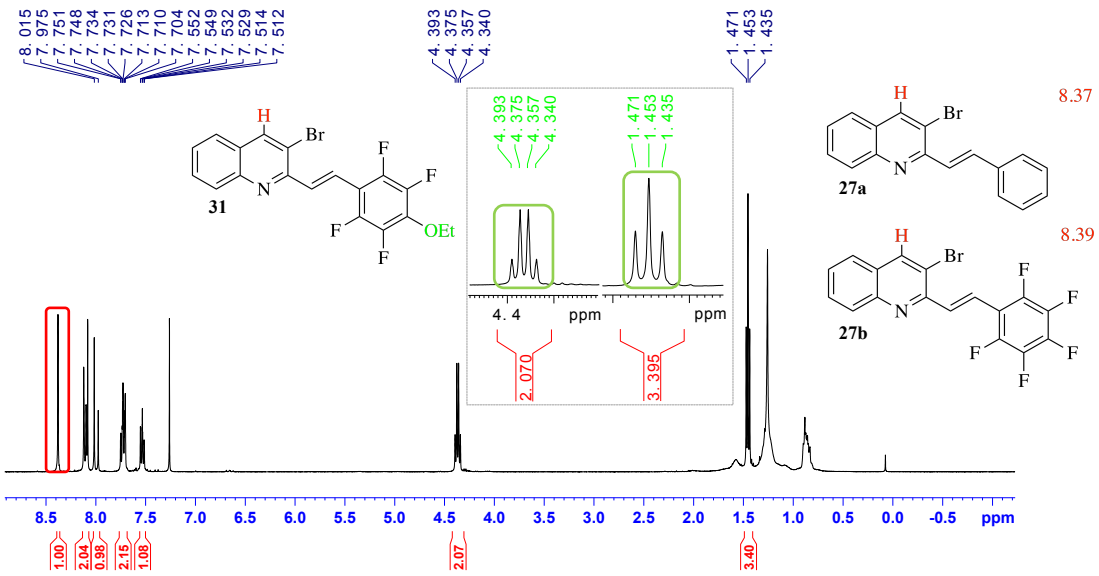

Figure 21: ^{1}H-NMR spectrum of compound **31**.

The chemical shift of the singlet in (*E*)-3-bromo-2-(4-ethoxy-2,3,5,6-tetrafluorostyryl)quinoline (**31**) corresponds well with those of compounds **27a** and **27b** ($\Delta\delta$ = 0.35, 0.37). The slight shift downfield observed in substitution product **31** is likely the result of the ethoxy group providing additional shielding through donation of its electrons. As this S_NA product was of little interest to this project, no more experimental data was gathered for compound **31**. Following the same reasoning, its synthesis is not described in the experimental section of the thesis.

2.2.4 Hydrogenation of the alkene moiety of coupling products 30

Previous work done by our group revealed that when subjecting coupling products such as compounds **30** to ring closure, the results would be undesirable ring closure at the alkene instead of on the quinoline.[60] To avoid such problems, it was decided to subject the alkenes to Pd/C catalyzed hydrogenations prior to attempting the MW-assisted ring closure.

Following a classical hydrogenation procedure, coupling products **30** were subjected to palladium-catalyzed hydrogenation to provide some interesting and unexpected results (Scheme 21). Coupling product **30a** was converted to 2-(2-phenetylquinolin-3-yl)aniline (**34a**) in near quan-

titative yields (91-96%). However, when compound **30b** was subjected to the same hydrogenation conditions, only trace amounts of 2-(2-(2-(perfluorophenyl)ethyl)quinolin-3-yl)aniline (**34b**) was detected on LRMS.

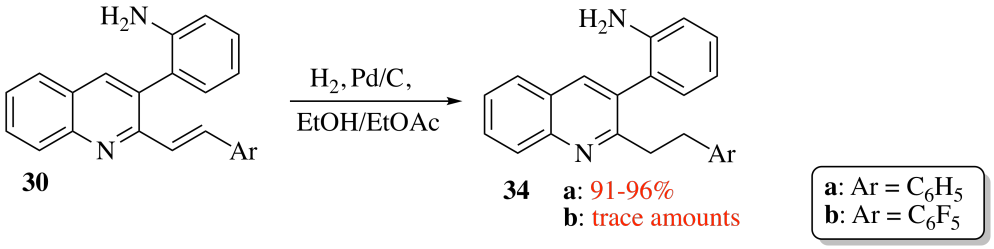

Scheme 21: Palladium-catalyzed hydrogenation of coupling products **30**.

These results prompted us to prolong the reaction time from 4 hours to 22 hours to examine if this could lead to the conversion of more starting material **30b** ($[M + H^+] = 413.2$) into product. LRMS was utilized to analyze the crude mixture after reaction times of 0.5, 1, 3 and 22 hours, respectively. Surprisingly, with increasing reaction time, the mass presumably belonging to the desired product **34b** ($[M + H^+] = 415.1$) disappeared entirely and the formation of several new masses was observed (441.3, 443.4, 447.3 and 501.4) (Figure 22). As this reaction was conducted using only 10 milligrams of starting material **30b**, no purification using chromatography was attempted. Nevertheless, the tentative identification of the compounds was attempted by turning to the literature, in an effort to understand why the reduction failed to yield the desired product **34b**.

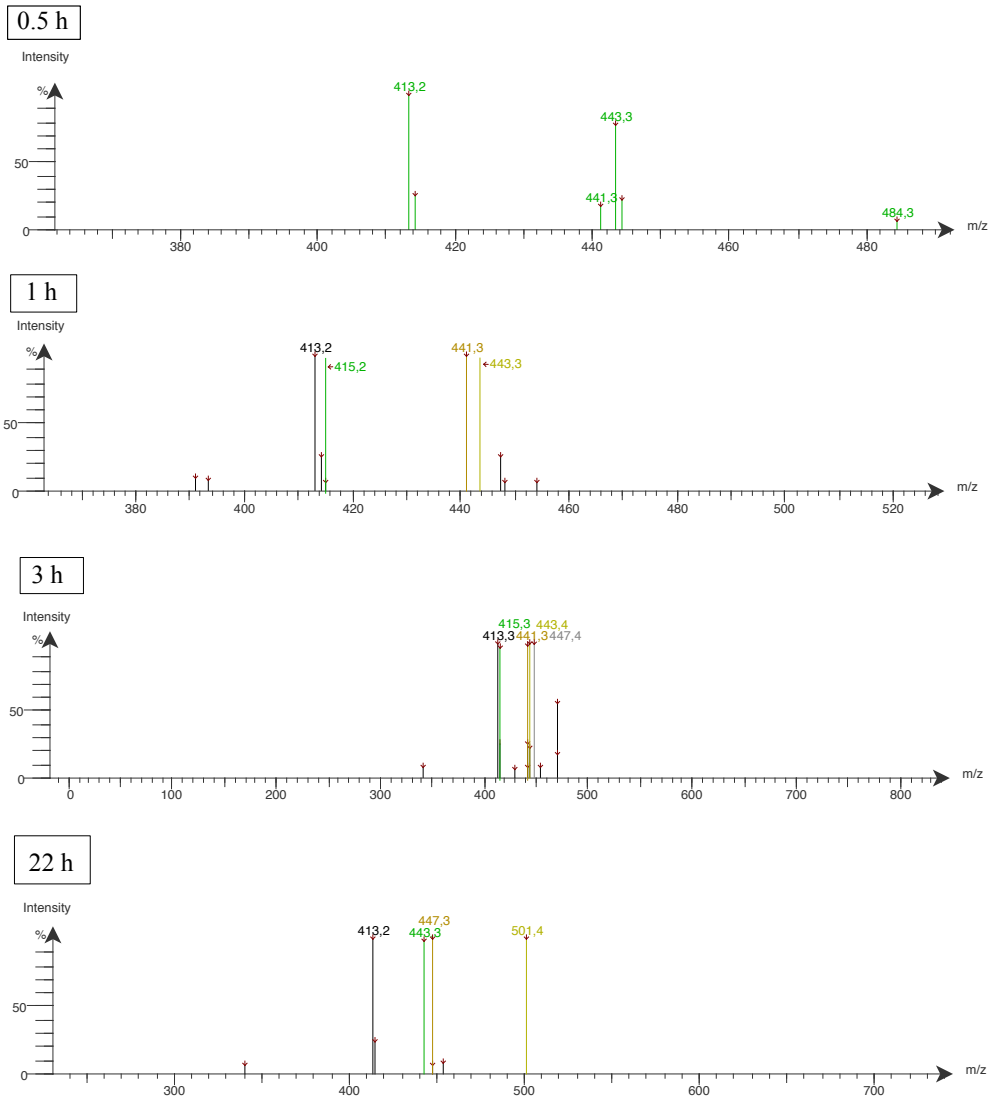

Figure 22: LRMS spectra of the crude mixture of the palladium-catalyzed hydrogenation to attempt the formation of compound **34b** at 0.5, 1, 3 and 22 hours.

During the conversion of nitro aryls to their primary amines, Sydnes and Isobe[61] discovered the formation of significant amounts of the corresponding secondary amines with prolonged reaction times. The secondary amine is thought to be the result of an alkylation reaction caused by the solvent being dehydrogenated by palladium to yield an acetaldehyde. Sydnes and Isobe[61] remarks that the ethanol used as the solvent likely is turned into acetaldehyde *via* an oxidative addition-type mechanism, in a manner similar to a proposal made by Sajiki *et al.* (Scheme 22).[62]

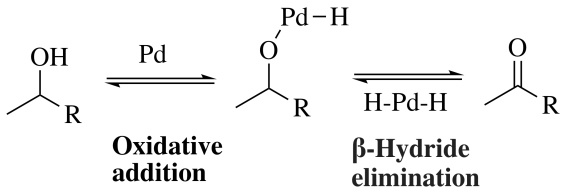

Scheme 22: Mechanistic proposal by Sajiki and coworkers[62] to account for the formation of ketones from their corresponding alcohols in the presence of Pd/C (10%).

Assuming a similar mechanism has occurred in our system, it could be possible that the two masses of 441.3 and 443.4, respectively are the results of an alkylation with and without the alkene being intact (Figure 23).

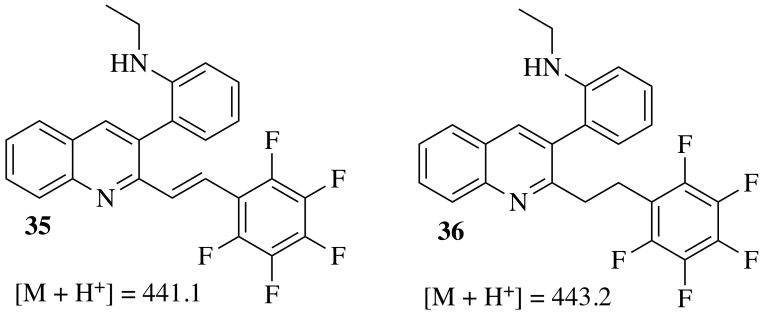

Figure 23: Possible structures which could account for the observed masses of 441.3 and 443.4 on LRMS.

The masses of 447.3 and 501.4 were harder to explain, but it is suggested that they are the result of a variety of reactions: alkylation of the free amine, reduction of the quinoline ring and an S_NA reaction (Figure 24).

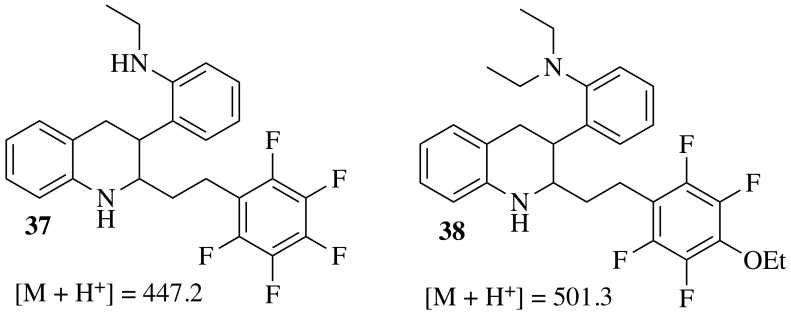

Figure 24: Possible structures belonging to the observed masses of 447.3 and 501.4 on LRMS.

Palladium is known to be capable of reducing quinolines but usually the conditions are harsh, requiring both high temperatures and applied pressures. However, even at room temperature palladium can be utilized to accomplish such hydrogenations, but most commonly it is assisted

by the presence of an acid.[63,64] It is possible that the prolonged reaction time was sufficient in our case to result in reduction of the quinoline moiety but without further experimentation this can not be said for certain.

The driving force of the reduction of alkenes *via* hydrogenation is the release of the energy stored in the π-bond. To understand the resistance displayed by the alkene in coupling product **30b** towards hydrogenation, it seemed natural to examine the mechanism of such reactions. As established in Section 1.4, the manner of which palladium-catalyzed reactions occur is not fully understood. Assuming the catalysis proceeds in a heterogeneous manner, the Horiuti-Polanyi mechanism is the most widely accepted (Figure 25).[65–67]

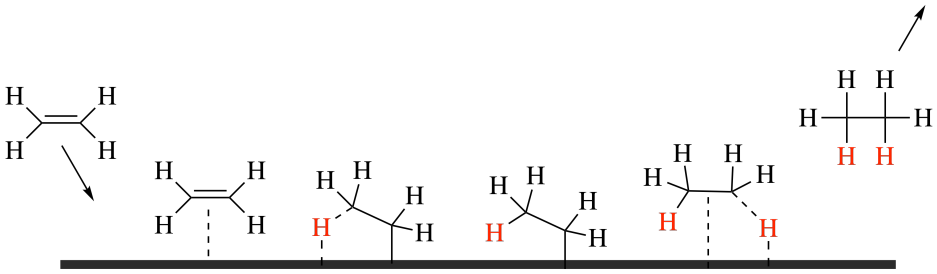

Figure 25: The Horiuti-Polanyi mechanism for the hydrogenation of alkenes.[66]

The catalysis is initiated by the alkene donating its π-electrons and binding to the palladium surface. Then, a σ-bond may be formed between the alkene and palladium and a proton chemisorbed onto the catalyst surface. The alkyl intermediate is subsequently formed into an alkane in a second half-hydrogenation step and moves away from the catalytic site. For the formation of the alkane to be successful, the alkenes affinity towards the catalyst can neither be too weak nor too strong.[65] Hence, it could be a possibility that coupling product **30b** is resistant to hydrogenation due to a low interaction with the catalytical site of palladium.

It has been known for some time that the introduction of R groups on an alkene leads to increased electrophilicity and thermodynamic stability.[68] Breaking a stable π-bond will consequently free less energy than breaking an unstable bond, making for a less favorable conversion. Additionally, alkenes with electron-accepting R groups will dissociate their electrons, resulting in fewer electrons available for formation of a σ-bond to the catalytic surface as seen in the Horiuti-Polanyi mechanism. With pentafluorophenyl as an R group, it seems plausible that the alkene in coupling product **30b** is too electron deficient to attach to the catalytical site and initiate catalysis.

Capable of reducing a wider selection of functional groups than palladium, including alkenes, aldehydes, ketones, nitriles, nitro compounds and more,[69] Raney-Nickel was chosen as the catalyst to attempt reduction of coupling product **30b**. Upon treatment with catalytical amounts of Raney-Nickel under hydrogen atmosphere, compound **34b** was obtained in excellent yields following purification (76%) (Scheme 23).

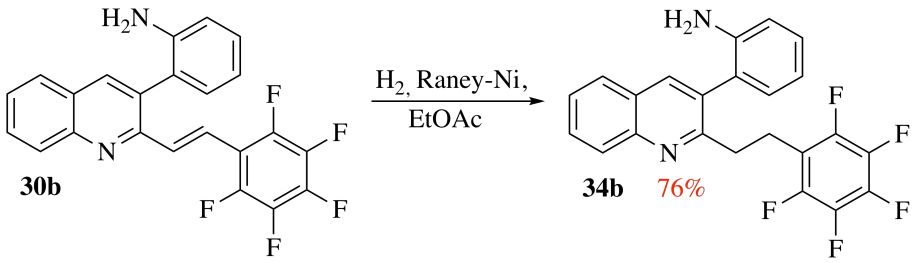

Scheme 23: Successful formation of compound **34b** using Raney-Nickel as the catalyst.

To confirm that the hydrogenations had indeed occurred, ^{1}H-NMR was used to look for the absence of the alkene signals of coupling products **30** and the appearance of new signals belonging to alkanes. Indeed, the signals corresponding to the *trans* alkenes of the coupling products (**30a**: δ 7.74 ppm, J = 15.9 Hz; δ 7.06, J = 15.9 Hz. **30b**: δ = 7.99 ppm, J = 16.1 Hz; δ 7.48 ppm, J = 16.1 Hz) was not observed (Figure 26).

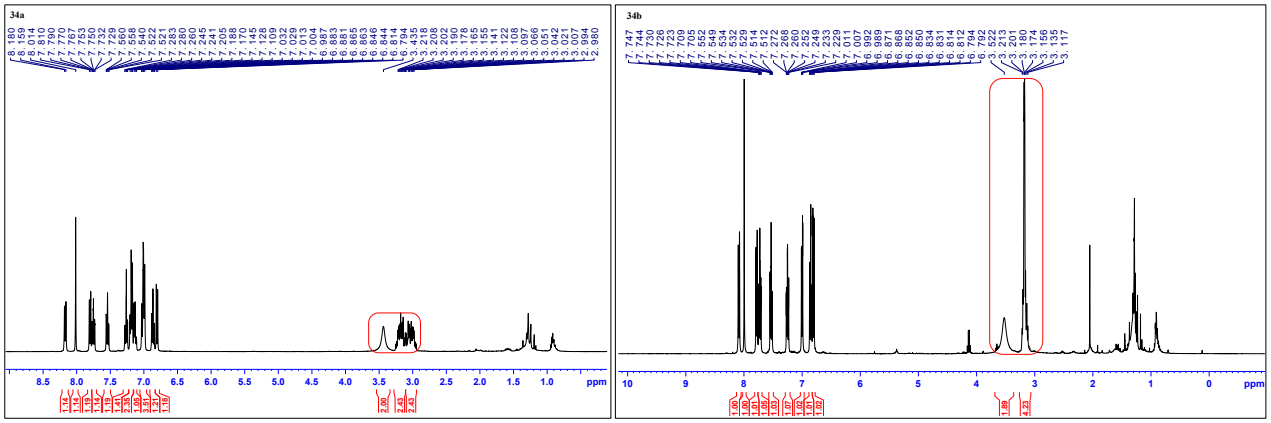

Figure 26: ^{1}H-NMR spectra of hydrogenation products **34**.

More over, signals corresponding well with alkane protons were observed in both compounds (**30a**: δ 3.25-3.10 ppm, δ 3.09-2.95 ppm; **30b**: δ 3.17-3.15 ppm). Reasuringly, there seems to be no evidence of any alkenylation of the free amine, as ^{1}H-NMR still shows the presence of a broad singlet. Additionally, analysis by ^{1}H-NMR would readily reveal any alkyl protons, if present.

2.2.5 Tandem C-H activation and C-N bond formation of hydrogenation products 34

Utilizing the conditions reported by Helgeland and Sydnes,[3] 6-phenethyl-5*H*-indolo[3,2-*c*]quinoline (**39a**) was furnished in excellent yields (87%). Despite performing well with compound **39a**, the unexpected challenges with the MW-assisted experiment containing $PdCl_2$(dppf) and hydrogen peroxide, prompted us to use the conditions reported by Bjørsvik and Elumalai[2] to synthesize the fluoro analogue. Upon purification, 6-(2-(perfluorophenyl)ethyl)-5*H*-indolo[3,2-*c*]quinoline (**39b**) was provided in modest yields (32-37%) (Scheme 24).

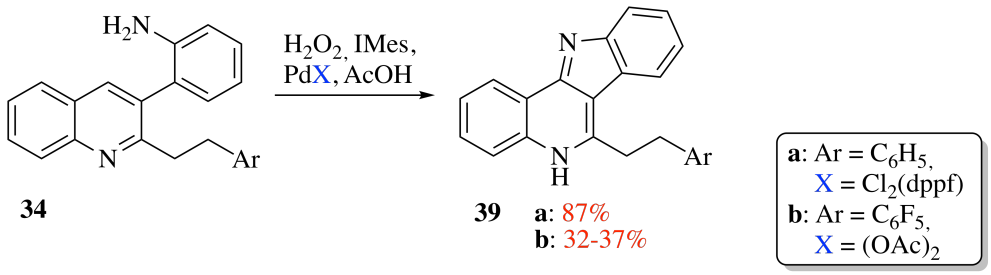

Scheme 24: MW assisted ring closure of **34** to yield indoloquinolines **39**.

This coincides well with the results obtained for the synthesis of 5*H*-indolo[3,2-*c*]quinoline (**13**) using the two different catalysts. The reasoning employed in Section 2.1.2 may also be applicable for this system, where the palladium acetate forms an unfavorable cyclic intermediate due to molecular strain, favoring the starting material over the cyclized product. Preferably, the two catalysts should be employed for ring closures of both compounds **34a** and **34b** for a more accurate comparison, but time constraints prevented us from realizing this.

Similarly to the $Pd(OAc)_2$ catalyzed reaction to form indoloquinoline **13**, unreacted starting material was observed in the crude mixture of indoloquinoline **39b**. A mass most likely representing the *N*-acetylation of the starting material as seen by Bjørsvik and Elumalai[2] and later by us, was also observed using LRMS (Figure 27).

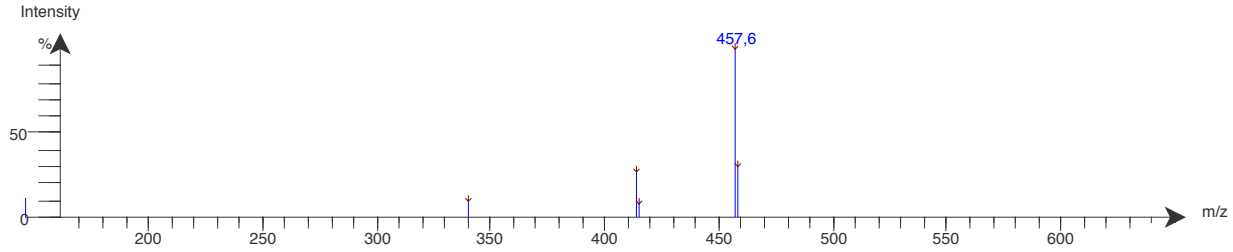

Figure 27: LRMS spectrum possibly representing *N*-acetylation of compound **34b**.

Due to difficult separations during purification, the compound believed to be *N*-(2-(2-(2-(perfluorophenyl)ethyl)quinolin-3-yl)phenyl)acetamide (**40**) (Figure 28) was not successfully isolated. To determine its presence confidently, analysis by NMR would be necessary.

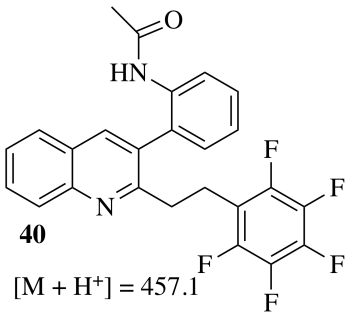

Figure 28: Structure of acetanilide **40**, a possible side product of the ring closure of compound **34b** assisted by palladium acetate.

Comparing the ^{1}H-NMR spectra of compounds **34a** and **39a** provided evidence for the successful ring closure of compound **34a**. As seen on Figure 29, the singlet at δ 8.01 ppm is not present after subjecting compound **34a** to tandem C-H activation and C-N bond formation.

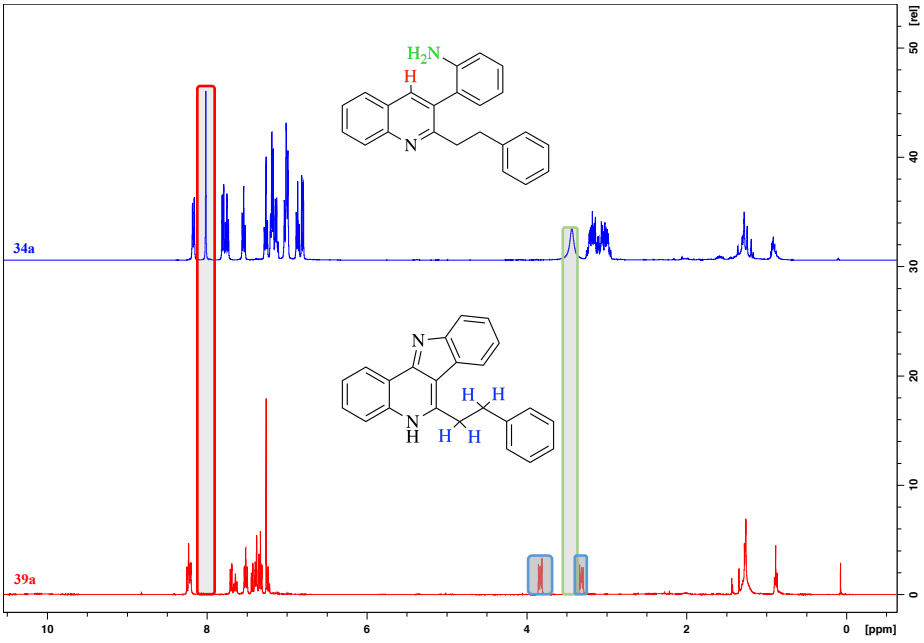

Figure 29: ^{1}H-NMR spectra of compounds **34a** and **39a**.

The additional absence of the broad singlet at δ 3.43 ppm supports the transformation into indoloquinoline **39a**. It can also be noted that the alkane protons have been shifted downfield

after the cyclization of compound **34a**, possibly due to increased anisotropy exhibited by the indoloquinoline.

2.2.6 *N*-Methylation of indoloquinolines 39

To conclude our synthetic pathway towards novel isocryptolepine (**4**) analogues, *N*-methylation of indoloquinolines **39** using the conditions described by Whittell and coworkers,[19] furnished 5-methyl-6-phenethyl-5*H*-indolo[3,2-*c*]quinoline (**41a**) and 5-methyl-6-(2-(perfluorophenyl)ethyl)-5*H*-indolo[3,2-*c*]quinoline (**41b**) in good to excellent yields upon purification (**41a**: 95%, **41b**: 66%) (Scheme 25).

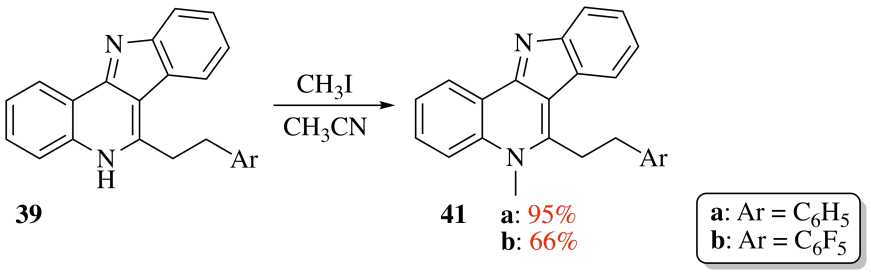

Scheme 25: *N*-Methylation of indoloquinolines **39** to yield isocryptolepine analogues **41**.

Despite being a low concentration sample, the ^{1}H-NMR spectrum of isocryptolepine analogue **41a** clearly shows the presence of a methyl group in the compound (Figure 30).

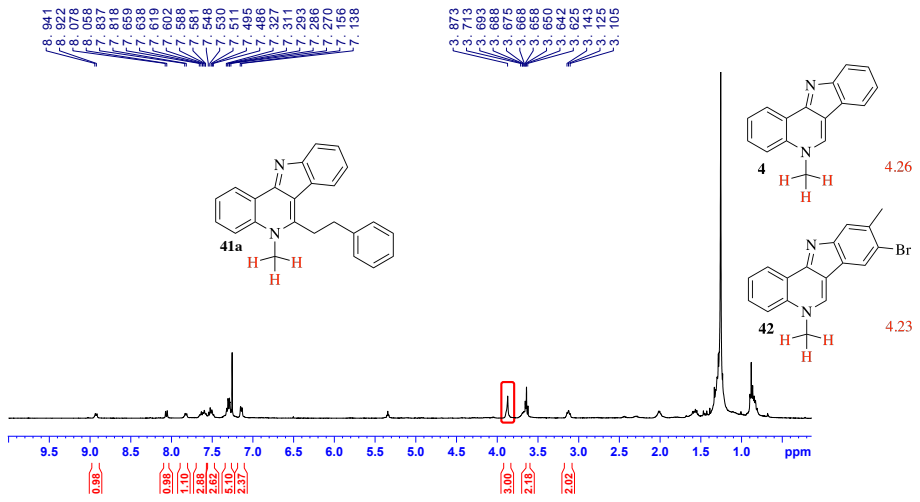

Figure 30: ^{1}H-NMR spectrum of isocryptolepine analogue **41a**.

The signal matches that of the natural product **4** ($\Delta\delta$ = 0.39)[3] and an 8-bromo-9-methyl analogue (**42**) ($\Delta\delta$ = 0.36)[19] to a satisfactory degree, indicating the methylation of the quinoline

was successful. There exists the possibility of methylation also occurring on the indole moiety in this reaction, forming a di-methylated product. However, this seems unlikely, as the nitrogen in quinoline is much more nucleophilic than the indole nitrogen. With the assistance of HSQC and HMBC, the methyl group was indeed confirmed to be located on the quinoline scaffold.

2.3 Concluding remarks

2.3.1 Synthesis of isocryptolepine (4)

Isocryptolepine (**4**) was successfully synthesized in four steps starting from 3-bromoquinoline (**10**). The synthesis was carried out using $Pd(OAc)_2$ as the catalyst, where $PdCl_2$(dppf) is reported to provide superior results at small scales.[3] Efforts towards a gram-scale synthesis of the natural product **4** was unsuccessful with both types of palladium. $PdCl_2$(dppf) turned out to be unsuitable for large-scale MW syntheses, while $Pd(OAc)_2$ yielded low conversions of the starting material **12** into indoloquinoline **13**, possibly due to steric effects of the bulky acetate ligands.

2.3.2 Synthesis of novel C6-alkylated isocryptolepine analogues

Over six steps, two novel isocryptolepine analogues (**41**) were synthesized starting from 3-bromoquinoline (**10**). The synthetic pathway was initiated by carrying out *N*-oxidation of 3-bromoquinoline (**10**) to furnish 3-bromoquinoline-*N*-oxide (**19**) in excellent yields following purification (81%). Having activated C2 of the quinoline scaffold, iodine-catalyzed direct C-H alkenylation was conducted using styrene and 2,3,4,5,6-pentafluorostyrene to yield the alkenylation products **27** in good to excellent yields after purification (**27a**: 61-89%, **27b**: 49-54%). During the formation of compound **27b**, a side product was formed in 24% yield. The compound was difficult to identify by ^{1}H NMR and was sent to UiT for X-ray analysis. Based on the preliminary results, the compound is tentatively identified as 3-bromo-2-(2-iodo-2-(perfluorophenyl)ethyl)quinoline (**28**).

Alkenylation products **27** were subjected to Suzuki-Miyaura cross coupling under the conditions reported by Helgeland and Sydnes[3] to yield coupling products **30** in good to excellent yields following purification (**30a**: 67-78%, **30b**: 51%). Due to worries that the low yield of coupling product **30b** was related to its poor solubility in EtOH/H_2O, the coupling was attempted using EtOH/THF. The results of the changed conditions was an S_NA reaction of the fluorine in the *para* position of the pentaluorophenyl moiety to furnish compound **31**. No formation of the desired coupling product **30b** was observed as evident from LRMS analysis.

Upon subjecting coupling products **30** to Pd/C catalyzed hydrogenation, only formation of hydrogenation product **34a** was observed and isolated in excellent yields (91-96%). Suggestively, the alkene of compound **34b** was resistant to reduction due to increased stability as a result of the highly electron-deficient nature of the pentafluorophenyl moiety accepting its π-electrons. When Raney-Nickel was utilized as catalyst during the reduction, the desired product **34b** was furnished in 76% yield after purification.

Tandem C-H activation and C-N bond formation of compounds **34** yielded indoloquinolines **39** in modest to excellent yields after purification (**39a**: 87%, **39b**: 32-37%). The modest yield of indoloquinoline **39b** is believed to be due to the unfavorable conversion of starting material following the same reasoning which was discussed for the formation of indoloquinoline **13**.

To conclude the synthetic pathway, indoloquinolines **39** were subjected to a standard *N*-methylation to yield the novel C6-alkylated isocryptolepine analogues **41** in good to excellent yields following purification (**41a**: 95%, **41b**: 66%). Biological evaluation of the analogues will be conducted by Associate Professor Hanne R. Hagland's group at the CORE fascilities located in Stavanger, Norway. The antimalarial assay is to be conducted by Professor Vicky Avery's group in Brisbane, Australia.

2.4 Future work

In order to successfully conduct a gram-scale synthesis of isocryptolepine (**4**), optimization of the MW-assisted ring closure of indoloquinoline **13** would be a logical starting point. Exploration of other palladium catalysts might prove useful, as would the use of different ligands. Bjørsvik and Elumalai[2] report using $Pd(tfa)_2$ as a catalyst, which should be considered being tested for the ring closure of the quinoline scaffold.

More over, MW-syntheses may be unsuitable for the scale-up of such reactions and other synthetic pathways should be investigated. The one-pot synthesis of isocryptolepine (**4**) as reported by Aksenov and coworkers[20] could yield promising results. One-pot syntheses also provide for a much greener chemistry, allowing for the use of less chemicals by eliminating several purification steps.

Regarding the synthesized isocryptolepine analogues **41**, their biological activity is uncertain at this stage as they are still undergoing testing. However, the compounds seem to be highly insoluble in water, which could affect their biological availability. Thus, it is of interest to introduce water-soluble moieties at various sites of the indoloquinoline scaffold to increase

the biological availability. Examplewise, introduction of functional groups such as guanidine through some linker at C6 (Figure 31) may provide useful results.

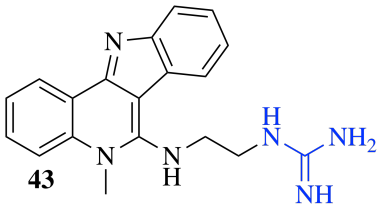

43

Figure 31: C6-substituted isocryptolepine analogue containing a guanidine moiety (in blue).

3 Experimental

3.1 General

3.1.1 Solvents and reagents

All chemicals were obtained from Merck, VWR or Sigma Aldrich and used as supplied. When specified, dichloromethane (DCM) was dried by storing over 4 Å molecular sieves.

3.1.2 Spectroscopic and spectrometric analysis

Nuclear magnetic resonance (NMR) spectra were recorded on a Bruker Ascend^{TM} 400 series, operating at 400 MHz for ^{1}H and ^{19}F and 100 MHz for ^{13}C, respectively. The chemical shifts (δ) are expressed in ppm relative to residual chloroform-d (^{1}H, 7.26 ppm; ^{13}C, 77.16 ppm), DMSO-d_6 (^{1}H, 2.50 ppm; ^{13}C, 39.52 ppm), methanol-d_4 (^{1}H, 3.31 ppm; ^{13}C, 49.00 ppm), acetone-d_6 (^{1}H, 2.09 ppm; ^{13}C, 30.60 ppm)[70] or α,α,α-trifluorotoluene (^{19}F, -63.72 ppm).[71] Coupling constants (*J*) are given in Hertz (Hz) and the multiplicity is reported as: singlet (s), doublet (d), triplet (t), doublet of doublets (dd), doublet of doublet of doublets (ddd), triplet of doublets (td), multiplet (m) and broad singlet (bs). The assignments of signals in various NMR spectra was often assisted by conducting heteronuclear single-quantum correlation spectroscopy (HSQC) and/or heteronuclear multiple bond correlation spectroscopy (HMBC).

Infrared (IR) spectra were recorded on an Agilent Cary 630 FTIR spectrophotometer. Samples were analyzed either as a thin film on NaCl plates or by placing the sample directly onto the crystal of an attenuated total reflectance (ATR) module.

Melting points (mp) were determined on a Stuart SMP20 melting point apparatus and are uncorrected.

The microwave (MW) assisted experiments were performed in a CEM Focused Microwave^{TM} Synthesis System, model type Discover that operated at 0-300 W at a temperature of 118 °C, a pressure range of 0-290 psi, with reactor vial volumes of 10 or 35 mL.

Low resolution mass spectra were obtained on an Advion expression^{s} CMS mass spectrometer operating at 3.5 kV in electrospray ionization (ESI) mode. The low resolution mass spectrometer (LRMS) was routinely used to monitor reactions and identify the various components of reaction mixtures.

Samples for high resolution mass spectrometry (HRMS) were prepared and sent to Dr. Bjarte Holmelid at the University of Bergen (UiB) for analysis.

Compound **28** was recrystallized using ethanol and sent to Dr. Ronny Helland at the University of Tromsø (UiT) for X-ray analysis.

3.1.3 Chromatography

Thin-layer chromatography (TLC) was carried out using aluminum backed 0.2 mm thick silica gel plates from Merck (type: 60 F_{254}). The spots were detected with ultraviolet (UV) (extinction at λ = 254 nm or fluorescent at λ = 366 nm). Flash chromatography (FC) was carried out with silica gel (particle size 40-63 μm), with solvent gradients as indicated in the experimental procedures. Dry vacuum flash chromatography[72] (DVFC) was carried out by dry-packing the column with approximately 5 cm of silica gel (particle size 19-37 μm). The crude mixute, which had previously been evaporated onto celite, was then added on top of the silica layer. The column was eluted by the addition of 20 mL of the eluent system as indicated by the experimental procedures. The polarity of the eluent was usually increased by 0.5-1% in increments of 4 fractions.

Automated flash chromatography was carried out using an Interchim puriFlash® 215 chromatography system. The sample was evaporated onto celite and then dry-loaded into a specialized column. This was then attached to a second column filled with 40 μm silica gel particles. The eluent was flushed through the columns using an applied pressure of 26 bar. Full overview of the parameters utilized can be found in the Appendix.

3.2 Methods

2-(Quinolin-3-yl)aniline (12)[3]

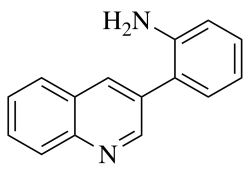

3-Bromoquinoline (**10**) (3.3 mL, 24.0 mmol), 2-aminophenylboronic acid hydrochloride (**11**) (4.6 g, 26.4 mmol) and potassium carbonate (9.9 g, 72.1 mmol) were dissolved in EtOH/H_2O (5/1, 38 mL) under a nitrogen atmosphere. $PdCl_2$(dppf) (0.6 g, 0.8 mmol) was added and the reaction mixture was stirred at 60 °C for 15 h. The reaction mixture was cooled to ambient

temperature and the volatiles were removed under reduced pressure. The concentrate was evaporated onto celite and purified by silica gel column chromatography (PE/Et_2O, 7/3 → 1/1 v/v, followed by PE/EtOAc, 1/1 → 4/6 v/v, respectively). Concentration of the relevant fractions [R_f = 0.27 (PE/EtOAc, 7/3 v/v)] gave compound **12** as yellow crystals (4.4 g, 84%).

mp: 132-135 °C.
IR (ATR): ν_{max} 3414, 3317, 3218, 3025, 1634, 1490, 1306, 948, 915, 738 cm^{-1}.
^{1}**H-NMR** (400 MHz, $CDCl_3$): δ 9.03 (d, J = 2.0 Hz, 1H), 8.25 (d, J = 2.0 Hz, 1H), 8.14 (d, J = 8.4 Hz, 1H), 7.83-7.81 (m, 1H), 7.75-7.71 (m, 1H), 7.59-7.55 (m, 1H), 7.25-7.19 (m, 2H), 6.92-6.88 (m, 1H), 6.84-6.82 (m, 1H), 3.80 (bs, 2H).
^{13}**C-NMR** (100 MHz, $CDCl_3$): δ 151.5, 147.1, 144.1, 135.5, 132.5, 130.9, 129.6, 129.5, 129.2, 127.9, 127.8, 127.1, 123.7, 119.1, 116.0.
Spectroscopic and spectrometric data are in accordance with previously reported data.[3]

5*H*-Indolo[3,2-*c*]quinoline (13)

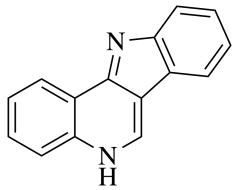

2-(Quinolin-3-yl)aniline (**12**) (70.0 mg, 0.3 mmol) in acetic acid (0.8 mL) was added to a premixed solution of $Pd(OAc)_2$ (14.7 mg, 0.06 mmol), IMes (4.9 mg, 0.02 mmol), H_2O_2 (35 wt%, 7.3 μL, 0.09 mmol) and acetic acid (0.2 mL). The reaction mixture was introduced into a sealed reactor tube, which was placed in the cavity of a microwave oven for 10 min. at 118 °C. The reaction mixture was then transferred to a 50 mL round-bottom flask using EtOAc and concentrated *in vacuo*. The concentrate was evaporated onto celite and purified by two consecutive separations by silica gel DVFC (DCM/EtOAc, 1/1 → 45/55 v/v and DCM/EtOAc, 1/1 v/v, respectively). Concentration of the relevant fractions [R_f = 0.21 (DCM/EtOAc, 2/8, v/v)] gave compound **13** as a pale yellow solid (36.9 mg, 53%).

mp: 333-336 °C (lit.[3] 340-341 °C).
IR (ATR): ν_{max} 3139, 3044, 2925, 2852, 2763, 1568, 1512, 1459, 1338, 1237, 733 cm^{-1}.
^{1}**H-NMR** (400 MHz, $(CD_3)_2CO$-d_6): δ 11.86 (bs, 1H), 9.61 (s, 1H), 8.50 (ddd, J = 8.3 Hz, 6.7 Hz, 0.6 Hz, 1H), 8.34-8.32 (m, 1H), 8.22-8.19 (m, 1H), 7.77-7.71 (m, 2H), 7.68-7-64 (m, 1H), 7.52-7.48 (m, 1H), 7.39-7.35 (m, 1H).

^{13}**C-NMR** (100 MHz, $(CD_3)_2CO$-d_6): δ 146.7, 145.3, 141.1, 140.1, 130.6, 128.9, 126.6, 126.5, 123.4, 122.6, 121.8, 120.8, 118.2, 115.8, 112.7.
Spectroscopic data are in accordance with previously reported data.[3]

Isocryptolepine (4)

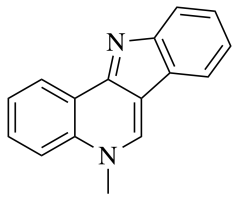

To a solution of 5*H*-indolo[3,2-*c*]quinoline (**13**) (34.0 mg, 0.2 mmol) in acetonitrile (2.0 mL), iodomethane (1.0 mL, 15.6 mmol) was added and the resulting mixture refluxed for 19 h. The volatiles were then removed under reduced pressure and the concentrate was evaporated onto celite. Purification by silica gel DVFC ($CHCl_3$/MeOH, 95/5 v/v) and concentration of the relevant fractions [R_f = 0.18 ($CHCl_3$/MeOH, 95/5 v/v)] to give the hydroiodide salt of isocryptolepine. To obtain isocryptolepine as the free base, its hydroiodide salt was dissolved in DCM (20 mL), aqueous ammonia (25%, 15 mL) was added and the reaction mixture was stirred at ambient temperature for 10 min. The organic layer was separated and the aqueous layers were extracted with $CHCl_3$ (3 x 10 mL) and the combined organic layers were washed with brine (2 x 10 mL), dried ($MgSO_4$), filtered and concentrated *in vacuo* to give isocryptolepine (**4**) as a pale yellow crystalline solid (24.3 mg, 69%).

mp: 188-192 °C (lit.[3] 185-187 °C).
IR (NaCl): ν_{max} 3049, 2923, 2852, 1638, 1598, 1455, 1351 cm^{-1}.
^{1}**H-NMR** (400 MHz, DMSO-d_6): δ 9.38 (s, 1H), 8.77 (dd, J = 8.0 Hz, 1.4 Hz, 1H), 8.14-8.11 (m, 1H), 8.07 (d, J = 8.6 Hz, 1H), 7.86 (ddd, J = 8.6 Hz, 7.0 Hz, 1.6 Hz, 1H), 7.80-7.78 (m, 1H), 7.74-7.70 (m, 1H), 4.28 (s, 3H).
^{13}**C-NMR** (100 MHz, DMSO-d_6): δ 154.1, 152.3, 138.4, 135.5, 129.6, 129.3, 125.5, 125.3, 123.9, 120.9, 119.8, 119.5, 118.3, 117.6, 116.1, 42.2.
Spectroscopic and spectrometric data are in accordance with previously reported data.[3]

3-Bromoquinoline-*N*-oxide (19)

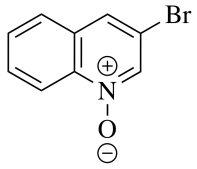

3-Bromoquinoline (**10**) (3.3 mL, 24.0 mmol) and H_2O_2 (35 wt%, 6.0 mL, 24.0 mmol) in acetic acid (35 mL) was stirred at 100 °C for 4 h. Saturated aqueous K_2CO_3 (30 mL) was then added and the mixture was extracted with $CHCl_3$ (3 x 15 mL). The combined organic layers were dried ($MgSO_4$), filtered and concentrated *in vacuo*. The concentrate was evaporated onto celite and purified by silica gel column chromatography (PE/EtOAc, 8/2 $\rightarrow$ 7/3 v/v). Concentration of the relevant fractions [R_f = 0.25 (PE/EtOAC, 1/1 v/v)] gave compound **19** as an off-white solid (4.3 g, 81%).

mp: 108-110 °C (lit.[48] 97–99 °C).
IR (NaCl): ν_{max} 3102, 3054, 2926, 1555, 1497, 1078, 841, 769 cm^{-1}.
^{1}**H-NMR** (400 MHz, $CDCl_3$): δ 8.61 (d, J = 8.9 Hz, 1H), 8.57 (s, 1H), 7.84 (s, 1H), 7.74-7.69 (m, 2H), 7.63-7.59 (m, 1H).
^{13}**C-NMR** (100 MHz, $CDCl_3$): δ 140.6, 137.3, 130.6, 130.2, 129.8, 128.0, 127.4, 119.9, 114.3.
Spectroscopic and spectrometric data are in accordance with previously reported data.[48]

***N*-(2-(Quinolin-3-yl)phenyl)acetamide (24)**

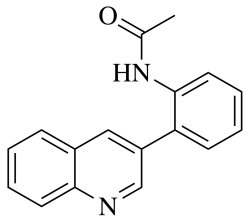

2-(Quinolin-3-yl)aniline (**12**) (500.0 mg, 2.3 mmol) in acetic acid (2.5 mL) was added to a pre-mixed solution of $Pd(OAc)_2$ (102.0 mg, 0.5 mmol), IMes (34.5 mg, 0.1 mmol), H_2O_2 (35 wt%, 0.05 mL, 0.7 mmol) and acetic acid (0.5 mL). The reaction mixture was introduced into a sealed reactor tube, which was placed in the cavity of a microwave oven for 10 min. at 118 °C. The reaction mixture was then transferred to a 250 mL round-bottom flask using EtOAc and concentrated *in vacuo*. The concentrate was evaporated onto celite and purified by an Interchim

puriFlash 215 chromatography system (see Appendix for parameters) followed by silica gel DVFC (PE/DCM, 1/1 v/v). Concentration of the relevant fractions [R_f = 0.36 (EtOAc/DCM, 8/2 v/v)] gave compound **24** as an orange solid (27.3 mg, 3%) and recovered starting material **12** as an orange solid (247.7 mg, 25%).

mp: 73-76 °C.
IR (ATR): ν_{max} 3233, 3181, 3052, 2962, 2924, 2855, 1662, 1491, 1288, 751 cm^{-1}.
^{1}**H-NMR** (400 MHz, $CDCl_3$): δ 8.88 (bs, 1H), 8.16-8.09 (m, 3H), 7.84 (d, J = 7.9 Hz, 1H), 7.77-7.73 (m, 1H), 7.62-7.58 (m, 1H), 7.46-7.42 (m, 1H), 7.34-7.28 (m, 3H), 2.00 (s, 3H).
^{13}**C-NMR** (100 MHz, $CDCl_3$): δ 168.8, 150.8, 147.3, 136.2, 135.1, 130.7, 130.2, 130.1, 129.4, 129.2, 128.1, 127.5, 125.5, 123.9, 24.4.
LRMS (ESI): Calcd for $C_{17}H_{15}N_2O$ [M + H^+] 263.1, found 263.3.
HRMS: Sample send to UiB for analysis.

(*E*)-3-Bromo-2-styrylquinoline (27a)[30]

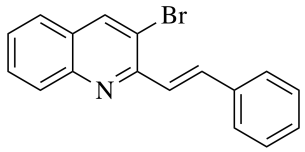

3-Bromoquinoline-*N*-oxide (**19**) (400.0 mg, 1.8 mmol), styrene (2.0 mL, 17.8 mmol) and I_2 (30.0 mg, 5 mol %) were dissolved in dry DCM (2.2 mL) and stirred at 120 °C in a dry sealed tube under an air atmosphere for 16 h. The mixture was then cooled to ambient temperature, concentrated *in vacuo* and evaporated onto celite. Purification by silica gel column chromatography (PE/DCM, 7/3 $\rightarrow$ 1/1 v/v) and concentration of the relavant fractions [R_f = 0.35 (PE/DCM, 7/3 v/v)] gave compound **27a** as a pale yellow solid (488.9 mg, 89%).

mp: 124-127 °C (lit.[30] 103-105 °C).
IR (NaCl): ν_{max} 3058, 2923, 1578, 1496, 996, 744 cm^{-1}.
^{1}**H-NMR** (400 MHz, $CDCl_3$): δ 8.37 (s, 1H), 8.08 (dd, J = 8.5 Hz, 0.6 Hz, 1H), 8.05 (d, J = 15.6 Hz, 1H), 7.71 (d, J = 15.6 Hz, 1H), 7.71-7.69 (m, 4H), 7.53-7.49 (m, 2H), 7.44-7.40 (m, 1H), 7.37-7.32 (m, 1H).
^{13}**C-NMR** (100 MHz, $CDCl_3$): δ 152.8, 146.7, 139.2, 137.1, 136.5, 130.0, 129.2, 128.9, 128.7, 127.7, 126.9, 126.5, 124.9, 118.5.
Spectroscopic data are in accordance with previously reported data.[30]

(*E*)-2-(2-Styrylquinolin-3-yl)aniline (30a)

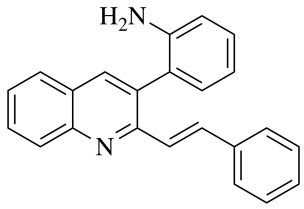

(*E*)-3-Bromo-2-styrylquinoline (**27a**) (488.9 mg, 1.6 mmol), 2-aminophenylboronic acid hydrochloride (**11**) (301.4 mg, 1.7 mmol) and potassium carbonate (655.1 mg, 4.7 mmol) were dissolved in EtOH/H_2O (5/1, 48 mL) under a nitrogen atmosphere. $PdCl_2$(dppf) (57.8 mg, 0.08 mmol) was added and the reaction mixture was stirred at 70 °C for 19 h. The mixture was cooled to ambient temperature and the volatiles were removed under reduced pressure. The concentrate was evaporated onto celite and purified by silica gel column chromatography (PE/EtOAc, 95/5 $\rightarrow$ 9/1 v/v). Concentration of the relevant fractions [R_f = 0.18 (PE/DCM, 3/7 v/v)] gave compound **30a** as a pale yellow solid (397.0 mg, 78%).

mp: 120-123 °C.
IR (NaCl): ν_{max} 3463, 3380, 3207, 3056, 1615, 1495, 1300, 1161, 973, 791, 748, 690 cm^{-1}.
^{1}**H-NMR** (400 MHz, CD_3OD): δ 8.04 (s, 1H), 8.00 (d, *J* = 8.5 Hz, 1H), 7.78 (d, *J* = 9.1 Hz, 1H), 7.74 (d, *J* = 15.9 Hz, 1H), 7.67-7.63 (m, 1H), 7.47-7.42 (m, 1H), 7.32-7.30 (m, 2H), 7.22-7.13 (m, 4H), 7.06 (d, *J* = 15.9 Hz, 1H), 6.96 (dd, *J* = 7.5 Hz, 1.4 Hz, 1H), 6.81 (dd, *J* = 8.1 Hz, 0.8 Hz, 1H), 6.73 (td, *J* = 7.4 Hz, 1.1 Hz, 1H). The NH_2 signal is not visible due to deuterium exchange with CD_3OD.
^{13}**C-NMR** (100 MHz, CD_3OD): δ 155.9, 148.7, 146.5, 139.5, 138.2, 136.6, 134.2, 132.0, 131.1, 130.5, 129.8, 129.7, 129.2, 129.1, 128.8, 128.2, 127.5, 126.5, 125.2, 119.1, 116.8.
LRMS (ESI): Calcd for $C_{23}H_{19}N_2$ [M + H^+] 323.2, found 323.4.
HRMS: Sample sent to UiB for analysis.

2-(2-Phenethylquinolin-3-yl)aniline (34a)

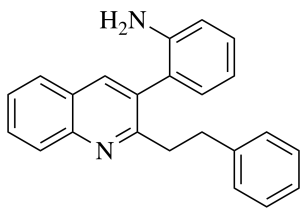

(*E*)-3-Bromo-2-(2-Styrylquinolin-3-yl)aniline (**30a**) (397.0 mg, 1.2 mmol) was dissolved in EtOAc (8 mL) and EtOH (14 mL) followed by addition of Pd/C (10%, 79.0 mg) under an N_2 atm. The resulting reaction mixture was then stirred at room temperature as H_2 was introduced slowly (1 atm, balloon) for 4 h. The volatiles were removed under reduced pressure and the concentrate was evaporated onto celite. Purification by silica gel column chromatography (PE/EtOAc, 8/2 v/v) and concentration of the relevant fractions [R_f = 0.22 (PE/EtOAc, 8/2 v/v)] gave compound **34a** as a yellow oil (371.0 mg, 93%).

IR (NaCl): ν_{max} 3456, 3371, 3202, 3059, 3026, 2925, 2854, 1616, 1498, 1301, 791, 751 cm^{-1}.
^{1}**H-NMR** (400 MHz, $CDCl_3$): δ 8.17 (d, J = 8.4 Hz, 1H), 8.01 (s, 1H), 7.80 (d, J = 8.1 Hz, 1H), 7.77-7.73 (m, 1H), 7.56-7.52 (m, 1H), 7.28-7.24 (m, 1H), 7.20-7.17 (m, 2H), 7.14-7.11 (m, 1H), 7.03-6.98 (m, 4H), 6.86 (td, J = 7.4 Hz, 0.9 Hz, 1H), 6.80 (d, J = 8.0 Hz, 1H), 3.43 (bs, 2H), 3.25-3.10 (m, 2H), 3.09-2.95 (m, 2H).
^{13}**C-NMR** (100 MHz, $CDCl_3$): δ 161.5, 147.6, 144.1, 142.1, 137.7, 132.4, 130.7, 129.7, 129.3, 128.8, 127.6, 126.3, 125.8, 124.7, 118.6, 115.5, 38.7, 35.6.
LRMS (ESI): Calcd for $C_{23}H_{21}N_2$ [M + H^+] 325.2, found 325.4.
HRMS: Sample sent to UiB for analysis.

6-Phenethyl-5*H*-indolo[3,2-*c*]quinoline (39a)

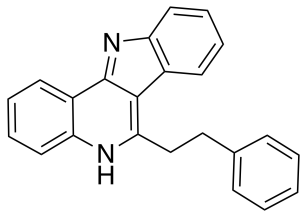

2-(2-Phenethylquinolin-3-yl)aniline (**34a**) (371.0 mg, 1.1 mmol) in acetic acid (6 mL) was added to a premixed solution of $PdCl_2$(dppf) (167.4 mg, 0.2 mmol), IMes (17.4 mg, 0.057 mmol), H_2O_2 (35 wt%, 0.3 mL, 0.3 mmol) and acetic acid (6 mL). The reaction mixture was introduced into a sealed reactor tube, which was placed in the cavity of a microwave oven for 40 min. at 118 °C. The reaction mixture was then transferred to a 100 mL round-bottom flask using EtOAc and concentrated *in vacuo*. The concentrate was evaporated onto celite and purified by two concecutive separations by flash chromatography (*n*-heptane/Et_2O, 2/8 v/v and *n*-heptane/Et_2O 8/2 $\rightarrow$ 7/3, respectively), where the column was packed with a slurry of Et_3N and silica gel followed by flashing with the relevant eluent. Concentration of the relevant fractions [R_f = 0.11 (*n*-heptane/Et_2O, 2/8)] gave compound **39a** as a white solid (320.0 mg, 87%).

mp: 184-187 °C.
IR (NaCl): ν_{max} 3056, 2924, 2850, 1564, 1512, 1361, 1247, 879, 742 cm^{-1}.
^{1}**H-NMR** (400 MHz, $CDCl_3$): δ 8.25 (d, *J* = 8.3 Hz, 1H), 8.21 (d, *J* = 8.3 Hz, 1H), 8.17 (d, *J* = 7.9 Hz, 1H), 7.75 (d, *J* = 8.1 Hz, 1H), 7.58-7.50 (m, 2H), 7.48-7.38 (m, 4H), 7.35-7.31 (m, 2H), 7.25-7.21 (m, 1H), 3.85-3.81 (m, 2H), 3.32-3.28 (m, 2H). The NH signal is not visible due to exchange with deuterium.
^{13}**C-NMR** (100 MHz, $CDCl_3$): δ 157.8, 141.8, 140.9, 138.8, 128.8, 128.7, 128.6, 126.3, 125.7, 125.5, 122.8, 121.9, 121.8, 120.8, 116.1, 113.5, 111.9, 39.4, 34.7.
LRMS (ESI): Calcd for $C_{23}H_{19}N_2$ [M + H^+] 323.2, found 323.2.
HRMS: Sample sent to UiB for analysis.

5-Methyl-6-phenethyl-5*H*-indolo[3,2-*c*]quinoline (41a)

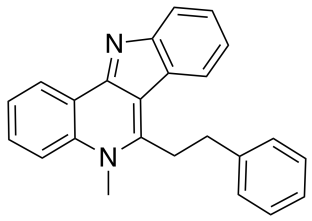

To a solution of 6-phenethyl-5*H*-indolo[3,2-*c*]quinoline (**39a**) (300.0 mg, 0.9 mmol) in acetonitrile (10 mL), iodomethane (5.8 mL, 93.0 mmol) was added and the resulting mixture refluxed for 22 h. The volatiles were then removed under reduced pressure and the concentrate was evaporated on celite. Purification by silica gel column chromatography ($CHCl_3$/MeOH, 99/1 v/v) and concentration of the relevant fractions [R^f = 0.13 ($CHCl_3$/MeOH, 9/1)] gave the hydroiodide salt of **41a**. To obtain **41a** as a free base, its hydroiodide salt was dissolved in $CHCl_3$ (30 mL), aqueous ammonia (25%, 20 mL) was added and the reaction mixture was stirred at ambient temperature for 20 min. The organic layer was separated and the aqueous layers were extracted with $CHCl_3$ (3 x 15 mL) and the combined organic layers were washed with brine (20 mL) and dest. H_2O (20 mL), dried ($MgSO_4$), filtered and concentrated *in vacuo* to give **41a** as a pale yellow oil (297.0 mg, 95%).

IR (ATR): ν_{max} 2918, 2850, 1586, 1458, 1338, 1020, 738, 692 cm^{-1}.
^{1}**H-NMR** (400 MHz, $CDCl_3$): δ 8.93 (d, *J* = 7.5 Hz, 1H), 8.06 (d, *J* = 8.0 Hz, 1H), 7.82 (d, *J* = 8.0 Hz, 1H), 7.66-7.58 (m, 3H), 7.55-7.49 (m, 3H), 7.32-7.27 (m, 5H), 7.14 (d, *J* = 7.3 Hz, 2H), 3.87 (s, 3H), 3.65 (t, *J* = 7.0 Hz, 2H), 3.12 (t, *J* = 7.0 Hz, 2H).

^{13}**C-NMR** (100 MHz, $CDCl_3$): δ 151.5, 138.9, 136.4, 134.2, 130.2, 129.9, 129.8, 129.7, 128.9, 128.2, 127.5, 127.1, 126.4, 125.7, 125.4, 121.5, 120.5, 116.7, 70.5, 63.0, 35.8.
LRMS (ESI): Calcd for $C_{24}H_{21}N_2$ [M + H^+] 337.2, found 337.3.
HRMS: Sample sent to UiB for analysis.

(*E*)-3-Bromo-2-(2-(perfluorophenyl)vinyl)quinoline (27b)[30]

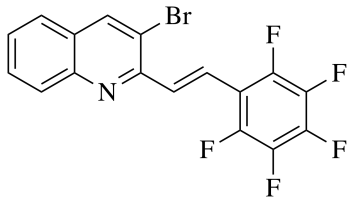

3-Bromoquinoline-*N*-oxide (**19**) (400.0 mg, 1.8 mmol), 2,3,4,5,6-pentafluorostyrene (2.5 mL, 17.8 mmol) and I_2 (30.0 mg, 5 mol %) were dissolved in dry DCM (3 mL) and stirred at 120 °C in a dry sealed tube under an air atmosphere for 18 h. The mixture was then cooled to ambient temperature, concentrated *in vacuo* and evaporated onto celite. Purification by silica gel column chromatography (PE/DCM, 99/1 $\rightarrow$ 6/4 v/v) and concentration of the relevant fractions [R^f = 0.18 (PE/DCM, 9/1 v/v)] gave compound **27b** as white crystals (386.5 mg, 54%) and compound **28** as pale yellow crystals (173.6 mg, 24%).

27b:
mp: 169-172 °C.
IR (ATR): ν_{max} 3054, 2987, 1422, 1266, 896 cm^{-1}.
^{1}**H-NMR** (400 MHz, $CDCl_3$): δ 8.39 (s, 1H), 8.13 (d, J = 16.0 Hz, 1H), 8.11 (dd, J = 8.4 Hz, 0.8 Hz, 1H), 7.97 (d, J = 16.0 Hz, 1H), 7.76-7.71 (m, 2H), 7.57-7.53 (m, 1H).
^{13}**C-NMR** (100 MHz, $CDCl_3$): δ 151.9, 146.9-146.8 (m), 146.7, 144.4-144.2 (m), 142.1-141.8 (m), 139.6, 139.5-139.2 (m), 136.8-136.5 (m), 132.9 (td, J_{CF} = 6.5 Hz, 2.4 Hz), 130.4, 129.7, 128.9, 127.8, 126.6, 120.7 (d, J_{CF} = 2.2 Hz), 118.6, 112.0 (td, J_{CF} = 9.5 Hz, 4.4 Hz).
^{19}**F-NMR** (400 MHz, $CDCl_3$): δ -141.8, -155.4, -163.5.
LRMS (ESI): Calcd for $C_{17}H_8BrF_5N$ [M + H^+] 400.0, found 399.9.
HRMS: Sample sent to UiB for analysis.

28:
mp: 151-154 °C.
IR (ATR): ν_{max} 3065, 2925, 2856, 1499, 1118, 980, 781 cm^{-1}.

^{1}H-NMR (400 MHz, $CDCl_3$): δ 8.35 (s, 1H), 8.00 (dd, J = 8.0 Hz, 0.8 Hz, 1H), 7.76-7.71 (m, 2H), 7.58-7.54 (m, 1H), 5.86 (dd, J = 16.8 Hz, 9.7 Hz, 1H), 5.59 (bs, 1H), 3.77 (dd, J = 9.9 Hz, 2.7 Hz, 1H), 3.48 (dd, J = 17.2 Hz, 2.7 Hz, 1H).
^{13}C-NMR (100 MHz, $CDCl_3$): δ 157.3, 146.7-145.5 (m), 145.7, 144.3-144.1 (m), 142.3-142.0 (m), 139.5, 139.2-138.9 (m), 136.7-136.4 (m), 130.5, 128.8, 128.2, 127.6, 126.8, 118.4, 116.2-115.8 (m), 64.3, 41.8.
^{19}F-NMR (400 MHz, $CDCl_3$): δ -142.0, -155.1, -162.0.
HRMS: Sample sent to UiB for analysis.

(*E*)-2-(2-(2-(Perfluorophenyl)vinyl)quinolin-3-yl)aniline (30b)

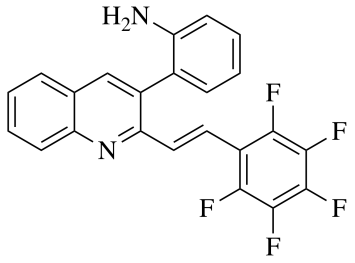

(*E*)-3-Bromo-2-(2-(perfluorophenyl)vinyl)quinoline (**27b**) (50.0 mg, 0.1 mmol), 2-aminophenylboronic acid hydrochloride (**11**) (24.0 mg, 0.1 mmol) and potassium carbonate (52.0 mg, 0.4 mmol) were dissolved in EtOH/H_2O (5/1, 6 mL) under an argon atmosphere. $PdCl_2$(dppf) (5.0 mg, 0.006 mmol) was added and the reaction mixture was stirred at 60 °C for 24 h. The mixture was cooled to ambient temperature and the volatiles were removed under reduced pressure. The concentrate was evaporated onto celite and purified by silica gel DVFC (PE/EtOAc, 99/1 $\rightarrow$ 92/8 v/v). Concentration of the relevant fractions [R_f = 0.24 (PE/EtOAc, 9/1 v/v)] gave compound **30b** as off-white crystals (26.3 mg, 51%).

mp: 200-204 °C.
IR (ATR): ν_{max} 2922, 2853, 1618, 1519, 1493, 957, 746 cm^{-1}.
^{1}H-NMR (400 MHz, $CDCl_3$): δ 8.19 (d, J = 8.5 Hz, 1H), 8.12 (s, 1H), 7.99 (d, J = 16.1 Hz, 1H), 7.80 (dd, J = 8.4 Hz, 1.1 Hz, 1H), 7.78-7.74 (m, 1H), 7.58-7.54 (m, 1H), 7.48 (d, J = 16.1 Hz, 1H), 7.32-7.26 (m, 1H), 7.11 (dd, J = 7.6 Hz, 1.5 Hz, 1H), 6.89 (td, J = 7.5 Hz, 1.2 Hz, 1H), 6.84 (dd, J = 8.1 Hz, 0.9 Hz, 1H), 3.62 (bs, 2H).
^{13}C-NMR (100 MHz, $CDCl_3$): δ 153.1, 147.7, 146.7-144.5 (m), 144.2, 144.2-144.0 (m), 141.8-141.5 (m), 139.2-138.9 (m), 138.2, 136.7-136.4 (m), 133.7-133.5 (m), 132.6, 131.1, 130.2, 129.8, 129.6, 128.0, 127.6, 127.2, 123.5, 119.2-119.1 (m), 118.9, 115.7, 112.4 (td, J_{CF}

= 13.7 Hz, 4.1 Hz).
^{19}**F-NMR** (400 MHz, $CDCl_3$): δ -142.1, -156.2, -163.8.
LRMS (ESI): Calcd for $C_{23}H_{14}F_5N_2$ [M + H^+] 413.1, found 413.2.
HRMS: Sample sent to UiB for analysis.

2-(2-(2-(Perfluorophenyl)ethyl)quinolin-3-yl)aniline (34b)

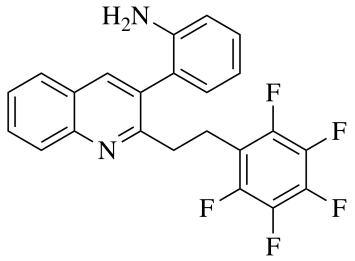

(*E*)-2-(2-(2-(perfluorophenyl)vinyl)quinolin-3-yl)aniline (**30b**) (196.4 mg, 0.5 mmol) was dissolved in EtOAc (5 mL) under an argon atm. Raney-Ni (approx. 200 mg) was added and the resulting reaction mixture was stirred at room temperature as H_2 was introduced slowly (1 atm, balloon) for 6 h. Raney-Ni was then filtered off using a celite pad and the volaties were removed under reduced pressure and the concentrate was evaporated onto celite. Purification by silica gel DVFC (PE/DCM, 9/1 v/v) and concentration of the relevant fractions [R_f = 0.22 (PE/DCM, 4/6 v/v)] gave compound **34b** as a pale yellow oil (151.2 mg, 76%).

IR (ATR): ν_{max} 3031, 2926, 2855, 1733, 1617, 1498, 947, 748 cm^{-1}.
^{1}**H-NMR** (400 MHz, $CDCl_3$): δ 8.10 (d, J = 8.2 Hz, 1H), 8.02 (s, 1H), 7.80 (d, J = 8.0 Hz, 1H), 7.76-7.72 (m, 1H), 7.57-7.53 (m, 1H), 7.24 (td, J = 8.0 Hz, 1.6 Hz, 1H), 3.48 (bs, 2H), 3.17-3.15 (m, 4H).
^{13}**C-NMR** (100 MHz, $CDCl_3$): δ 159.5, 147.4-147.2 (m), 146.6-146.4 (m), 144.3-144.1 (m), 143.9, 141.2-140.8 (m), 138.7-138.4 (m), 137.9-137.7 (m), 136.3-136.1 (m), 132.3, 130.5, 129.9, 129.6, 128.7, 127.5, 127.2, 126.7, 124.2, 118.7, 115.6, 115.0-114.6 (m), 34.9, 21.6.
^{19}**F-NMR** (400 MHz, $CDCl_3$): δ -143.6, -158.3, -163.4.
LRMS (ESI): Calcd for $C_{23}H_{16}F_5N_2$ [M + H^+] 415.1, found 415.3.
HRMS: Sample sent to UiB for analysis.

6-(2-(Perfluorophenyl)ethyl)-5*H*-indolo[3,2-*c*]quinoline (39b)

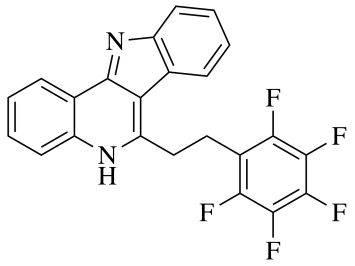

2-(2-(2-(Perfluorophenyl)ethyl)quinolin-3-yl)aniline (**34b**) (55.0 mg, 0.1 mmol) in acetic acid (1 mL) was added to a premixed solution of $Pd(OAc)_2$ (6.0 mg, 0.03 mmol), IMes (2.0 mg, 6.5 μmol), H_2O_2 (35 wt%, 3.7 μL, 0.04 mmol) and acetic acid (0.6 mL). The reaction mixture was introduced into a sealed tube, which was placed in the cavity of a microwave oven for 40 min. at 118 °C. The reaction mixture was then transferred to a 100 mL round-bottom flask using EtOAc and concentrated *in vacuo*. The concentrate was evaporated onto celite and purified by two consecutive separations by silica gel DVFC (PE/DCM, 1/1 $\rightarrow$ 0/100 v/v and PE/DCM, 1/1 v/v, respectively). Concentration of the relevant fractions [R_f = 0.52 (EtOAc/DCM, 8/2 v/v))] gave compound **39b** as an off-white solid (20.2 mg, 37%).

mp: 218-220 °C.
IR (ATR): ν_{max} 2925, 2854, 1504, 1456, 965, 746 cm^{-1}.
^{1}**H-NMR** (400 MHz, $CDCl_3$/DMSO-d_6): δ 11.92 (bs, 1H), 8.34-8.32 (m, 1H), 8.06-8.03 (m, 2H), 7.59-7.55 (m, 2H), 7.49-7.44 (m, 1H), 7.38-7.34 (m, 1H), 7.24-7.22 (m, 1H), 3.69-3.67 (m, 2H), 3.35-3.34 (m, 2H).
^{13}**C-NMR** (100 MHz, $CDCl_3$/DMSO-d_6): δ 155.3, 140.9, 138.9, 138.0, 128.0, 124.9, 121.9, 121.7, 120.9, 120.6, 116.3, 114.5, 112.6, 111.7, 35.7, 20.6. Not all quarternary carbons are visible and no C-F couplings were observed.
^{19}**F-NMR** (400 MHz, $CDCl_3$/DMSO-d_6): δ -144.2, -159.2, -164.3.
LRMS (ESI): Calcd for $C_{23}H_{14}F_5N_2$ [M + H^+] 413.1, found 413.2.
HRMS: Sample sent to UiB for analysis.

5-Methyl-6-(2-(perfluorophenyl)ethyl)-5*H*-indolo[3,2-*c*]quinoline (41b)

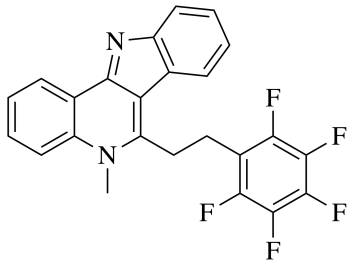

To a solution of 6-(2-(perfluorophenyl)ethyl)-5*H*-indolo[3,2-*c*]quinoline (**39b**) (30.0 mg, 0.07 mmol) in acetonitrile (3 mL), iodomethane (0.5 mL, 7.3 mmol) was added and the resulting mixture was refluxed for 18 h. The volatiles were then removed under reduced pressure and the concentrate was evaporated onto celite. Purification by silica gel DVFC ($CHCl_3$/MeOH, 9/1 v/v) and concentration of the relevant fractions [R_f = 0.14 ($CHCl_3$/MeOH, 9/1 v/v)] gave the hydroiodide salt of **41b**. To obtain **41b** as a free base, its hydroiodide salt was dissolved in DCM (30 mL), aqueous ammonia (25%, 15 mL) was added and the reaction mixture was stirred at ambient temperature for 15 min. The organic layer was separated and the aqueous layers extracted with $CHCl_3$ (3 x 15 mL) and the combined organic layers were washed with brine (2 x 15 mL), dest. H_2O (1 x 20 mL), dried ($MgSO_4$), filtered and concentrated *in vacuo* to give **41b** as a pale yellow solid (20.6 mg, 66%).

mp: 233-235 °C.
IR (ATR): ν_{max} 2919, 2851, 1735, 1504, 1462, 1038, 967, 743 cm^{-1}.
^{1}**H-NMR** (400 MHz, $CDCl_3$/DMSO-d_6): δ 8.47 (d, J = 7.8 Hz, 1H), 7.88-7.84 (m, 1H), 7.68 (d, J = 6.0 Hz, 1H), 7.58-7.53 (m, 1H), 7.43-7.40 (m, 2H), 7.29-7.27 (m, 2H), 7.15-7.12 (m, 1H), 7.02-6.99 (m, 1H), 4.03 (s, 3H), 3.63-3.58 (m, 4H).
^{13}**C-NMR** (100 MHz, $CDCl_3$/DMSO-d_6): δ 152.7, 136.2, 131.6, 128.5, 126.8, 126.7, 123.7, 122.2, 120.6, 119.9, 117.8, 115.4, 113.4, 112.8, 69.1, 60.4, 21.3. Not all quarternary carbons are visible and no C-F couplings were observed.
^{19}**F-NMR** (400 MHz, $CDCl_3$/DMSO-d_6): δ -144.6, -157.1, -163.0.
LRMS (ESI): Calcd for $C_{24}H_{16}F_5N_2$ [M + H^+] 427.1, found 427.4.
HRMS: Sample sent to UiB for analysis.

References

[1] Aroonkit, P.; Thongsornkleeb, C.; Tummatorn, J.; Krajangsri, S.; Mungthin, M.; Ruchirawat, S. *Eur. J. Med. Chem.* **2015**, *94*, 56–62.

[2] Bjørsvik, H.-R.; Elumalai, V. *Eur. J. Org. Chem.* **2016**, 5474–5479.

[3] Helgeland, I. T. U.; Sydnes, M. O. *SynOpen* **2017**, *1*, 41–44.

[4] Perlmann, P. *Malaria: Molecular and Clinical Aspects*; CRC Press, Boca Raton, 1999, Available from: ProQuest Ebook Central, Accessed: 6 January 2018.

[5] World Health Organization, *Guidelines for the Treatment of Malaria, 3rd edition*. 2015.

[6] Andersson, J.; Forssberg, H.; Zierath, J. R. *Nobelförsamlingen* **2015**, 1–11, Available from: www.nobelprize.org/nobel_prizes/medicine/laureates/2015/press.html, Accessed: 11 July 2018.

[7] World Health Organization, *World Malaria Report 2017*. Available from: www.who.int/malaria/publications/world-malaria-report-2017/en/, Accessed: 11 July 2018.

[8] Wang, N.; Wicht, K. J.; Imai, K.; Wang, M.; Ngoc, T. A.; Kiguchi, R.; Kaiser, M.; Egan, T. J.; Inokuchi, T. *Bioorg. Med. Chem.* **2014**, *22*, 2629–2642.

[9] Achan, J.; Talisuna, A. O.; Erhart, A.; Yeka, A.; Tibenderana, J. K.; Baliraine, F. N.; Rosenthal, P. J.; D'Alessandro, U. *Malar. J.* **2011**, *10*, 144.

[10] Mishra, M.; Mishra, V. K.; Kashaw, V.; Iyer, A. K.; Kashaw, S. K. *Eur. J. Med. Chem.* **2017**, *125*, 1300–1320.

[11] Harvey, A. L. *Drug Discov. Today* **2008**, *13*, 894–901.

[12] Qiu, S.; Sun, H.; Zhang, A.-I.; Xu, H.-Y.; Yan, G.-L.; Han, Y.; Wang, X.-J. *Chin. J. Nat. Med.* **2014**, *12*, 401–406.

[13] Dias, D. A.; Urban, S.; Roessner, U. *Metabo.* **2012**, *2*, 303–336.

[14] Ligon, B. L. *Semin. Pediatr. Infect. Dis.* **2004**, *15*, 52–57.

[15] Su, X.-Z.; Miller, L. H. *Sci. China Life Sci.* **2015**, *58*, 1175–1179.

[16] Lavrado, J.; Moreira, R.; Paulo, A. *Curr. Med. Chem.* **2010**, *17*, 2348–2370.

[17] Agarwal, P. K.; Sawant, D.; Sharma, S.; Kundu, B. *Eur. J. Org. Chem.* **2009**, *2*, 292–303.

[18] Yurovskaya, M. A.; Alekseyev, R. S. *Chem. Heterocycl. Compd.* **2014**, *49*, 1400–1425.

[19] Whittell, L. R.; Batty, K. T.; Wong, R. P. M.; Bolitho, E. M.; Fox, S. A.; Davis, T. M. E.; Murray, P. E. *Bioorg. Med. Chem.* **2011**, *19*, 7519–7525.

[20] Aksenov, A. V.; Aksenov, D. A.; Orazova, N. A.; Aksenov, N. A.; Griaznov, G. D.; Carvalho, A. D.; Kiss, R.; Mathieu, V.; Kornienko, A.; Rubin, M. *J. Org. Chem.* **2017**, *82*, 3011–3018.

[21] Tenguh, S. C.; Klonis, N.; Duffy, S.; Lucantoni, L.; Avery, V. M.; Hutton, C. A.; Baell, J. B.; Tilley, L. *J. Med. Chem.* **2013**, *56*, 6200–6215.

[22] Miyaura, N.; Suzuki, A. *Chem. Rev.* **1995**, *95*, 2457–2483.

[23] Miyaura, N.; Yamada, K.; Suzuki, A. *Tetrahedron Lett.* **1979**, *36*, 3437–3440.

[24] Suzuki, A. *J. Organomet. Chem.* **1999**, *576*, 147–168.

[25] Melchor, M. G. *A Theoretical Study of Pd-Catalyzed C-C Cross-Coupling Reactions*; Springer Science & Business Media: Barcelona, 2013; pp 113–115.

[26] Zalesskiy, S. S.; Ananikov, V. P. *Organometallics* **2012**, *31*, 2302–2309.

[27] Astruc, D. *Organometallic Chemistry and Catalysis*; Springer: Talence, 2007; pp 168–170.

[28] van Leeuwen, P. W. N. M. *Homogeneous Catalysis: Understanding the Art*; Springer Science & Business Media: Dordrecht, 2005; pp 286–299.

[29] Amatore, C.; Jutand, A.; Duc, G. L. *Chem. Eur. J.* **2011**, *17*, 2492–2503.

[30] Zhang, Z.; Pi, C.; Tong, H.; Cui, X.; Wu, Y. *Org. Lett.* **2017**, *19*, 440–443.

[31] Loupy, A. *Microwaves in Organic Synthesis: Second, Completely Revised and Enlarged Edition*; Wiley-VCH: Weinheim; vol. 1, 2006.

[32] Kolthoff, I. M.; Medalia, A. I. *J. Am. Chem. Soc.* **1949**, *71*, 3777–3783.

[33] Kumar, R. N.; Suresh, T.; Mohan, P. S. *Tetrahedron Lett.* **2002**, *43*, 3327–3328.

[34] Castejon, H.; Wiberg, K. B. *J. Am. Chem. Soc.* **1999**, *121*, 2139–2146.

[35] Tsang, W. C. P.; Zheng, N.; Buchwald, S. L. *J. Am. Chem. Soc.* **2005**, *127*, 14560–14561.

[36] Tsang, W. C. P.; Munday, R. H.; Brasche, G.; Zheng, N.; Buchwald, S. L. *J. Org. Chem.* **2008**, *73*, 7603–7610.

[37] Schwoegler, E. J.; Adkins, H. *J. Am. Chem. Soc.* **1939**, *61*, 3499–3502.

[38] Zhang, L.; Wang, X.-J.; Grinberg, N.; Krishnamurthy, D.; Senanayake, C. H. *Tetrahedron Lett.* **2009**, *50*, 2964–2966.

[39] Child, W. C.; Hay, A. J. *J. Am. Chem. Soc.* **1964**, *86*, 182–187.

[40] Wang, X.-J.; Yang, Q.; Liu, F.; You, Q.-D. *Synth. Commun.* **2008**, *38*, 1028–1035.

[41] Chakraborty, M.; Umrigar, V.; Parikh, P. A. *Int. J. Chem. React. Eng.* **2008**, *6*, 1–12.

[42] Charville, H.; Jackson, D. A.; Hodges, G.; Whiting, A.; Wilson, M. R. *Eur. J. Org. Chem.* **2011**, 5981–5990.

[43] Sharley, D. D. S.; Williams, J. M. J. *Chem. Commun.* **2017**, *53*, 2020–2023.

[44] Pan, F.; Lei, Z.-Q.; Wang, H.; Li, H.; Sun, J.; Shi, Z.-J. *Angew. Chem. Int. Ed.* **2013**, *52*, 2063 –2067.

[45] Annamalai, P.; Chen, W.-Y.; Raju, S.; Hsu, K.-C.; Upadhyay, N. S.; Cheng, C.-H.; Chuang, S.-C. *Adv. Synth. Catal.* **2016**, *358*, 1–8.

[46] Hubrich, J.; Himmler, T.; Rodefeld, L.; Ackermanna, L. *Adv. Synth. Catal.* **2015**, *357*, 474–480.

[47] Moseley, J. D.; M.Murray, P. *J. Chem. Technol. Biotechnol.* **2014**, *89*, 623–632.

[48] Bogányiab, B.; Kámána, J. *Tetrahedron* **2013**, *69*, 9512–9519.

[49] Zheng, Q.-Z.; Jiao, N. *Chem. Soc. Rev.* **2016**, *45*, 4590–4627.

[50] Neufeldt, S. R.; Sanford, M. S. *Acc. Chem. Res.* **2012**, *45*, 936–946.

[51] Mei, T.-S.; Kou, L.; Ma, S.; Engle, K. M.; Yu, J.-Q. *Synthesis* **2012**, *44*, 1778–1791.

[52] Kim, K. M.; Jeon, D. J.; Ryu, E. K. *Synthesis* **1998**, *6*, 835–836.

[53] Domingo, V.; Priesto, C.; Silva, L.; Rodilla, J. M. L.; del Moral, J. F. Q.; Barrero, A. F. *J. Nat. Prod.* **2016**, *79*, 831–837.

[54] Inturi, S. B.; Kalita, B.; Ahamed, A. J. *Tetrahedron Lett.* **2016**, *57*, 2227–2230.

[55] Kropp, P. J.; Daus, K. A.; Tubergen, M. W.; Kepler, K. D.; Wilson, V. P.; Craig, S. L.; Baillargeon, M. M.; Breton, G. W. *J. Am. Chem. Soc.* **1993**, *115*, 3071–3079.

[56] Irifune, S.; Kibayashi, T.; Ishii, Y.; Ogawa, M. *Synthesis* **1988**, *5*, 366–369.

[57] Lin-Vien, D.; Colthup, N. B.; Fateley, W. G.; Grasselli, J. G. *The Handbook of Infrared and Raman Characteristic Frequencies of Organic Molecules*; Elsevier: London, 1991; p 160.

[58] Garner, C. M.; Fisher, H. C. *Tetrahedron Lett.* **2006**, *47*, 7405–7407.

[59] Gutsche, C. S.; Ortwerth, M.; Gräfe, S.; Flanagan, K. J.; Senge, M. O.; Reissig, H.-U.; Kulak, N.; Wiehe, A. *Chem. Eur. J.* **2016**, *22*, 13953–13964.

[60] Helgeland, I. T. U.; Sydnes, M. O. *Unpublished work*, **2017**.

[61] Sydnes, M. O.; Isobe, M. *Tetrahedron Lett.* **2008**, *49*, 1199–1202.

[62] Esaki, H.; Ohtaki, R.; Maegawa, T.; Monguchi, Y.; Sajiki, H. *J. Org. Chem.* **2007**, *72*, 2143–2150.

[63] Katrizky, A. R.; Rachwal, S.; Rachwal, B. *Tetrahedron* **1996**, *52*, 15031–15070.

[64] Vierhapper, F. W.; Eliel, E. L. *J. Org. Chem.* **1975**, *40*, 2729–2734.

[65] Mattson, B.; Foster, W.; Greimann, J.; Hoette, T.; Le, N.; Mirich, A.; Wankum, S.; Cabri, A.; Reichenbacher, C.; Schwanke, E. *J. Chem. Educ.* **2013**, *90*, 613–619.

[66] Horiuti, I.; Polanyi, M. *J. Chem. Soc. Faraday Trans.* **1934**, *30*, 1164–1172.

[67] Ohno, S.; Wilde, M.; Mukai, K.; Yoshinobu, J.; Fukutani, K. *J. Phys. Chem. C* **2016**, *120*, 11481–11489.

[68] Bach, R. D.; Wolber, G. J.; Pross, A. *Isr. J. Chem.* **1983**, *23*, 97–104.

[69] Adkins, H.; Billica, H. R. *J. Am. Chem. Soc.* **1948**, *70*, 695–698.

[70] Fulmer, G. R.; Miller, A. J. M.; Sherden, N. H.; Gottlieb, H. E.; Nudelman, A.; Stoltz, B. M.; Bercaw, J. E.; Goldberg, K. I. *Organometallics* **2010**, *29*, 2176–2179.

[71] Jacobsen, N. E. *NMR Data Interpretation Explained: Understanding 1D and 2D NMR Spectra of Organic Compounds and Natural Products*; John Wiley & Sons: Hoboken, 2016; p 194.

[72] Pedersen, D. S.; Rosenbohm, C. *Synthesis* **2001**, *16*, 2431–2434.

4 Appendix

Structures

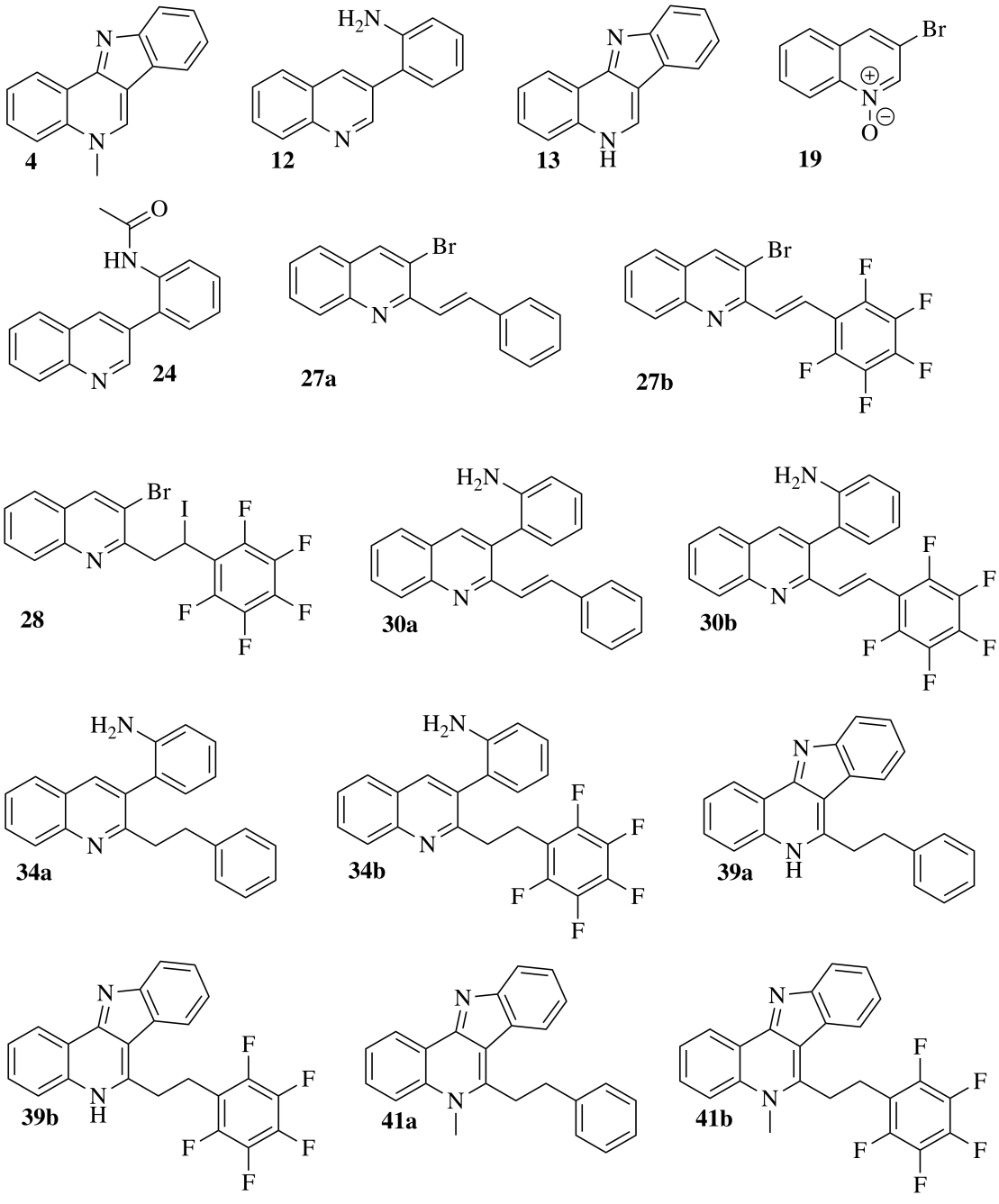

Interchim puriFlash 215 data

180612-1058-KSH36

Title : KATJA	Author :
Sample : KSH36	Column : PURIFLASH COLUMN 50 STD - 40.0 g (15 bar)
Solvent A : petroleum ether	Solvent C : methanol
Solvent B : ethyl acetate	Solvent D : dcm
Channel 1 : UV600:SCAN	Channel 2 : UV600:SIG2
Channel 3 : UV600:SIG1	
Equil+Inject Mode : Dry Load+Auto	Stop Mode : Pause
RUN Time : 6/12/2018 10:58:27 AM	

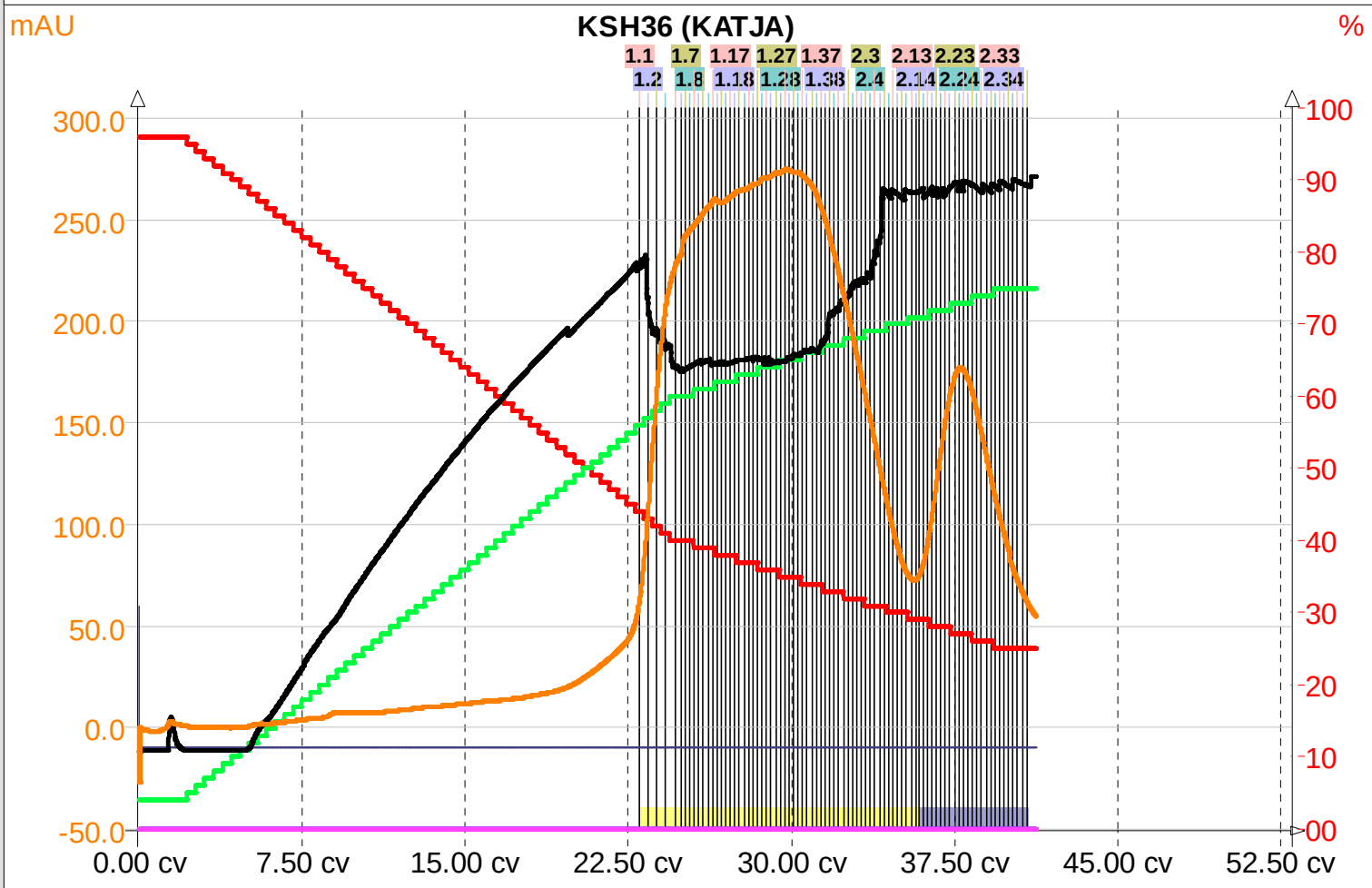

Peak Tracking

	25 mL				25 mL			
		067	066	045	044	023	022	001
		068	065	046	043	024	021	002
		069	064	047	042	025	020	003
		070	063	048	041	026	019	004
		071	062	049	040	027	018	005
	083	072	061	050	039	028	017	006
	082	073	060	051	038	029	016	007
	081	074	059	052	037	030	015	008
	080	075	058	053	036	031	014	009
	079	076	057	054	035	032	013	010
	078	077	056	055	034	033	012	011

<< RackSet #1 >>

<< RackSet #2 >>

180612-1058-KSH36

Collection Table

Tube	Peak	Rack	Pos.	RSet	Coll.	Volume	Surface	%Surface	Start Time	End Time	Begin	End
001/044	001	1	1/44	1	1	481.4	1133.0	30.2 %	00:42:25	01:00:56	22.98	33.01
045/058	001	2	1/14	1	1	135.6	415.6	11.1 %	01:00:56	01:06:09	33.01	35.83
001/058	001	-	-	-	-	617.1	1548.6	41.3 %	00:42:25	01:06:09	22.98	35.83
059/083	002	2	15/39	1	1	244.4	799.9	21.4 %	01:06:09	01:15:33	35.83	40.92
-	-	-	-	-	-	1118.9	1397.5	37.3 %	00:00:00	00:00:00	0.00	0.00

Elution Steps

N°	CV	Flow Rate	%A	%B	%C	%D
01	0.00	26.0	96	04	00	00
02	2.00	26.0	96	04	00	00
03	24.99	26.0	40	60	00	00
04	39.98	26.0	25	75	00	00
05	44.98	26.0	25	75	00	00

Detection Steps

N°	CV	WL (nm)	>> Scan	Gain	XIC <<	>> XIC	Collect	Threshold	F1
01	0.00	200	599				No		1
		254					Yes	60	1
		250					No		1

Collection Steps

N°	CV	Local	Volume	Mode	Action
01	0.00	Yes	20.0	Threshold	None
02	24.90	Yes	10.0	Threshold	None

Spectra for novel compounds

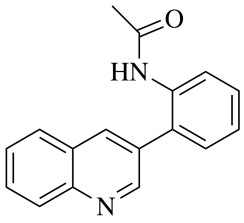

24

N-(2-(Quinolin-3-yl)phenyl)acetamide

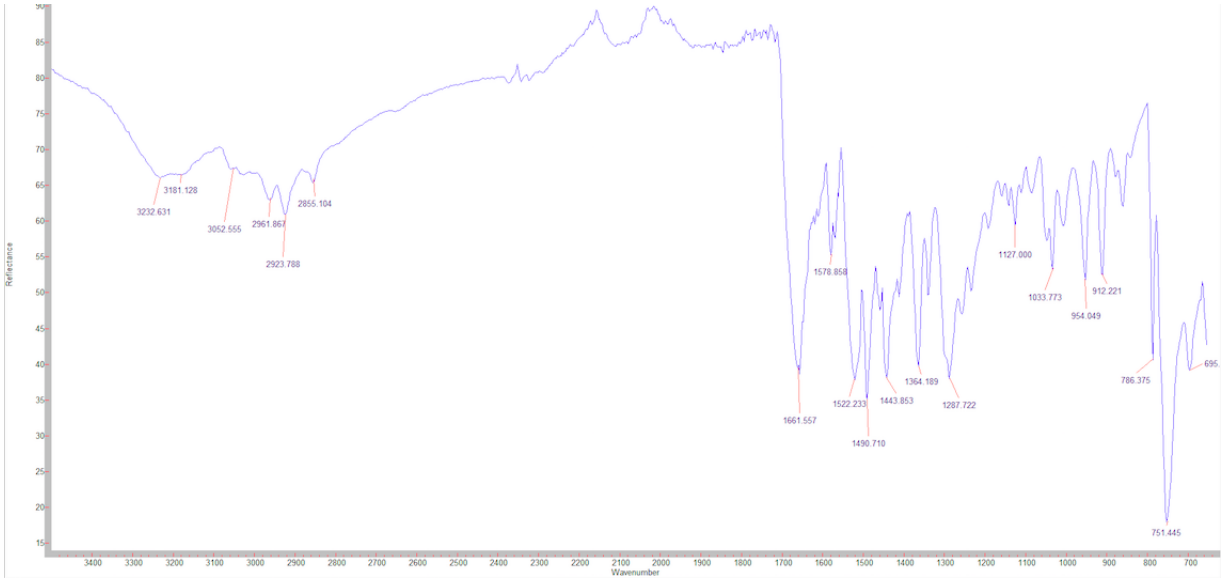

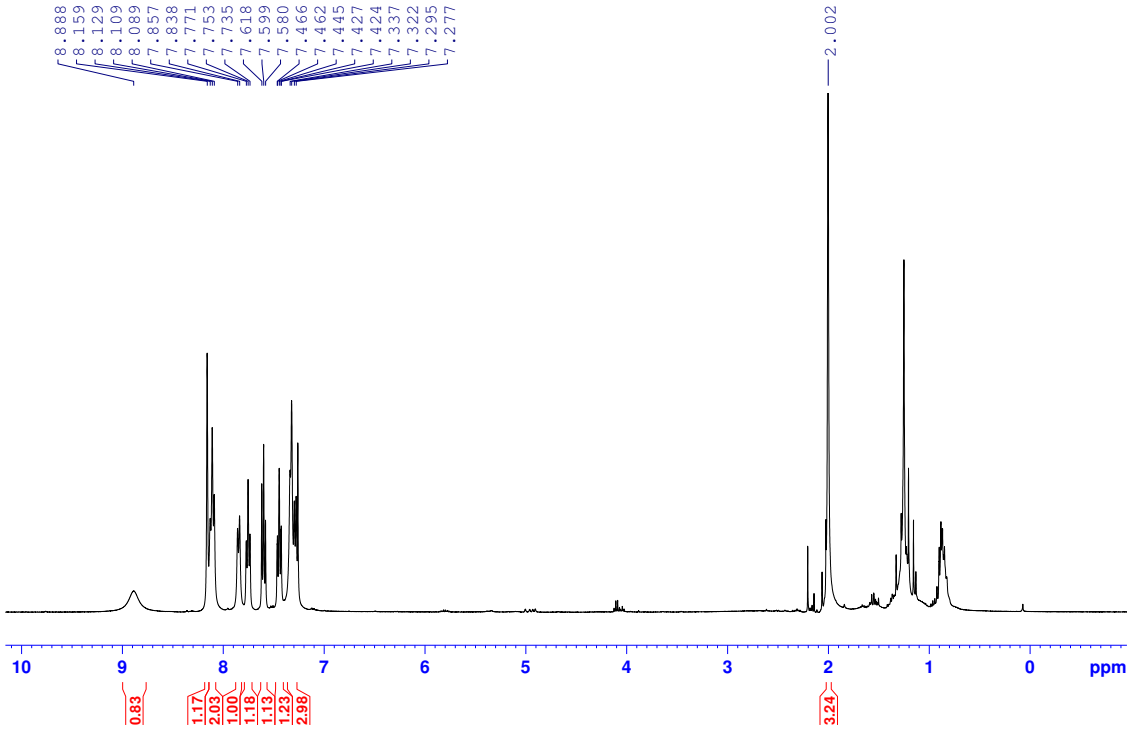
8.888
8.159
8.129
8.109
8.089
7.857
7.838
7.771
7.753
7.735
7.618
7.599
7.580
7.466
7.462
7.445
7.427
7.424
7.337
7.322
7.295
7.277
2.002
10
9
8
7
6
5
4
3
2
1
0
ppm
0.83
1.17
2.03
1.00
1.18
1.13
1.23
2.98
3.24

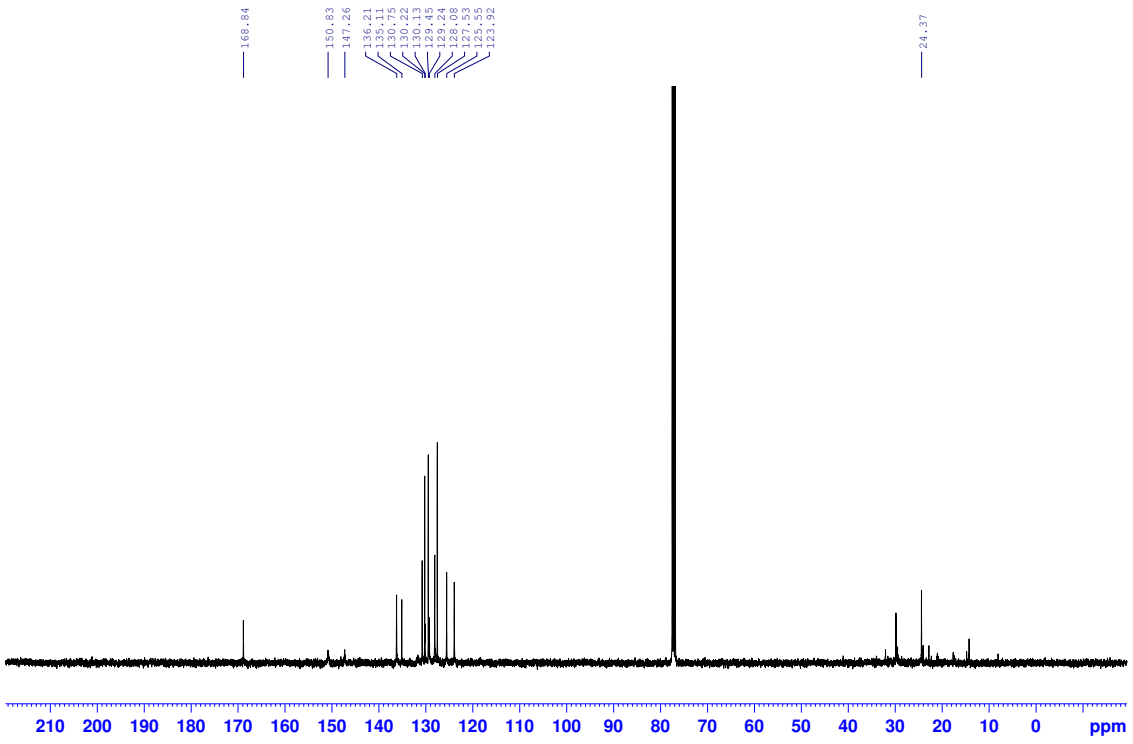
168.84
150.83
147.26
136.21
131.11
130.75
130.22
130.13
129.45
129.24
128.08
127.53
123.55
123.92
24.37
210
200
190
180
170
160
150
140
130
120
110
100
90
80
70
60
50
40
30
20
10
0
ppm

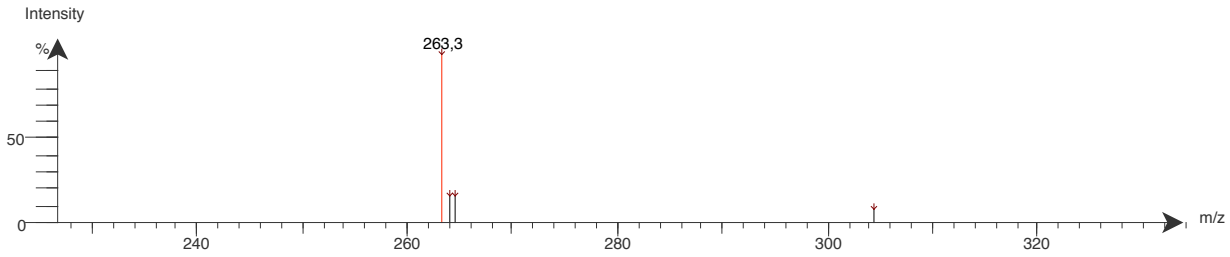
Intensity
%
263,3
50
0
240
260
280
300
320
m/z

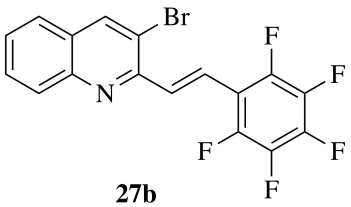

27b

(*E*)-3-Bromo-2-(2-(perfluorophenyl)vinyl)quinoline

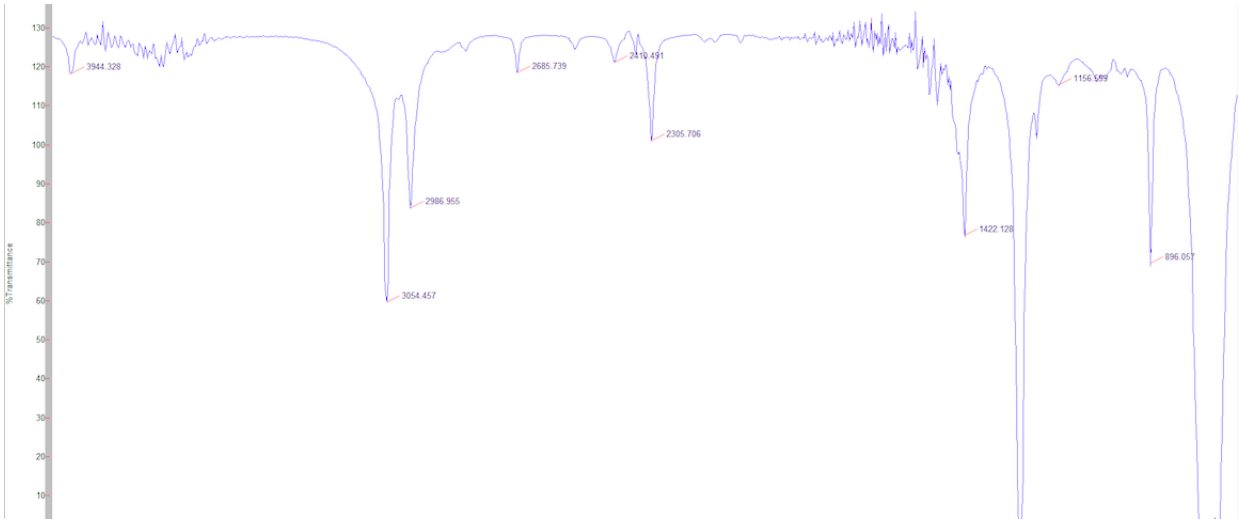

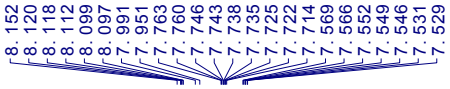

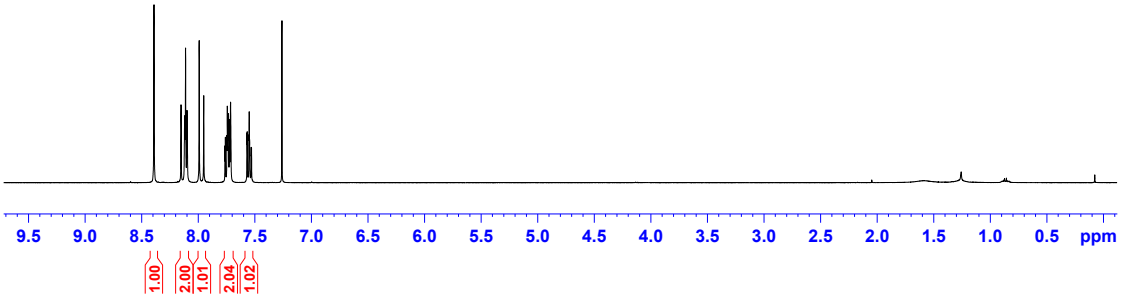

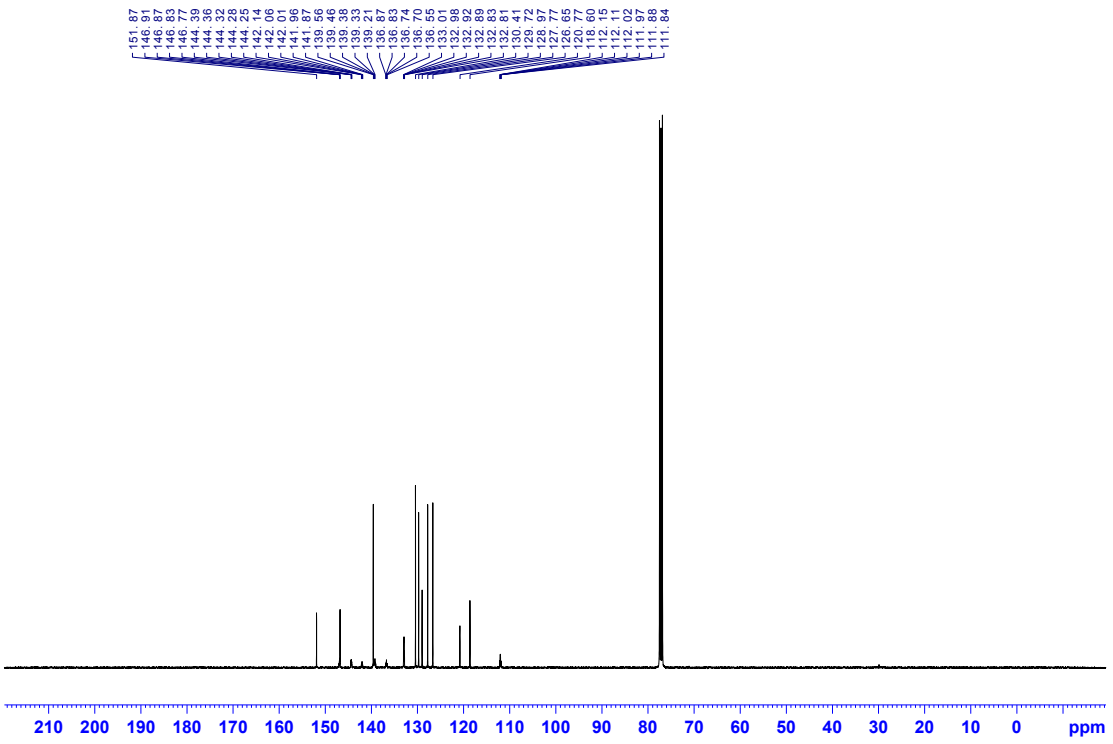
151.87
146.91
146.87
146.83
146.77
144.39
144.36
144.32
144.28
144.25
142.14
142.06
142.01
141.96
141.87
139.56
139.46
139.38
139.33
139.21
136.87
136.83
136.74
136.70
136.55
133.01
132.98
132.92
132.89
132.83
132.81
130.41
129.72
128.97
127.77
126.65
120.77
118.60
118.55
112.11
112.02
111.97
111.88
111.84
210 200 190 180 170 160 150 140 130 120 110 100 90 80 70 60 50 40 30 20 10 0 ppm

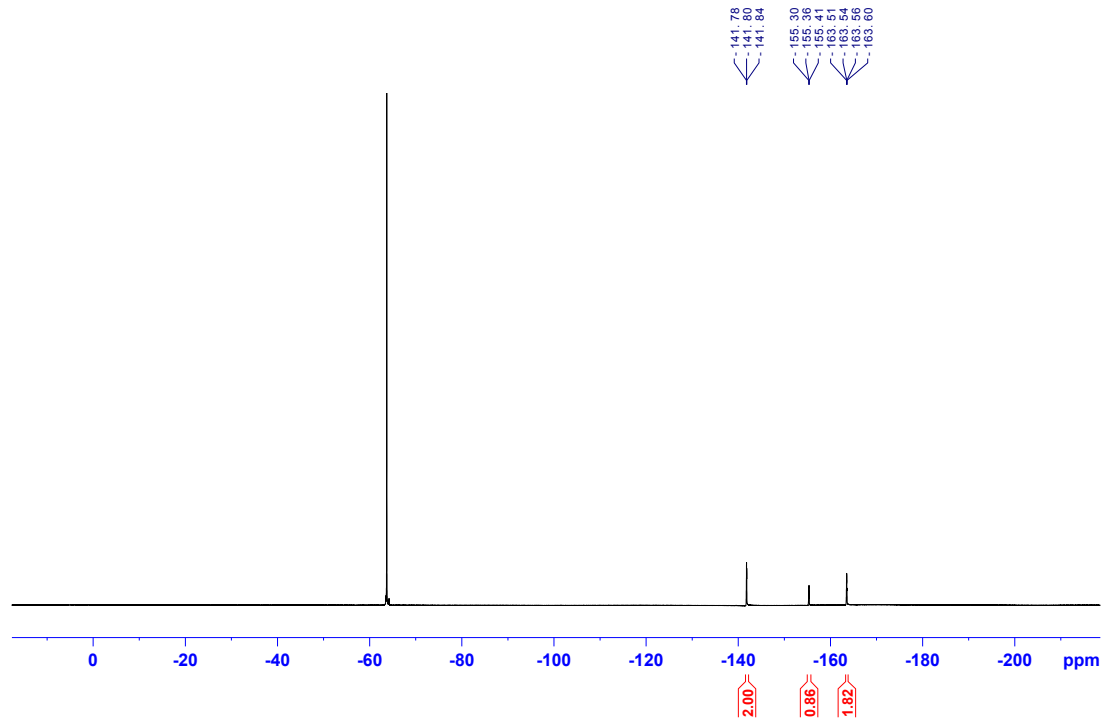
141.78
141.80
141.84
155.30
155.36
155.41
163.51
163.54
163.56
163.60
0 -20 -40 -60 -80 -100 -120 -140 -160 -180 -200 ppm
2.00
0.86
1.82

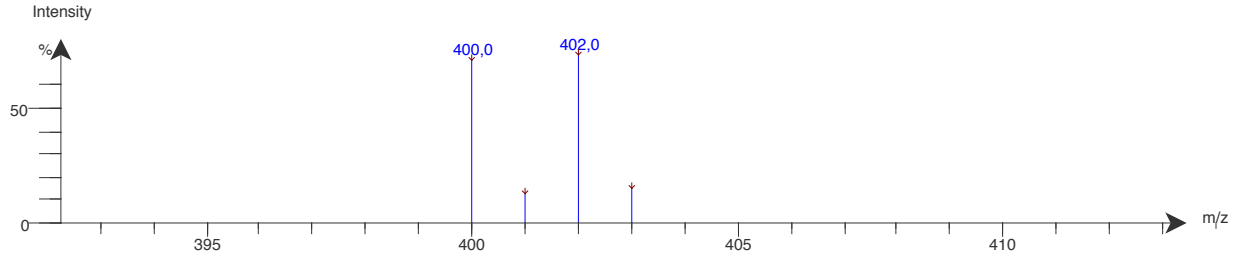
Intensity
%
50
0
400,0
402,0
395
400
405
410
m/z

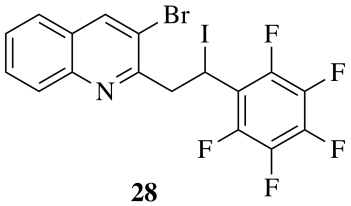

28

3-Bromo-2-(2-iodo-2-(perfluorophenyl)ethyl)quinoline

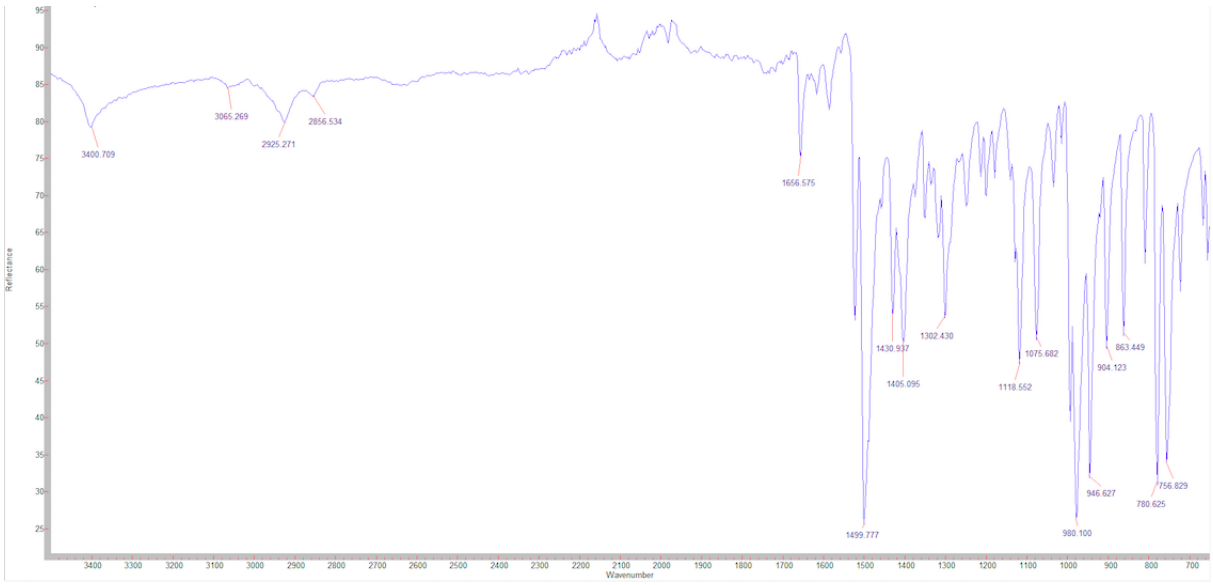

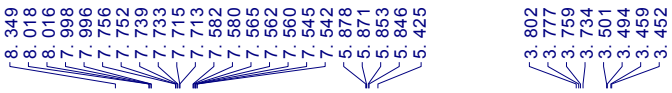

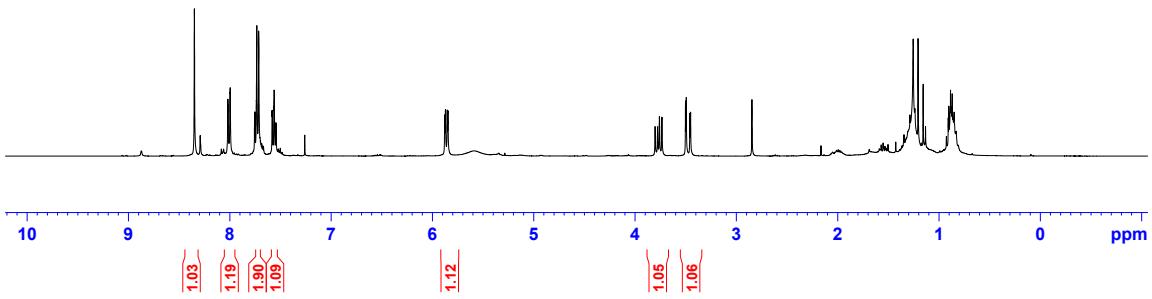

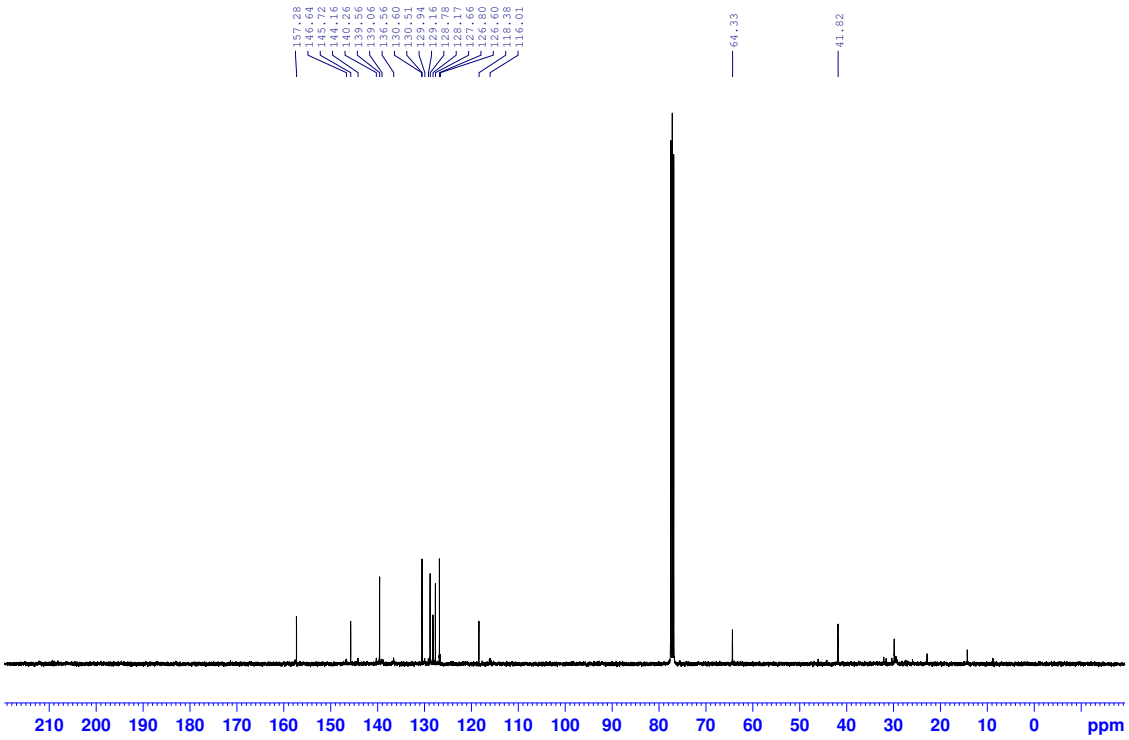
157.28
147.64
145.72
144.16
140.26
139.56
139.06
136.56
130.60
130.51
129.94
129.16
128.78
128.17
127.66
126.80
126.60
118.38
116.01
64.33
41.82
210 200 190 180 170 160 150 140 130 120 110 100 90 80 70 60 50 40 30 20 10 0 ppm

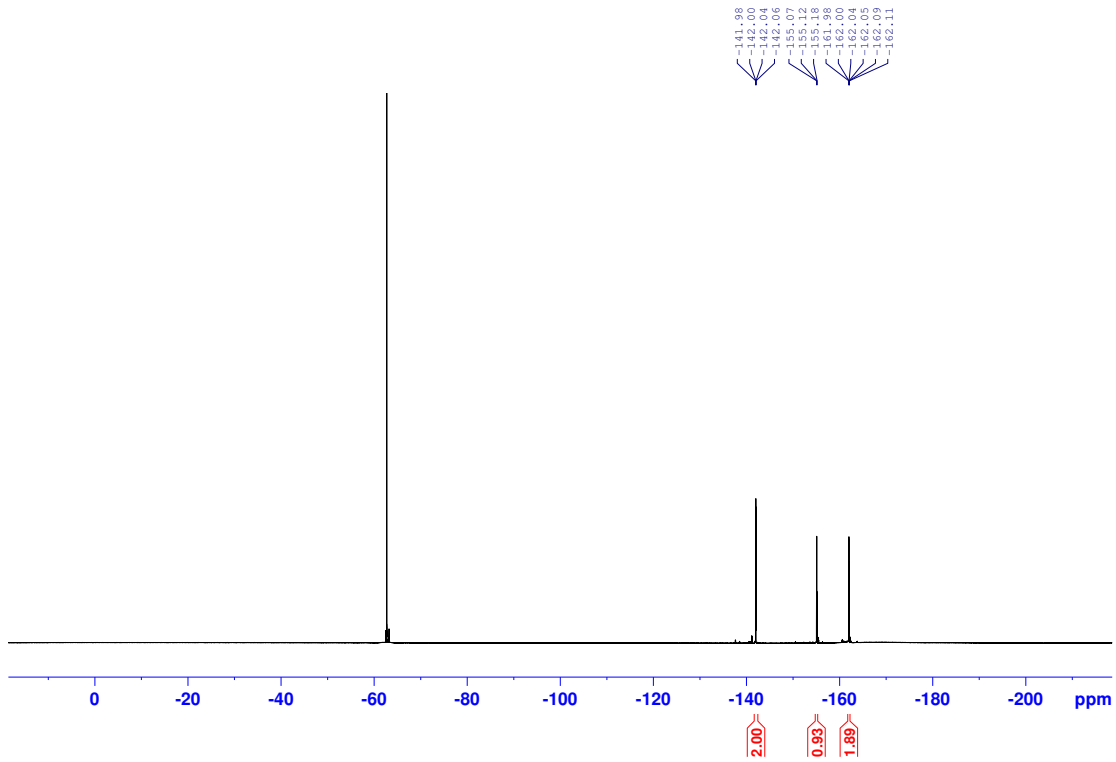
-141.98
-142.00
-142.04
-142.06
-155.07
-155.12
-155.18
-161.98
-162.00
-162.04
-162.05
-162.09
-162.11
0 -20 -40 -60 -80 -100 -120 -140 -160 -180 -200 ppm
2.00
0.93
1.89

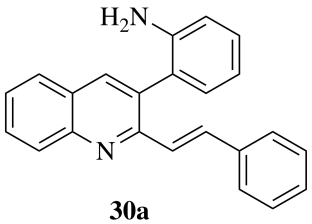

30a

(*E*)-2-(2-Styrylquinolin-3-yl)aniline

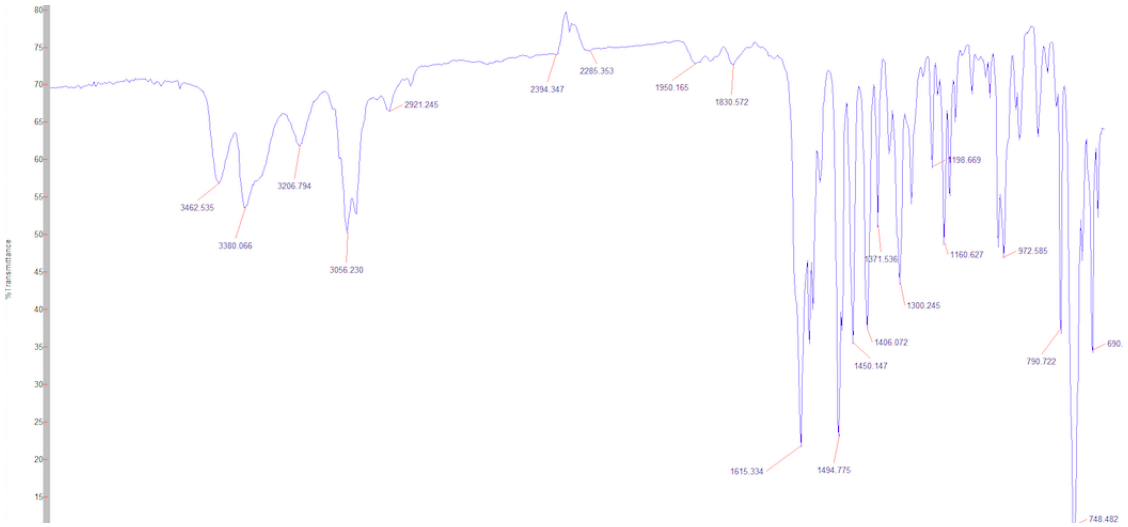

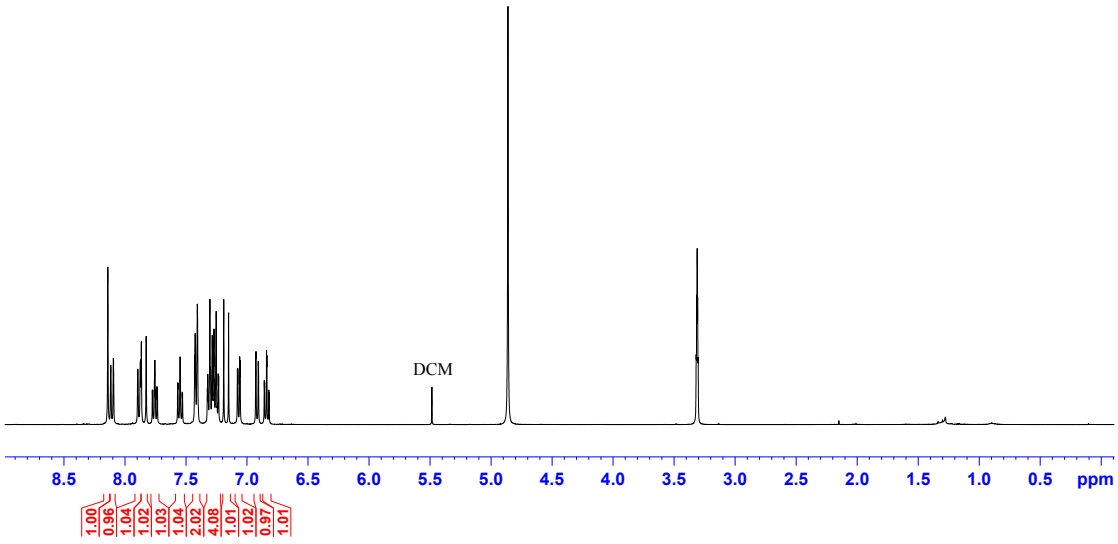

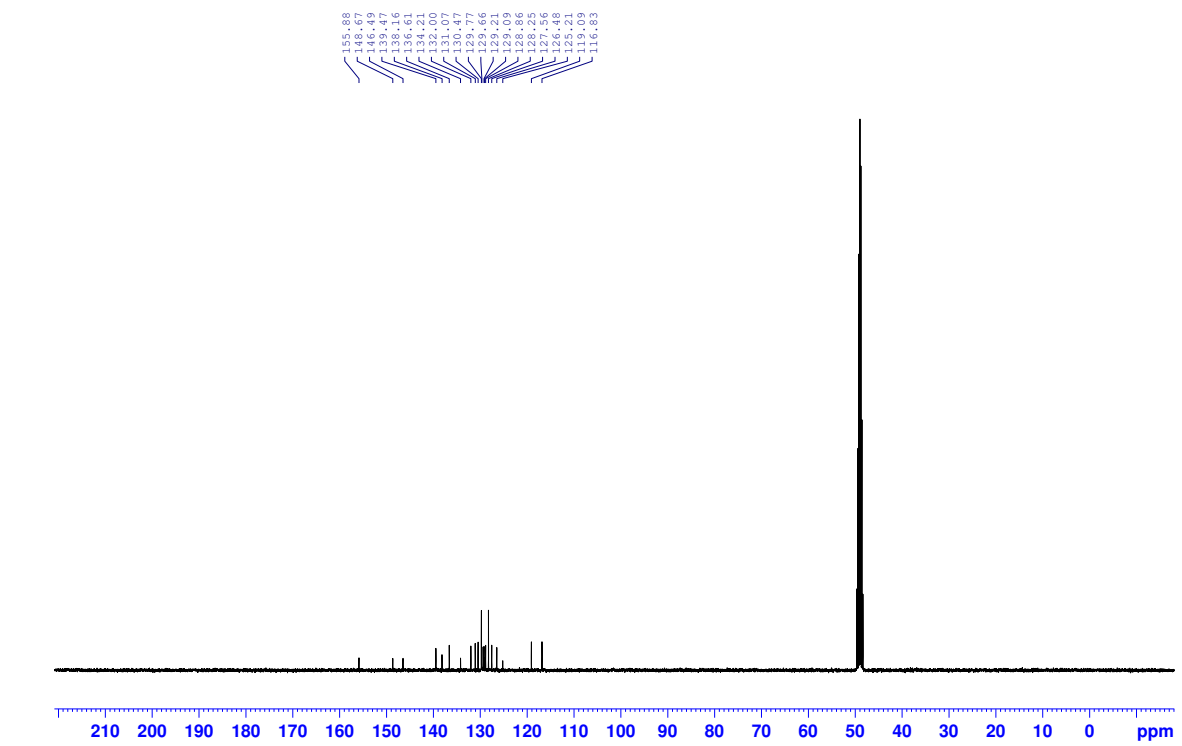
155.88
149.67
146.49
139.47
138.16
136.61
134.21
132.00
131.07
130.77
129.77
129.66
129.21
129.09
128.86
128.25
127.56
126.48
126.21
119.09
116.83
210 200 190 180 170 160 150 140 130 120 110 100 90 80 70 60 50 40 30 20 10 0 ppm

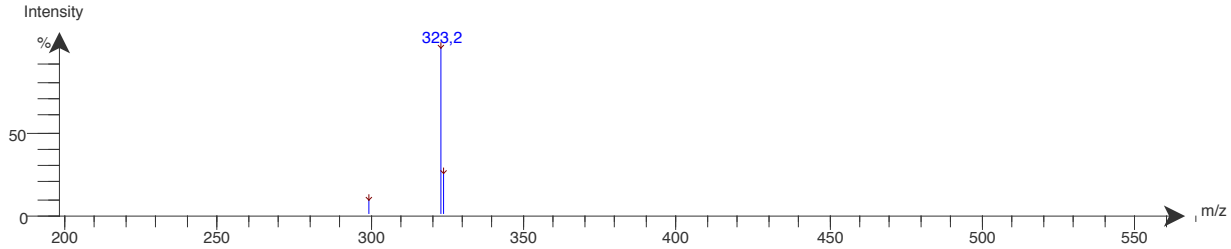
Intensity
%
323,2
50
0
200 250 300 350 400 450 500 550
m/z

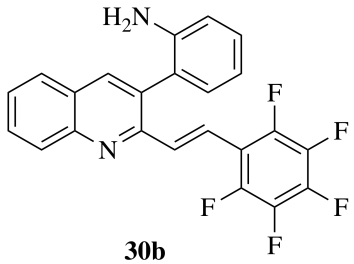

30b

(*E*)-2-(2-(2-(Perfluorophenyl)vinyl)quinolin-3-yl)aniline

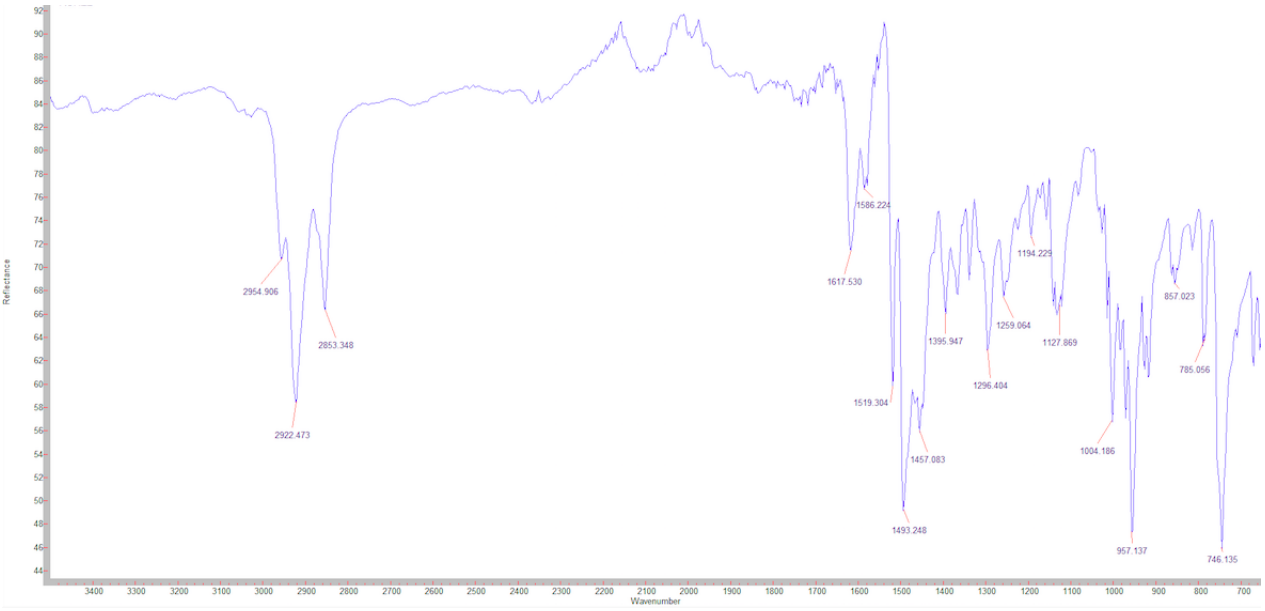

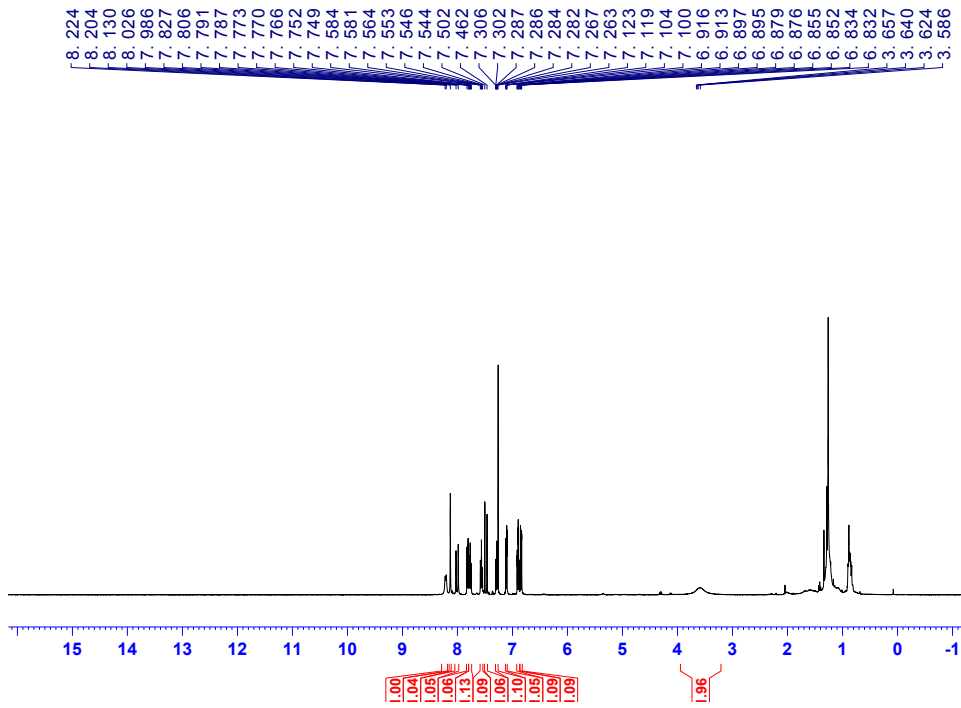
8.224
8.204
8.130
8.026
7.986
7.827
7.806
7.791
7.787
7.773
7.770
7.766
7.752
7.749
7.584
7.581
7.564
7.553
7.546
7.544
7.502
7.462
7.306
7.302
7.287
7.286
7.284
7.282
7.267
7.263
7.123
7.119
7.104
7.100
6.916
6.913
6.897
6.895
6.879
6.876
6.855
6.852
6.834
6.832
3.657
3.640
3.624
3.586
15 14 13 12 11 10 9 8 7 6 5 4 3 2 1 0 -1 -2 ppm
1.00 1.04 1.05 1.06 1.13 1.09 1.06 1.10 1.05 1.09 1.09
1.96

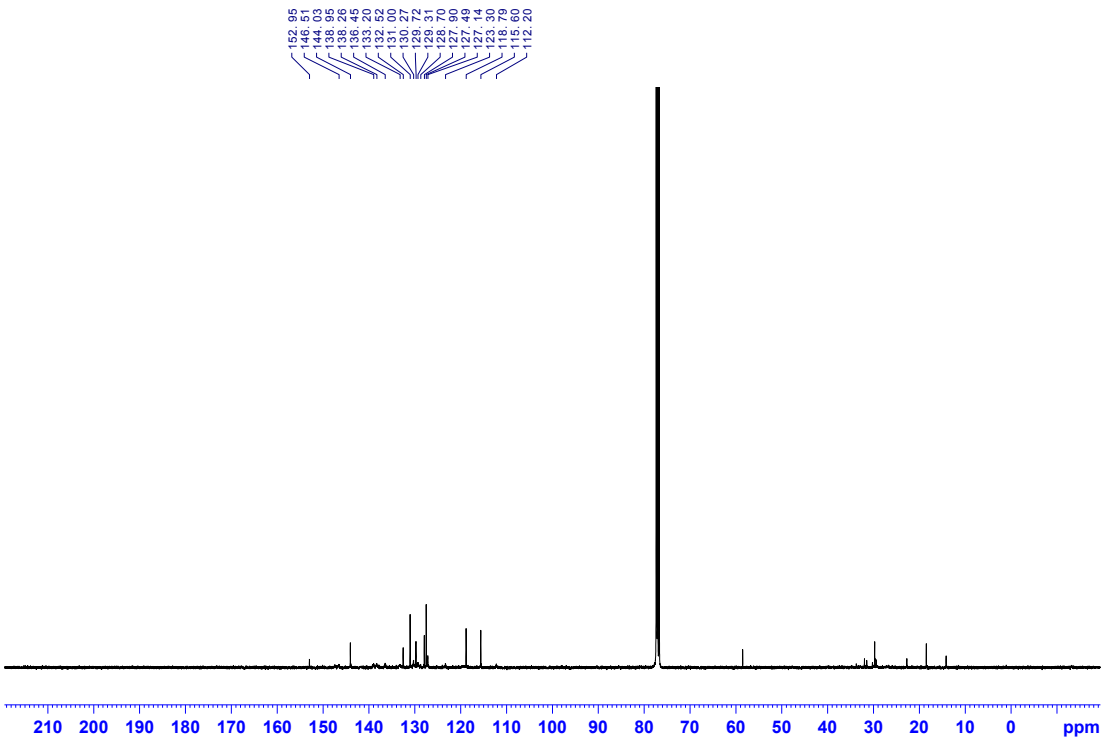
152.95
146.51
144.03
138.95
138.26
136.45
133.20
132.52
131.00
130.27
129.72
129.31
128.70
127.90
127.49
127.14
123.30
118.79
115.60
112.20
210 200 190 180 170 160 150 140 130 120 110 100 90 80 70 60 50 40 30 20 10 0 ppm

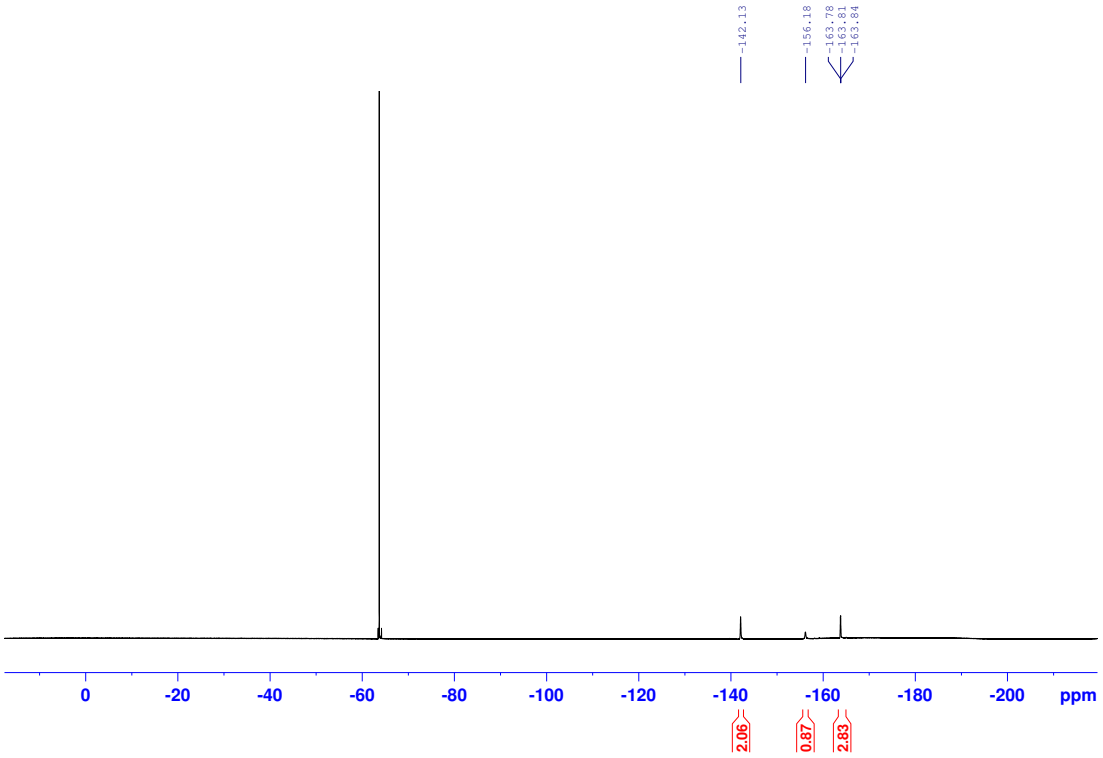
-142.13
-156.18
-163.78
-163.81
-163.84
0
-20
-40
-60
-80
-100
-120
-140
-160
-180
-200
ppm
2.06
0.87
2.83

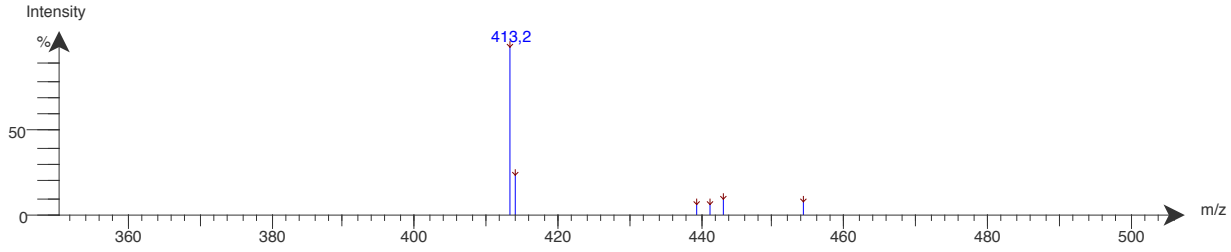
Intensity
%
50
0
413,2
360
380
400
420
440
460
480
500
m/z

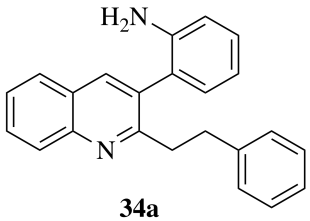

34a

2-(2-Phenethylquinolin-3-yl)aniline

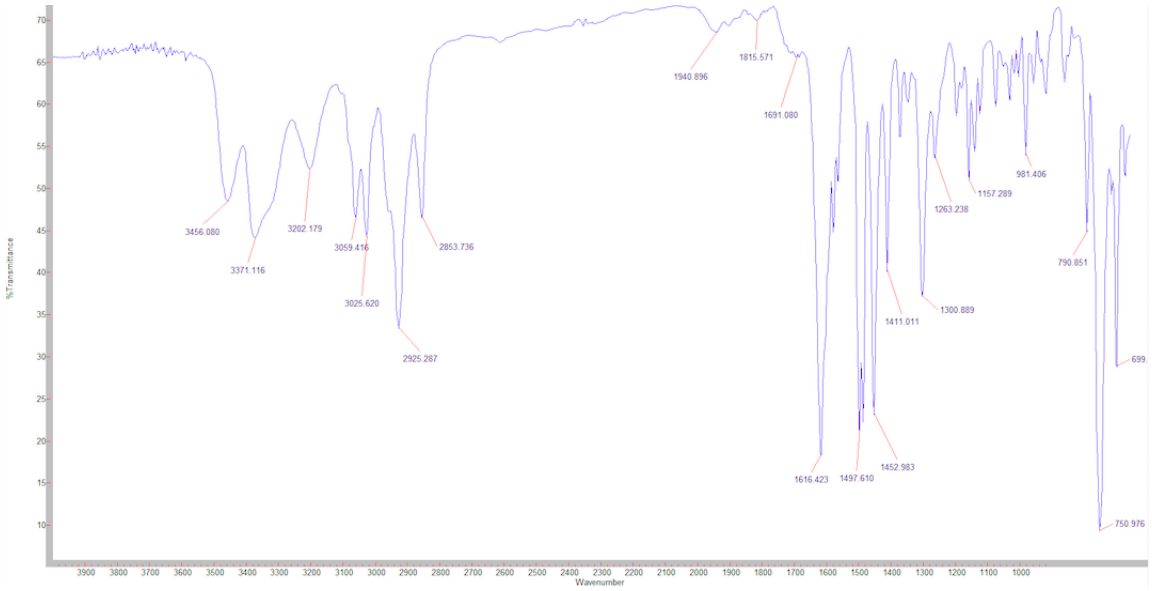

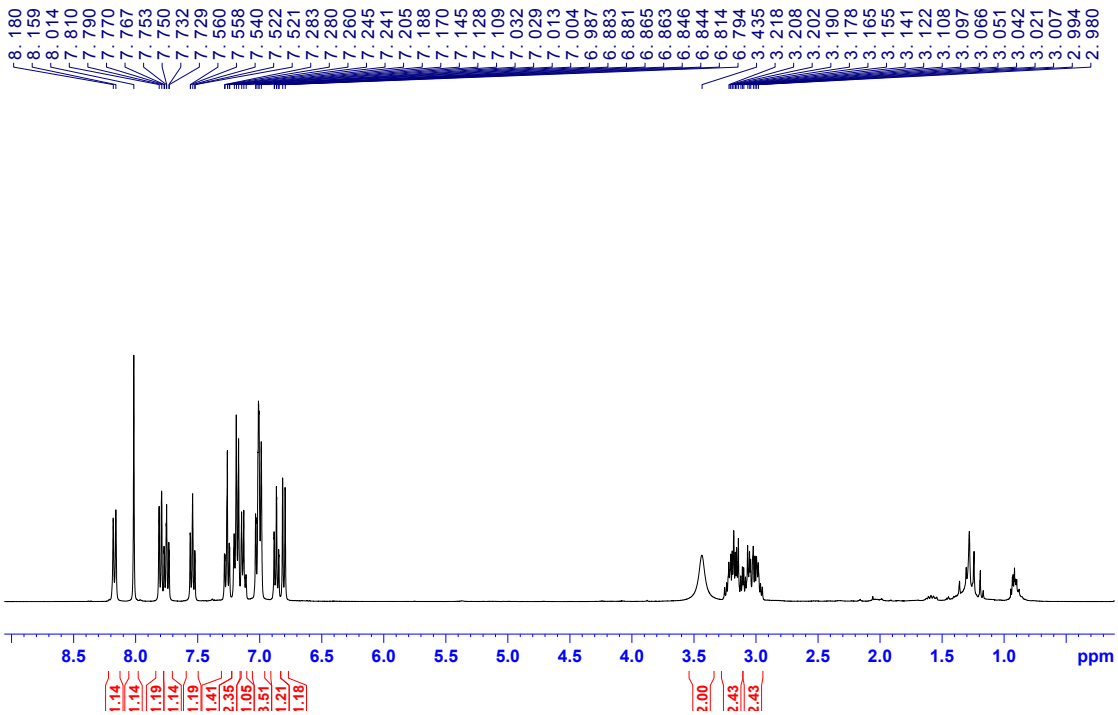
8.180
8.159
8.014
7.810
7.790
7.770
7.767
7.753
7.750
7.732
7.729
7.560
7.558
7.540
7.522
7.521
7.283
7.280
7.260
7.245
7.241
7.205
7.188
7.170
7.145
7.128
7.109
7.032
7.029
7.013
7.004
6.987
6.883
6.881
6.865
6.863
6.846
6.844
6.814
6.794
3.435
3.218
3.208
3.202
3.190
3.178
3.165
3.155
3.141
3.122
3.108
3.097
3.066
3.051
3.042
3.021
3.007
2.994
2.980
8.5
8.0
7.5
7.0
6.5
6.0
5.5
5.0
4.5
4.0
3.5
3.0
2.5
2.0
1.5
1.0
ppm
1.14
1.14
1.19
1.14
1.19
1.41
2.35
1.05
3.51
1.21
1.18
2.00
2.43
2.43

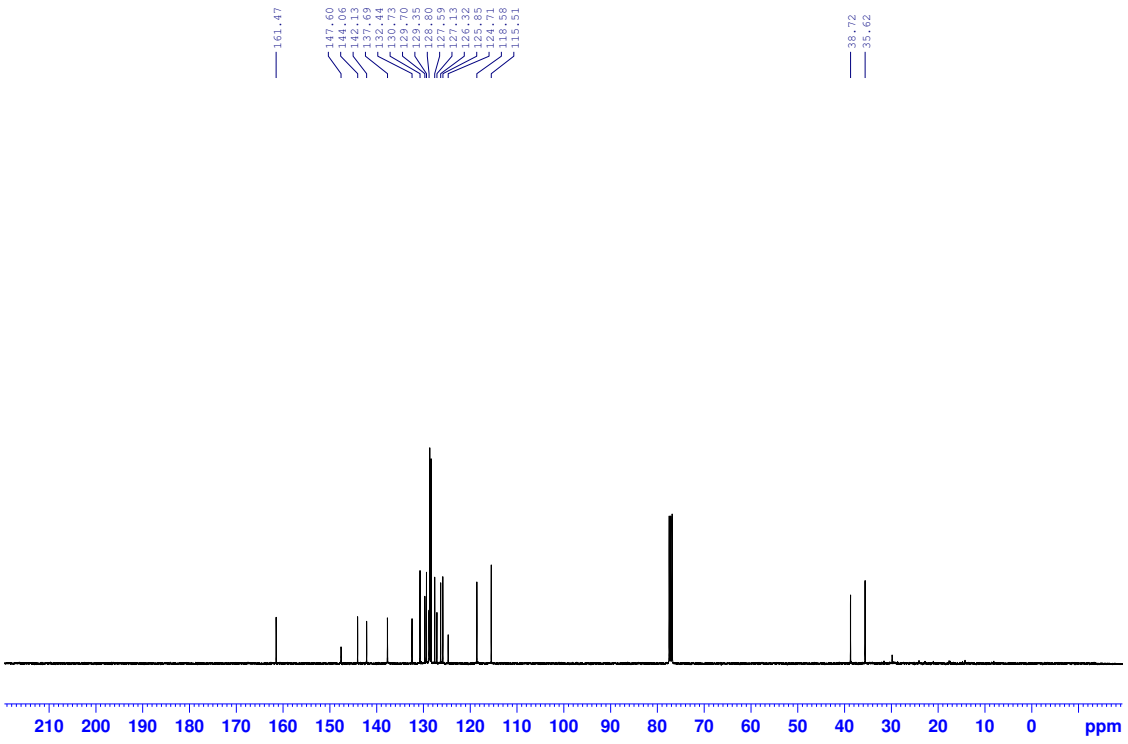
161.47
147.60
144.06
142.13
137.69
133.44
130.73
129.70
129.35
128.80
127.59
127.13
126.32
125.55
124.71
118.58
115.51
38.72
35.62
210
200
190
180
170
160
150
140
130
120
110
100
90
80
70
60
50
40
30
20
10
0
ppm

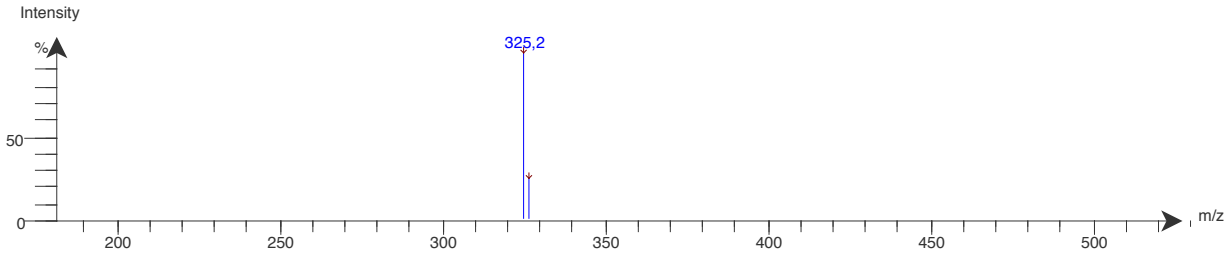
Intensity
%
325,2
50
0
200
250
300
350
400
450
500
m/z

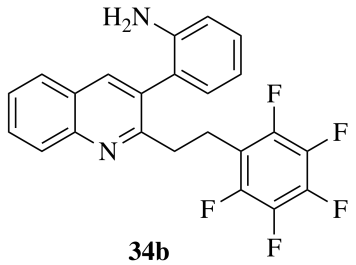

34b

2-(2-(2-(Perfluorophenyl)ethyl)quinolin-3-yl)aniline

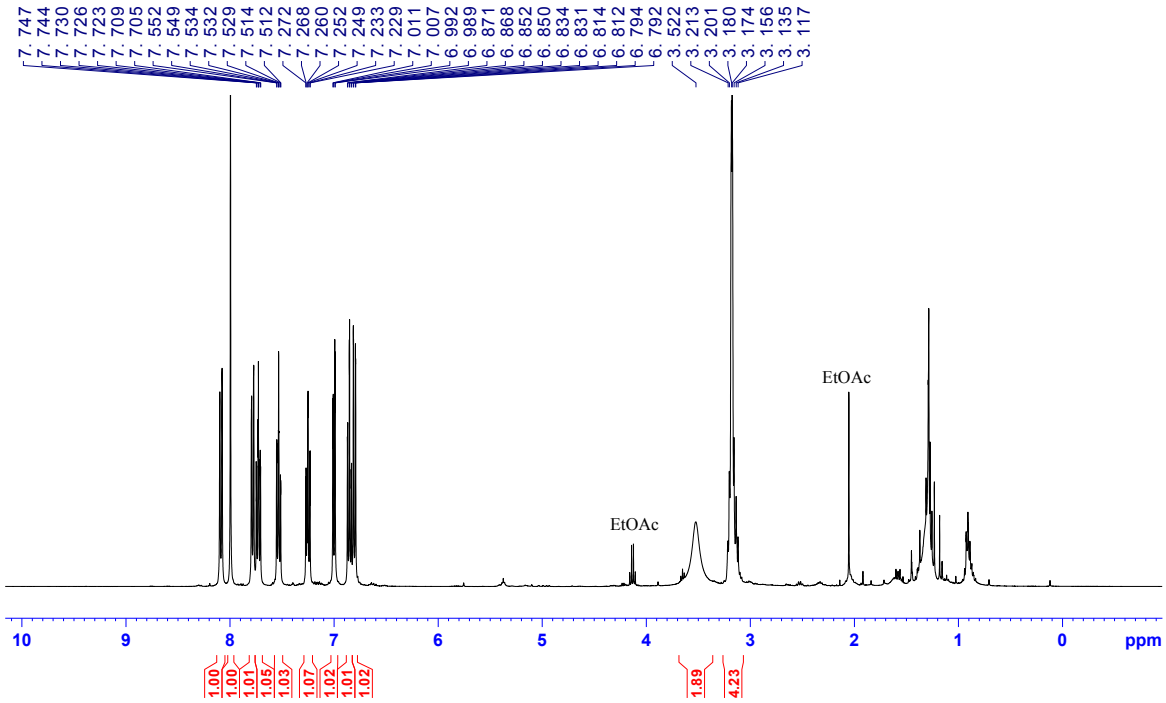
7.747
7.744
7.730
7.726
7.723
7.709
7.705
7.552
7.549
7.534
7.532
7.529
7.514
7.512
7.272
7.268
7.260
7.252
7.249
7.233
7.229
7.011
7.007
6.992
6.989
6.871
6.868
6.852
6.850
6.834
6.831
6.814
6.812
6.794
6.792
3.522
3.213
3.201
3.180
3.174
3.156
3.135
3.117
EtOAc
EtOAc
10
9
8
7
6
5
4
3
2
1
0
ppm
1.00
1.00
1.01
1.05
1.03
1.07
1.02
1.01
1.02
1.89
4.23

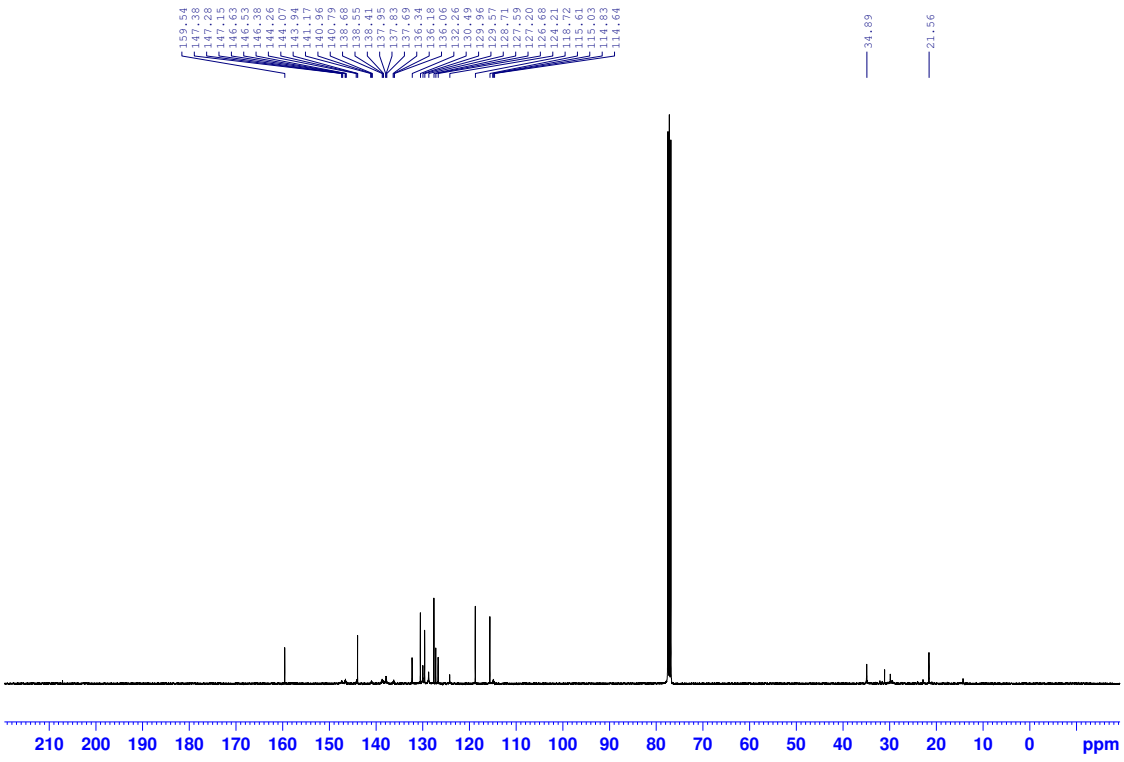
159.54
147.38
147.28
147.15
146.63
146.53
146.38
144.26
144.07
143.94
141.17
140.96
140.79
138.68
138.55
138.41
137.95
137.83
137.69
136.34
136.18
136.06
132.26
130.49
129.96
129.57
128.71
127.59
127.20
126.68
124.21
118.72
115.61
115.03
114.83
114.64
34.89
21.56
210
200
190
180
170
160
150
140
130
120
110
100
90
80
70
60
50
40
30
20
10
0
ppm

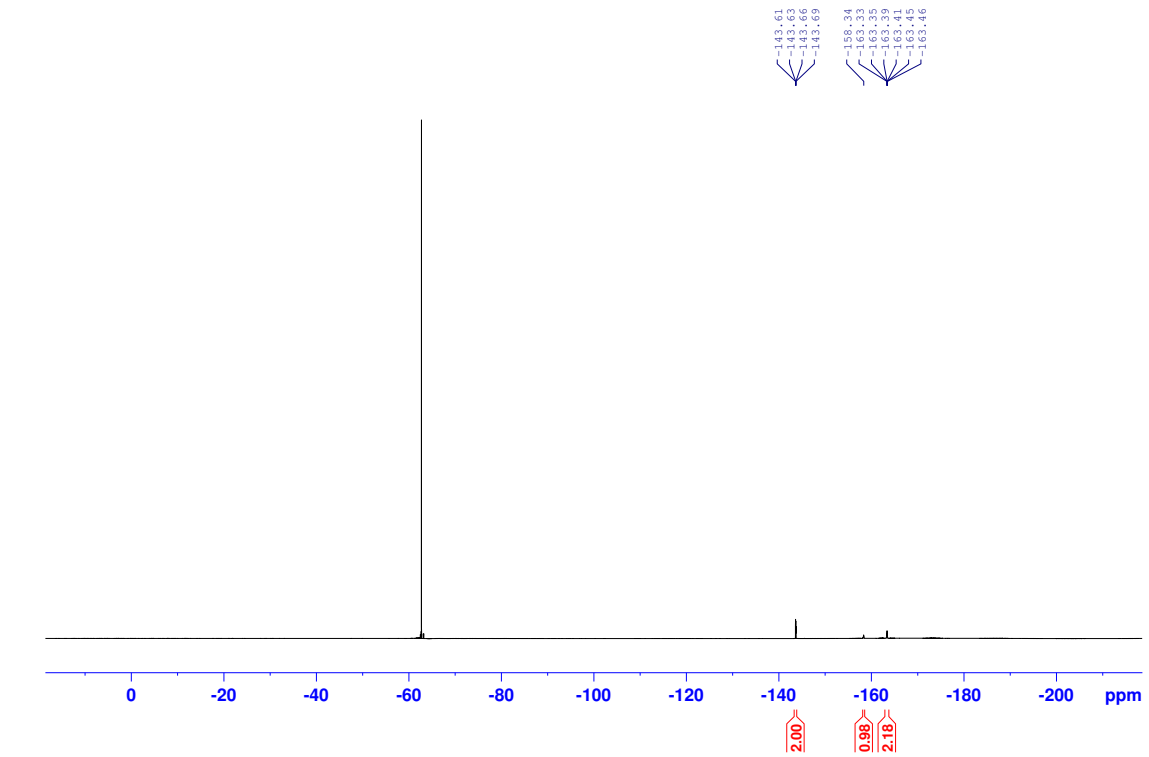
-143.61
-143.63
-143.66
-143.69
-158.34
-163.33
-163.35
-163.39
-163.41
-163.45
-163.46
0
-20
-40
-60
-80
-100
-120
-140
-160
-180
-200
ppm
2.00
0.98
2.18

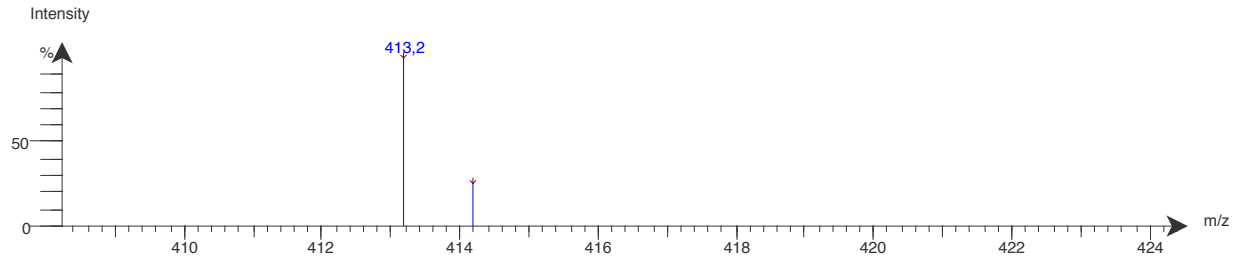
Intensity
%
50
0
413.2
410
412
414
416
418
420
422
424
m/z

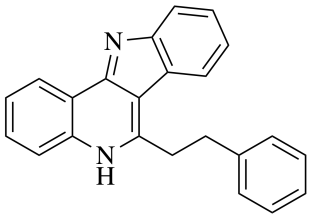

39a
6-Phenethyl-5*H*-indolo[3,2-*c*]quinoline

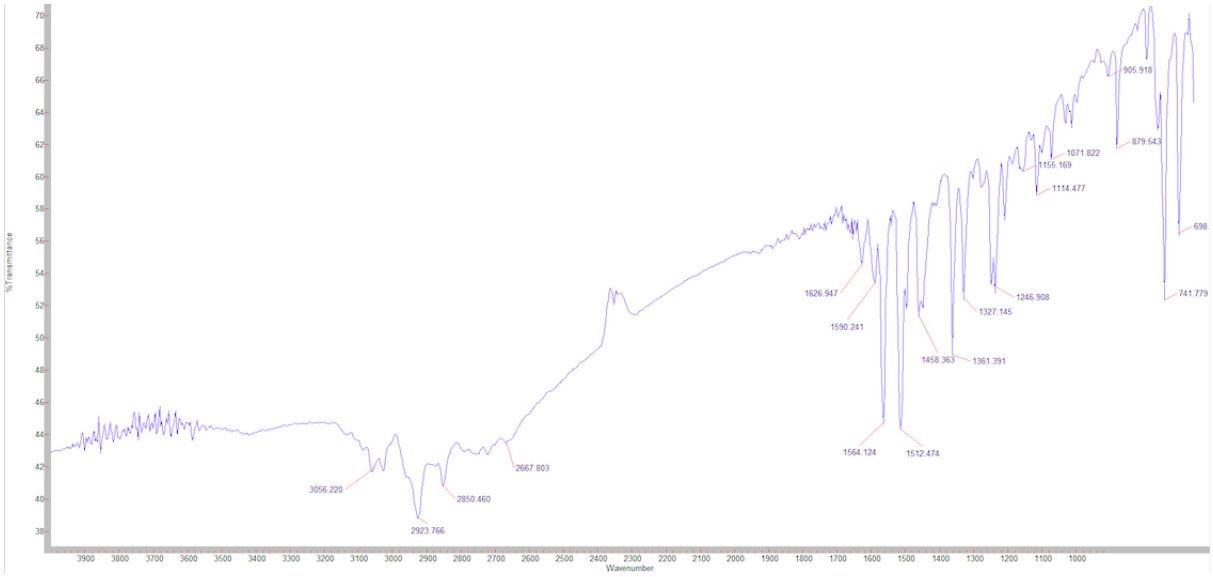

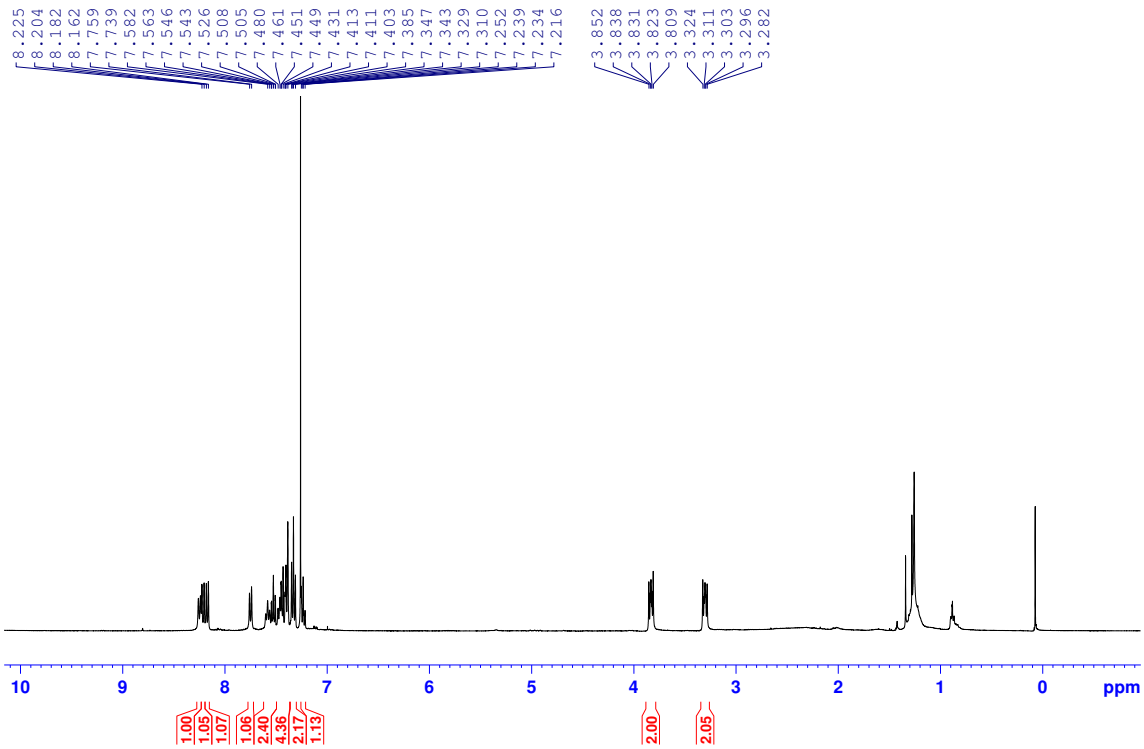
8.225
8.204
8.182
8.162
7.759
7.739
7.582
7.563
7.546
7.543
7.526
7.508
7.505
7.480
7.461
7.451
7.449
7.431
7.413
7.411
7.403
7.385
7.347
7.343
7.329
7.310
7.252
7.239
7.234
7.216
3.852
3.838
3.831
3.823
3.809
3.324
3.311
3.303
3.296
3.282
10 9 8 7 6 5 4 3 2 1 0 ppm
1.00 1.05 1.07 1.06 2.40 4.36 2.17 1.13 2.00 2.05

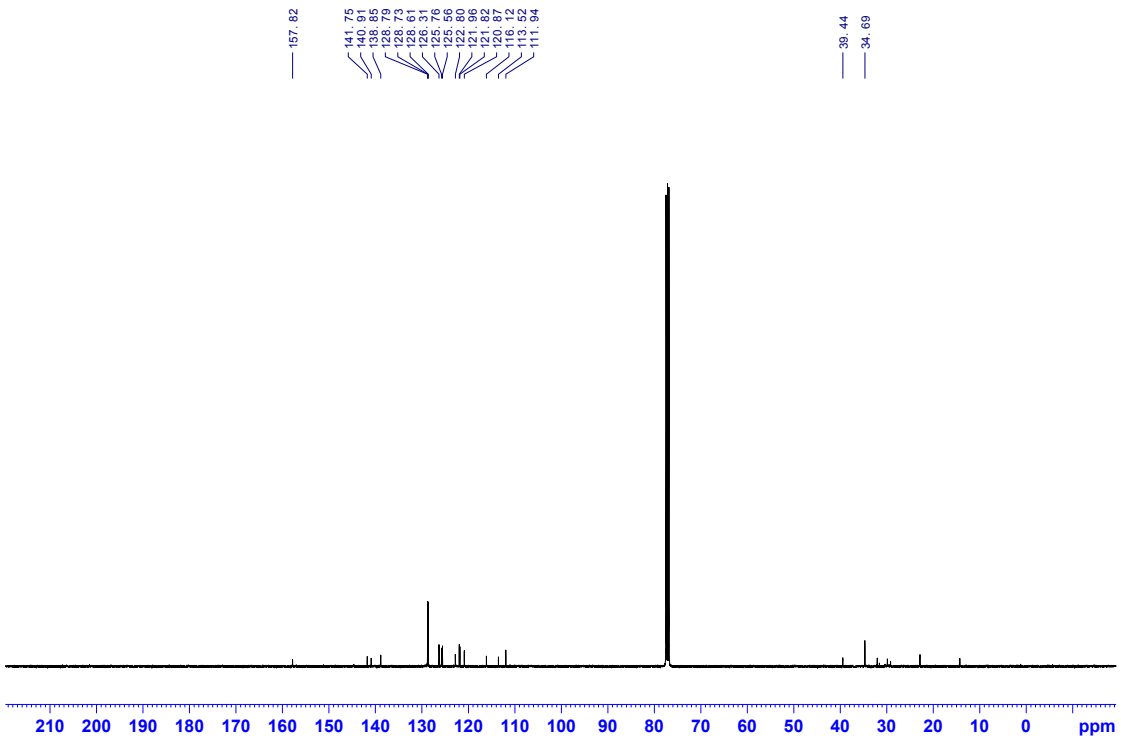
157.82
141.75
140.91
138.85
128.79
128.73
128.61
126.31
125.76
125.56
122.80
121.96
121.82
120.87
116.12
113.52
111.94
39.44
34.69
210 200 190 180 170 160 150 140 130 120 110 100 90 80 70 60 50 40 30 20 10 0 ppm

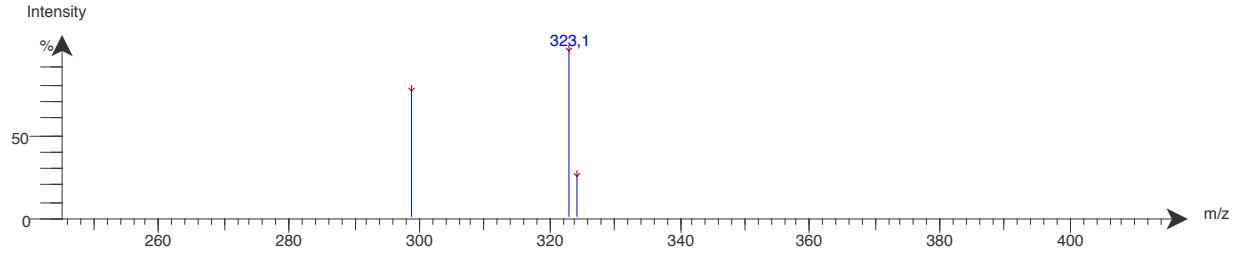
Intensity
%
50
0
323,1
260
280
300
320
340
360
380
400
m/z

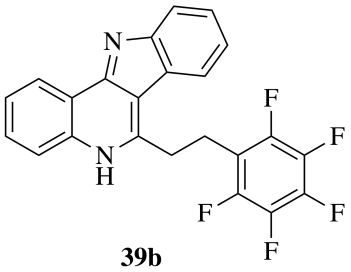

39b

6-(2-(Perfluorophenyl)ethyl)-5*H*-indolo[3,2-*c*]quinoline

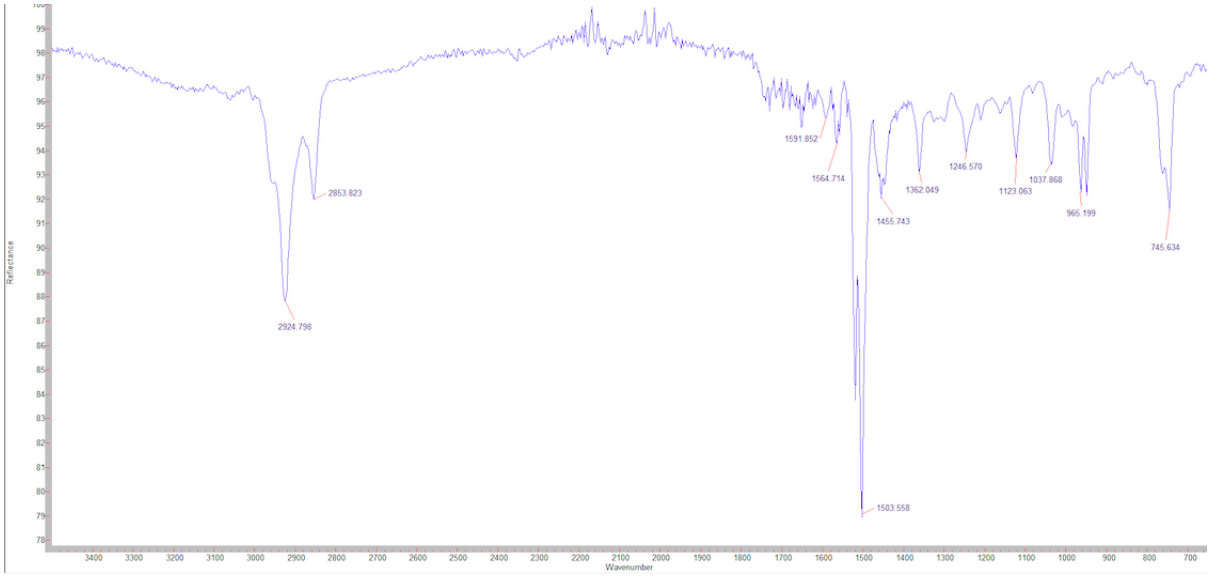

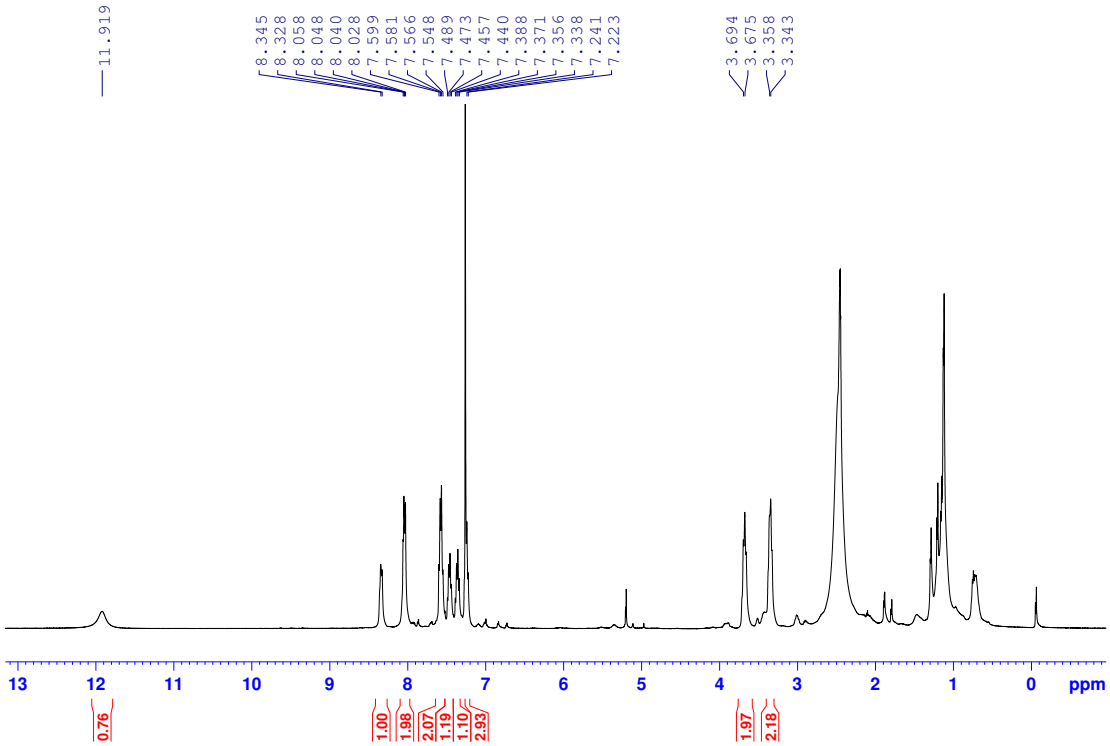
11.919
8.345
8.328
8.058
8.048
8.040
8.028
7.599
7.581
7.566
7.548
7.489
7.473
7.457
7.440
7.388
7.371
7.356
7.338
7.241
7.223
3.694
3.675
3.358
3.343
13 12 11 10 9 8 7 6 5 4 3 2 1 0 ppm
0.76
1.00
1.98
2.07
1.19
1.10
2.93
1.97
2.18

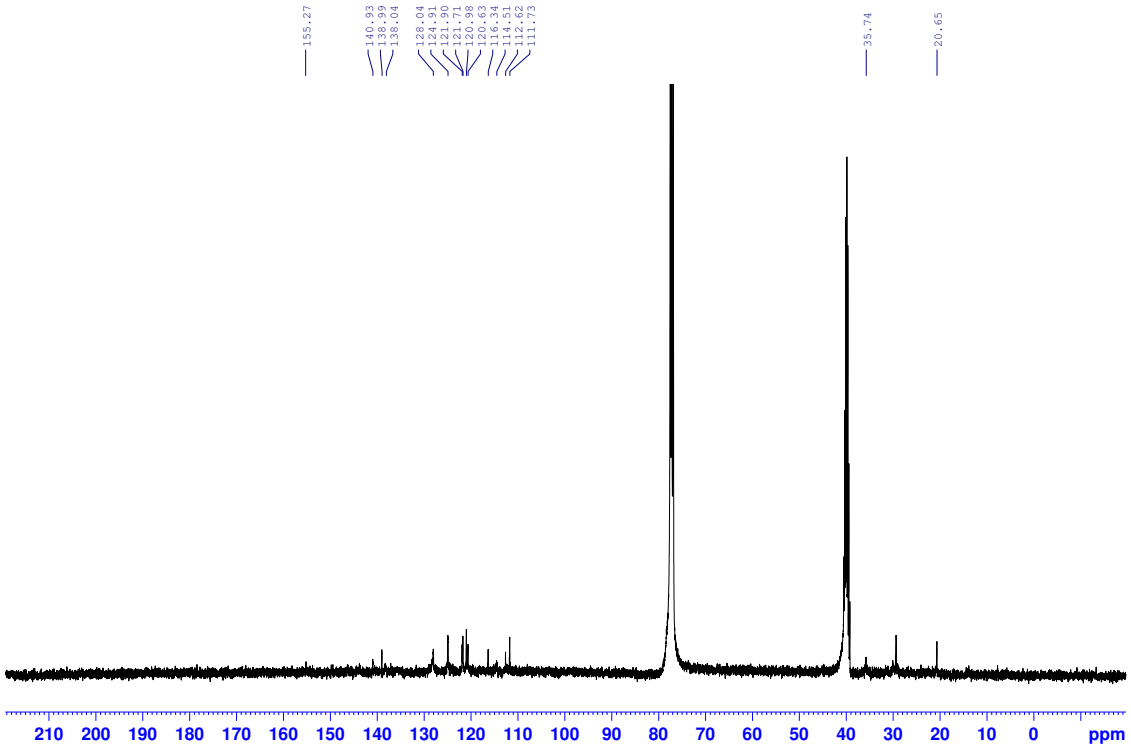
155.27
140.93
138.99
138.04
128.04
124.91
121.90
121.71
120.98
120.63
116.34
114.51
112.62
111.73
35.74
20.65
210 200 190 180 170 160 150 140 130 120 110 100 90 80 70 60 50 40 30 20 10 0 ppm

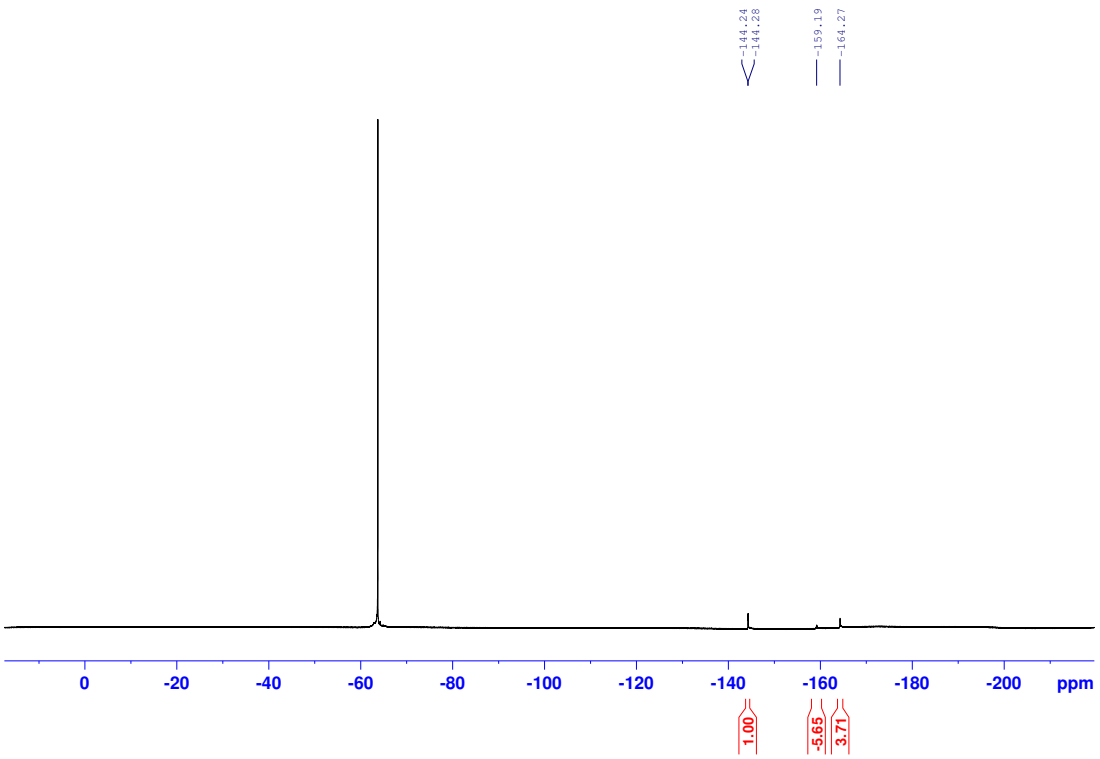
-144.24
-144.28
-159.19
-164.27
0
-20
-40
-60
-80
-100
-120
-140
-160
-180
-200
ppm
1.00
5.65
3.71

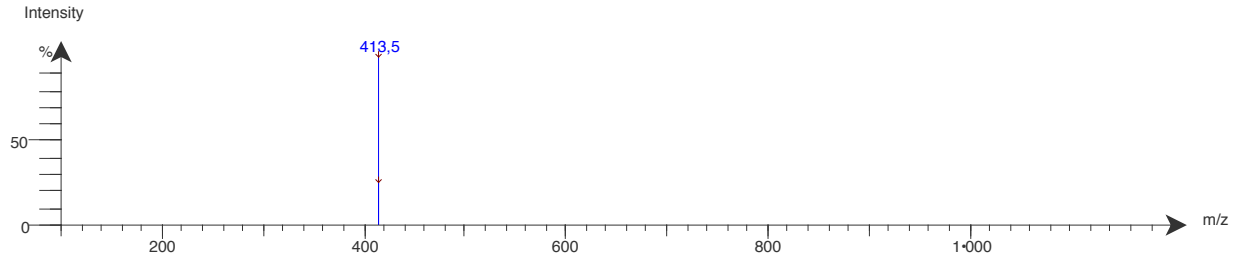
Intensity
%
413,5
50
0
200
400
600
800
1000
m/z

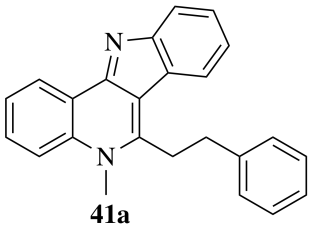

41a

5-Methyl-6-phenethyl-5*H*-indolo[3,2-*c*]quinoline

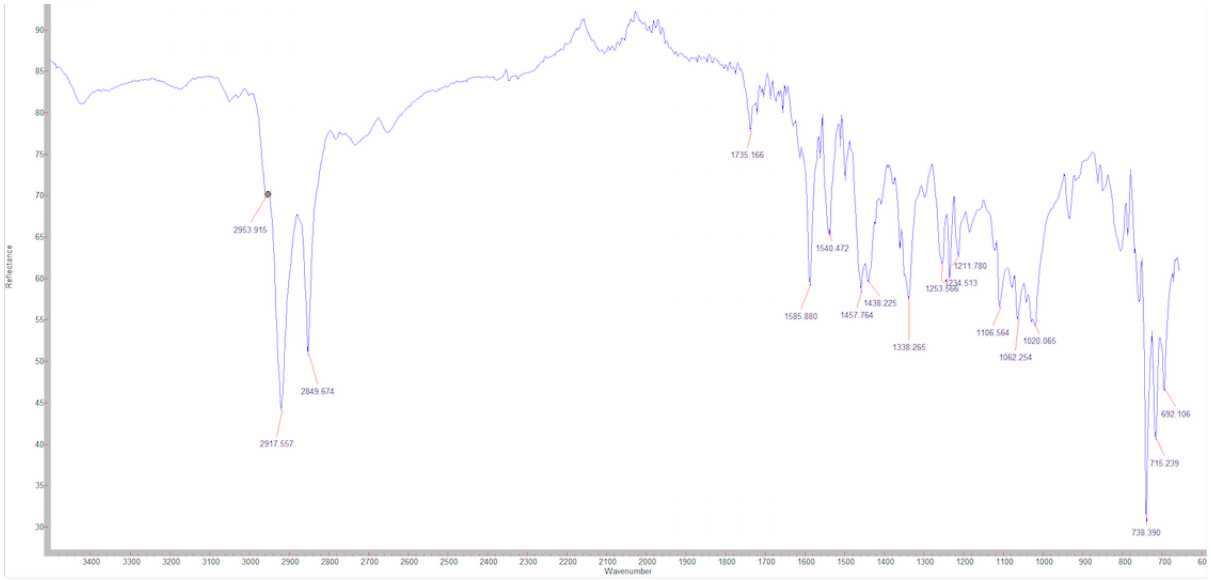

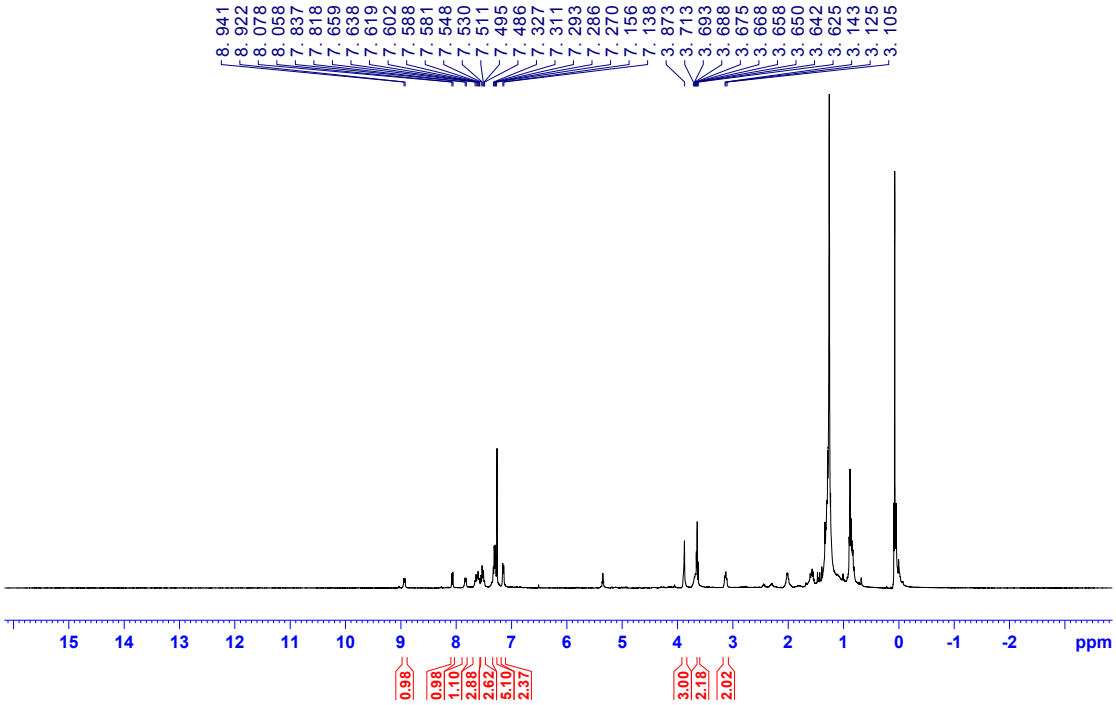
8.941
8.922
8.078
8.058
7.837
7.818
7.659
7.638
7.619
7.602
7.588
7.581
7.548
7.530
7.511
7.495
7.486
7.327
7.311
7.293
7.286
7.270
7.156
7.138
3.873
3.713
3.693
3.688
3.675
3.668
3.658
3.650
3.642
3.625
3.143
3.125
3.105
15 14 13 12 11 10 9 8 7 6 5 4 3 2 1 0 -1 -2 ppm
0.98
0.98
1.10
2.88
2.62
5.10
2.37
3.00
2.18
2.02

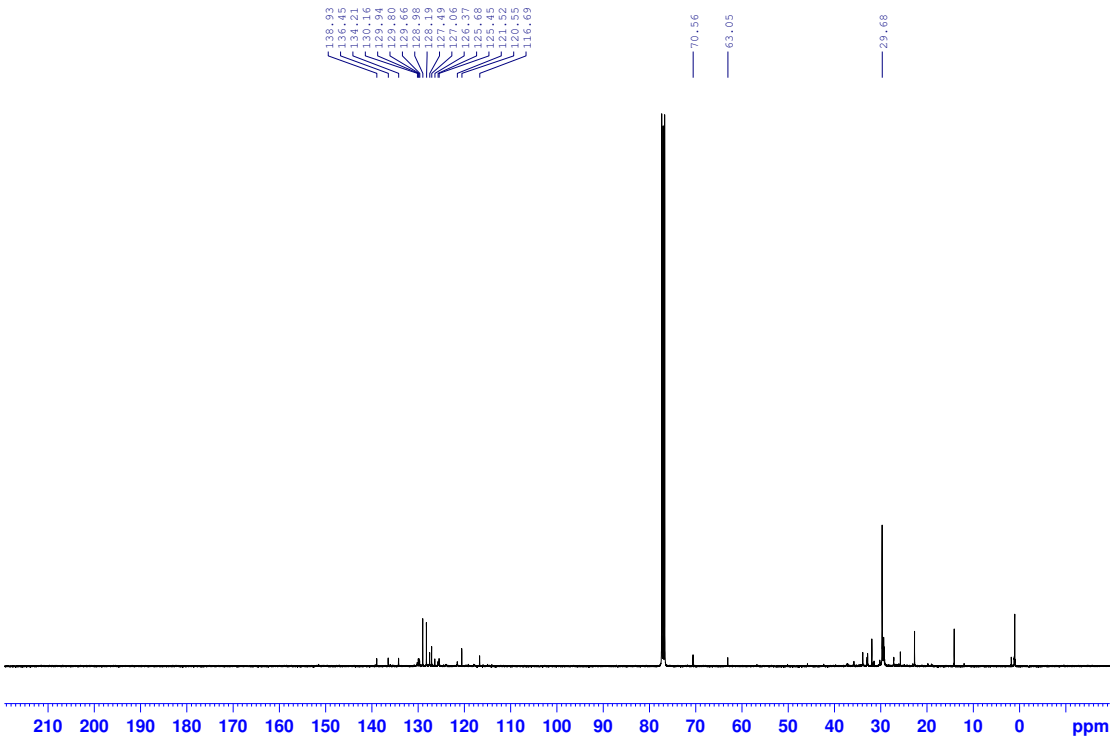
138.93
136.45
134.21
130.16
130.04
129.80
129.66
128.98
128.19
127.49
127.06
126.37
125.68
125.45
121.52
120.55
116.69
70.56
63.05
29.68
210 200 190 180 170 160 150 140 130 120 110 100 90 80 70 60 50 40 30 20 10 0 ppm

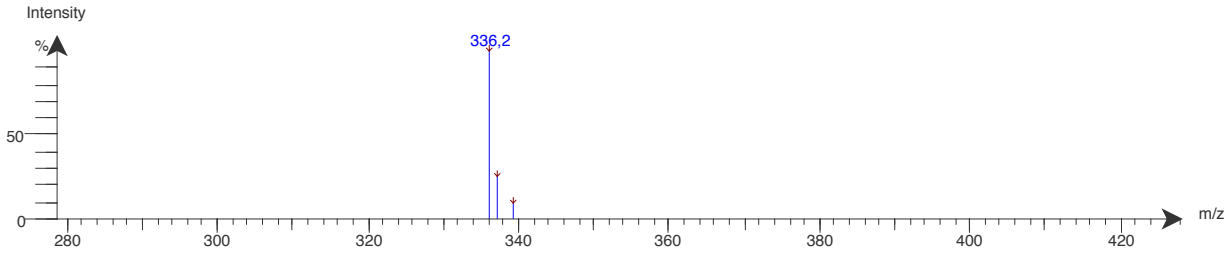
Intensity
%
50
0
336,2
280
300
320
340
360
380
400
420
m/z

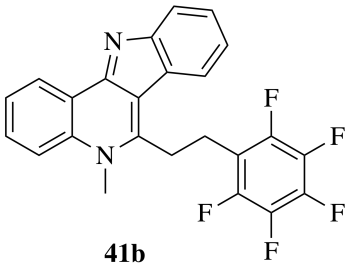

41b

5-Methyl-6-(2-(perfluorophenyl)ethyl)-5*H*-indolo[3,2-*c*]quinoline

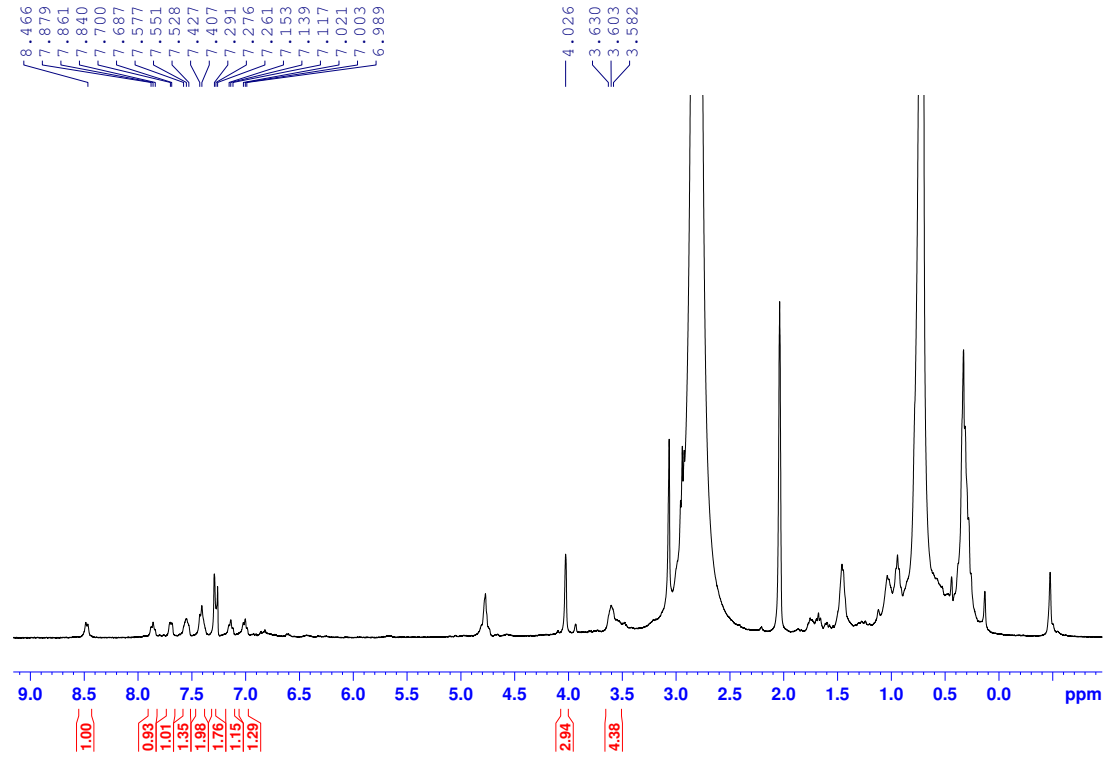
8.466
7.879
7.861
7.840
7.700
7.687
7.577
7.551
7.528
7.427
7.407
7.291
7.276
7.261
7.153
7.139
7.117
7.021
7.003
6.989
4.026
3.630
3.603
3.582
9.0 8.5 8.0 7.5 7.0 6.5 6.0 5.5 5.0 4.5 4.0 3.5 3.0 2.5 2.0 1.5 1.0 0.5 0.0 ppm
1.00
0.93
1.01
1.35
1.98
1.76
1.15
1.29
2.94
4.38

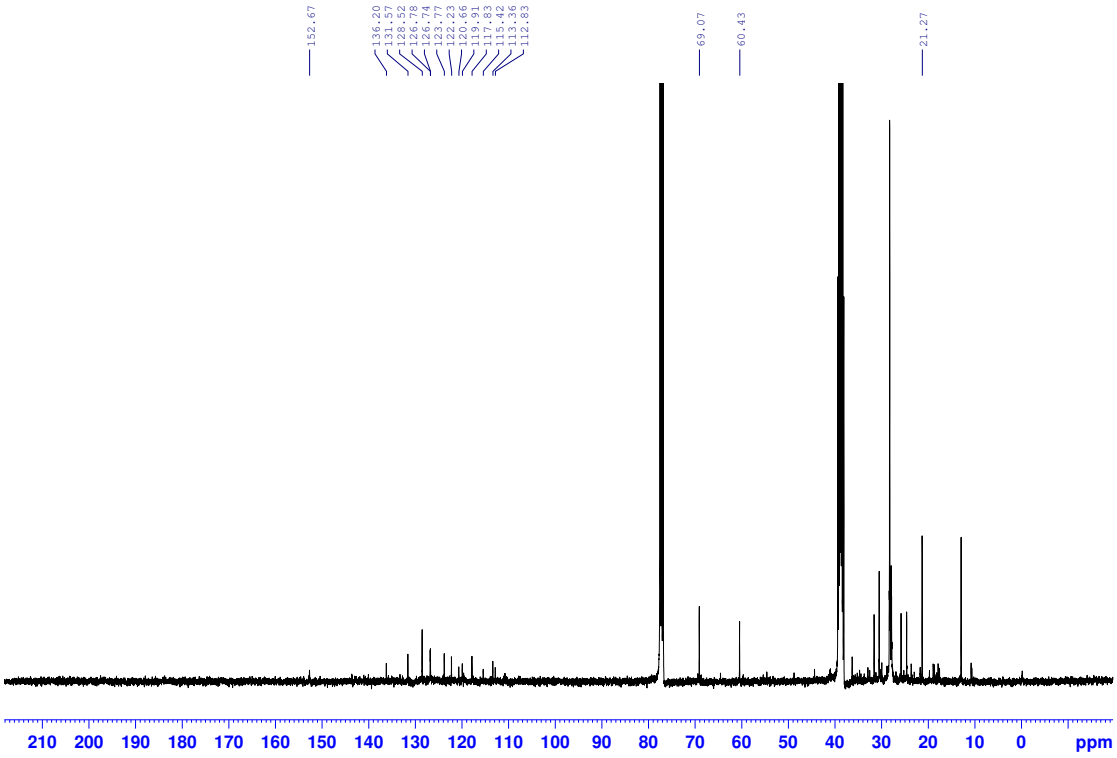
152.67
136.20
131.57
128.52
126.78
126.74
123.77
122.23
120.66
119.91
117.83
115.22
113.36
112.83
69.07
60.43
21.27
210 200 190 180 170 160 150 140 130 120 110 100 90 80 70 60 50 40 30 20 10 0 ppm

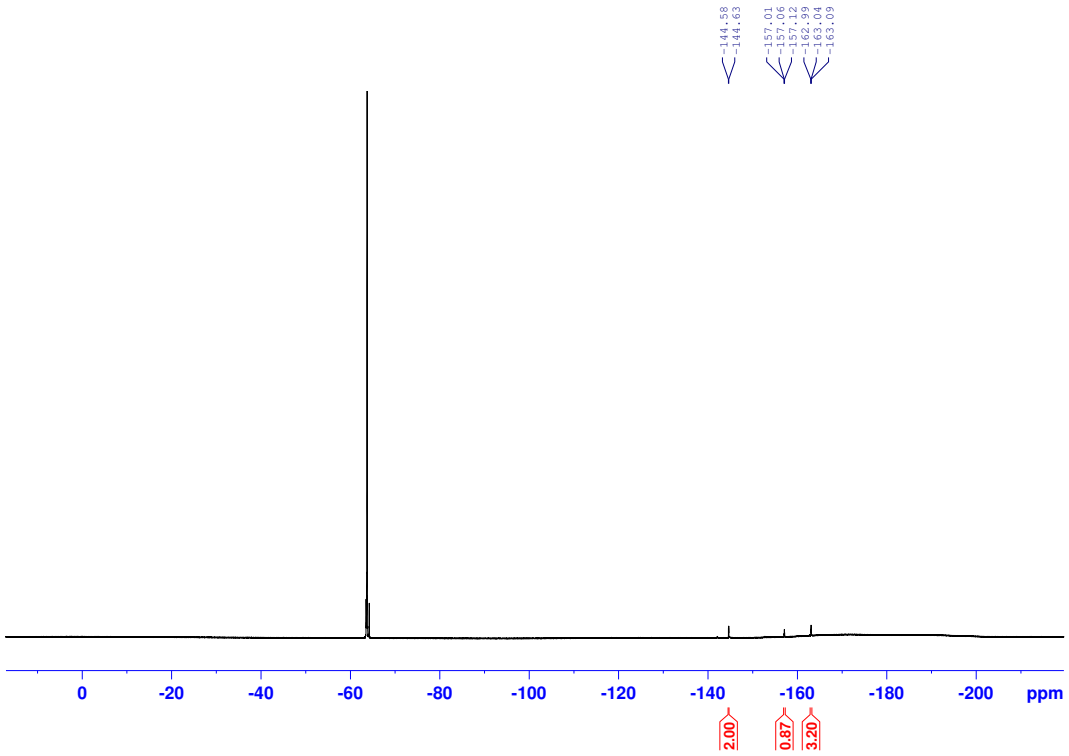
-144.58
-144.63
-157.01
-157.06
-157.12
-162.99
-163.04
-163.09
0
-20
-40
-60
-80
-100
-120
-140
-160
-180
-200
ppm
2.00
0.87
3.20

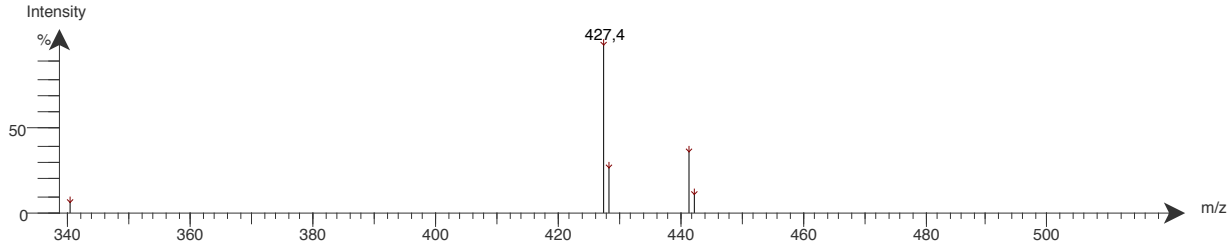
Intensity
%
50
0
427.4
340
360
380
400
420
440
460
480
500
m/z